Optimization of time-dependent routing problems considering dynamic paths and fuel consumption

Thèse

Hamza Heni

Doctorat en sciences de l'administration - opérations et systèmes de décision
Philosophiæ doctor (Ph. D.)

Québec, Canada

Optimization of time-dependent routing problems considering dynamic paths and fuel consumption

Thèse

Hamza Heni

Sous la direction de:

Jacques Renaud, directeur de recherche
Leandro C. Coelho, codirecteur de recherche

Résumé

Ces dernières années, le transport de marchandises est devenu un défi logistique à multiples facettes. L'immense volume de fret a considérablement augmenté le flux de marchandises dans tous les modes de transport. Malgré le rôle vital du transport de marchandises dans le développement économique, il a également des répercussions négatives sur l'environnement et la santé humaine. Dans les zones locales et régionales, une partie importante des livraisons de marchandises est transportée par camions, qui émettent une grande quantité de polluants. Le *Transport routier de marchandises* est un contributeur majeur aux émissions de gaz à effet de serre (GES) et à la consommation de carburant.

Au Canada, les principaux réseaux routiers continuent de faire face à des problèmes de congestion. Pour réduire significativement l'impact des émissions de GES reliées au transport de marchandises sur l'environnement, de nouvelles stratégies de planification directement liées aux opérations de routage sont nécessaires aux niveaux opérationnel, environnemental et temporel. Dans les grandes zones urbaines, les camions doivent voyager à la vitesse imposée par la circulation. Les embouteillages ont des conséquences défavorables sur la vitesse, le temps de déplacement et les émissions de GES, notamment à certaines périodes de la journée. Cette variabilité de la vitesse dans le temps a un impact significatif sur le routage et la planification du transport.

Dans une perspective plus large, notre recherche aborde les *Problèmes de distribution temporels* (Time-Dependent Distribution Problems – TDDP) *en considérant des chemins dynamiques dans le temps et les émissions de GES*. Considérant que la vitesse d'un véhicule varie en fonction de la congestion dans le temps, l'objectif est de minimiser la fonction de coût de transport total intégrant les coûts des conducteurs et des émissions de GES tout en respectant les contraintes de capacité et les restrictions de temps de service. En outre, les informations géographiques et de trafic peuvent être utilisées pour construire des multigraphes modélisant la *flexibilité des chemins* sur les grands réseaux routiers, en tant qu'extension du réseau classique des clients. Le réseau physique sous-jacent entre chaque paire de clients pour chaque expédition est explicitement considéré pour trouver des chemins de connexion. Les décisions de sélection de chemins complètent celles de routage, affectant le coût global, les émissions de GES, et le temps de parcours entre les nœuds. Alors que l'espace de recherche augmente, la résolution

des *Problèmes de distribution temporels* prenant en compte les chemins dynamiques et les vitesses variables dans le temps offre une nouvelle possibilité d'améliorer l'efficacité des plans de transport.

Une façon de réduire les émissions est de considérer la congestion et d'être en mesure de l'éviter. L'évitement des routes encombrées est possible, car les données de trafic requises sont facilement disponibles et, en même temps, ont un grand potentiel d'économies d'énergie et de coûts. Par conséquent, nous effectuons une analyse empirique des données historiques de trafic et d'expédition. Nous introduisons le **Problème du chemin le plus rapide dépendant du temps avec la minimisation des émissions**, dans lequel la fonction objectif comprend les coûts des émissions de GES, du conducteur et de congestion. Les coûts de déplacement sont affectés par le trafic en raison de l'évolution des niveaux de congestion en fonction de l'heure de la journée, des types de véhicules et de la charge transportée. Nous développons également des limites inférieures et supérieures dépendant du temps, qui sont à la fois précises et rapides à calculer. Les expériences numériques sont effectuées sur des *instances réelles* qui intègrent la variation du trafic tout au long de la journée. Nous étudions ensuite la qualité des trajectoires obtenues en considérant des vitesses variant avec le temps par rapport à celles basées uniquement sur des vitesses fixes.

Une variété de chemins alternatifs peut exister entre deux destinations si l'on considère tous les arcs individuels les reliant. Le **Problème de tournées des véhicules dépendant du temps avec minimisation des émissions et des coûts en considérant les chemins dynamiques** consiste à planifier les déplacements d'un parc de véhicules pour desservir un ensemble de clients sur un réseau dépendant du temps modélisé en multigraphe. La vitesse de déplacement sur chaque arc change avec le temps. Pour résoudre le problème, nous proposons une heuristique efficace du plus proche voisin, impliquant le calcul rapide de trajets point à point dépendant du temps en fonction de différentes mesures telles que le temps, la consommation de carburant ou le coût. Basées sur de nouvelles instances à grande échelle qui représentent de manière réaliste des opérations de transport de fret et qui capturent les périodes congestionnées en utilisant des réseaux routiers réels et de grands ensembles de données d'*observations de vitesse*, des expériences de calcul approfondies sont menées. Nous effectuons également une analyse de sensibilité pour évaluer les effets du choix du moment de départ, des décisions d'évitement de congestion et des demandes des clients sur les plans de routage résultants. Nous effectuons une évaluation approfondie de l'efficacité de notre méthode de solution par rapport à celle classique basée sur les limites de vitesse sans tenir compte de la congestion du trafic.

L'estimation de la consommation de carburant étant un élément clé de la logistique durable, la thèse contribue à proposer et à évaluer l'exactitude des modèles classiques et à développer de *nouveaux modèles de consommation* pour les tournées de véhicules. À partir de données réelles sur la consommation instantanée de carburant, d'observations de vitesses variables

dans le temps et de données de trafic liées à un grand nombre d'opérations de livraison, nous proposons des méthodes efficaces pour estimer la consommation de carburant. En effectuant une analyse de régression non linéaire en utilisant des *méthodes d'apprentissage supervisé*, à savoir les **Réseaux de neurones**, **Machines à vecteurs de support**, **Arbres d'inférence conditionnelle** et **Descente de gradient**, de nouveaux modèles de consommation pour améliorer la précision de la prévision sont développés. Notre objectif est d'estimer correctement la consommation pour un acheminement point à point dépendant du temps dans des conditions réalistes en tenant compte des opérations de transport de marchandises pendant l'heure de pointe, des schémas de conduite arrêt-départ, des états de ralenti et de la variation des charges. Nous comparons l'efficacité des modèles de consommation basés sur l'*apprentissage supervisé* par rapport au modèle CMEM (*Comprehensive Modal Emissions Model*) et la méthodologie d'estimation de la consommation de carburant provenant des transports (MEET) dans la prédiction de la consommation.

Cette thèse est organisée comme suit. Après un chapitre général d'introduction, nous présentons une étude bibliographique des thèmes étudiés, suivie de deux chapitres sur le problème de distribution temporel en considérant les trajectoires dynamiques et les émissions de GES sur un réseau dépendant du temps. Le quatrième chapitre se concentre sur les méthodes de prévision de la consommation de carburant en utilisant l'apprentissage supervisé. Des conclusions et orientations pour les travaux futurs sont présentées dans le dernier chapitre.

Mots clés: Routage dépendant du temps; chemins les plus rapides dépendant du temps; congestion; réseau routier; heuristique; émissions de gaz à effet de serre; modèles d'émission; apprentissage supervisé

Abstract

In recent years, freight transportation has evolved into a multi-faceted logistics challenge. The immense volume of freight has considerably increased the flow of commodities in all transport modes. Despite the vital role of freight transportation in the economic development, it also negatively impacts both the environment and human health. At the local and regional areas, a significant portion of goods delivery is transported by trucks, which emit a large amount of pollutants. Road freight transportation is a major contributor to greenhouse gas (GHG) emissions and to fuel consumption.

To reduce the significant impact of freight transportation emissions on environment, new alternative planning and coordination strategies directly related to routing and scheduling operations are required at the operational, environmental and temporal dimensions. In large urban areas, trucks must travel at the speed imposed by traffic, and congestion events have major adverse consequences on speed level, travel time and GHG emissions particularly at certain periods of day. This variability in speed over time has a significant impact on routing and scheduling.

From a broader perspective, our research addresses *Time-Dependent Distribution Problems* (TDDPs) *considering dynamic paths and GHG emissions*. Considering that vehicle speeds vary according to time-dependent congestion, the goal is to minimize the total travel cost function incorporating driver and GHG emissions costs while respecting capacity constraints and service time restrictions. Further, geographical and traffic information can be used to construct a multigraph modeling *path flexibility* on large road networks, as an extension to the classical customers network. The underlying physical sub-network between each pair of customers for each shipment is explicitly considered to find connecting road paths. Path selection decisions complement routing ones, impacting the overall cost, GHG emissions, the travel time between nodes, and thus the set of a feasible *time-dependent least cost paths*. While the search space increases, solving TDDPs considering dynamic paths and time-varying speeds may provide a new scope for enhancing the effectiveness of route plans.

One way to reduce emissions is to consider congestion and being able to route traffic around it. Accounting for and avoiding congested paths is possible as the required traffic data is available and, at the same time, has a great potential for both energy and cost savings. Hence,

we perform a large empirical analysis of historical traffic and shipping data. Therefore, we introduce the **Time-dependent Quickest Path Problem with Emission Minimization**, in which the objective function comprises GHG emissions, driver and congestion costs. Travel costs are impacted by traffic due to changing congestion levels depending on the time of the day, vehicle types and carried load. We also develop time-dependent lower and upper bounds, which are both accurate and fast to compute. Computational experiments are performed on *real-life instances* that incorporate the variation of traffic throughout the day. We then study the quality of obtained paths considering time-varying speeds over the one based only on fixed speeds.

A variety of *alternative paths* exist between a pair of customer nodes and each path is taken as a distinct sequence of arcs connecting the two nodes. The **Time-dependent Vehicle Routing Problem with Emission and Cost Minimization considering Dynamic Paths** consists of routing a fleet of vehicles to serve a set of customers across a time-dependent network modeled as a multigraph in which the traveling speed of each arc changes over time. To solve the problem we propose an efficient nearest neighbor improvement heuristic involving the fast computation of time-dependent point-to-point paths based on different measures such as time, fuel consumption, or cost. Based on new large-scale benchmark instances that realistically represent typical freight distribution operations and capture congested periods using real-life road networks and large data sets of *speed observations*, extensive computational experiments are conducted. We also carry out sensitivity analysis to assess the effects of departure time choice, congestion avoidance decisions and customer demands on the resulting routing plans. We perform an extensive assessment of the efficiency of our solution method compared to a classical one based on speed limits without regard to traffic congestion.

Since emission estimations is a key element of green logistics, this thesis proposes and assesses the accuracy of both classical and *new emission models* for vehicle routing. Based on real-world data of instantaneous fuel consumption, time-varying speeds observations, and traffic data related to a large set of shipping operations we propose effective methods to estimate GHG emissions. By carrying out nonlinear regression analysis using *supervised learning methods*, namely **Neural Networks**, **Support Vector Machines**, **Conditional Inference Trees**, and **Gradient Boosting Machines**, we develop new emission models to improve prediction accuracy. Our purpose is to correctly estimate emissions for time-dependent point-to-point routing under realistic conditions taking into account freight transportation operations during peak hour traffic congestion, stop-and-go driving patterns, idle vehicle states, and the variation of vehicle loads. Through extensive computational experiments under real data sets we compare the effectiveness of the proposed *machine learning* emissions models against the *Comprehensive Modal Emissions Model* (CMEM) and the *Methodology for Estimating air pollutant Emissions from Transport* (MEET) in the prediction of emissions.

This thesis is organized as follows. After a general introduction chapter, we present a literature

survey of the studied themes, followed by two chapters on the time-dependent distribution problem considering dynamic paths and GHG emissions on a time-dependent network. The fourth chapter focuses on emissions estimation using supervised learning methods. Conclusions and directions for future work are presented in the last chapter.

Keywords: Time-dependent routing; time-dependent quickest paths; traffic congestion; road network; heuristic; greenhouse gas emissions; emission models; supervised learning.

Contents

List of Tables

List of Figures

List of Abbreviations

CIT	Conditional Inference Trees
CMEM	Comprehensive Modal Emissions Model
FIFO	First-in, First-out
FSM	Flow Speed Model
GBM	Gradient Boosting Machines
GHG	Greenhouse Gas
GVRP	Green Vehicle Routing Problem
LTM	Link Travel Time Model
MCPP	Minimum-Cost Path Problem
MEET	Methodology for Estimating air pollutant Emissions from Transport
NN	Neural Networks
PRP	Pollution Routing Problem
QPP	Quickest Path Problem
SNNH	Static Nearest Neighbor Heuristic
SVM	Support Vector Machines
TD	Time-dependent
TD-Dijkstra	Time-dependent Dijkstra
TDDP	Time-dependent Distribution Problem
TDLCPP	Time-dependent Least Cost Path Problem
TDLEPP	Time-dependent Least Emission Path Problem
TDNNH	Time-dependent Nearest Neighbor Heuristic
TDNSIH	Time-dependent Neighborhood Search Improvement Heuristic
TDQPP	Time-dependent Quickest Path Problem
TDQPP-EM	Time-dependent Quickest Path Problem with Emission Minimization
TDSPP	Time-dependent Shortest Path Problem
TDTSP	Time-dependent Traveling Salesman Problem
TDVRP	Time-dependent Vehicle Routing Problem
TDVRP-ECMDP	Time-dependent Vehicle Routing Problem with Emission and Cost Minimization considering Dynamic Paths
VRP	Vehicle Routing Problem

To mom and dad, and to my
amazing grandparents...
You will always be in my heart.

The important thing is to not stop questioning. Curiosity has its own reason for existing.

Albert Einstein, 1955

Acknowledgments

First and foremost, I want to present not only my thanks, but also my admiration to my advisors, Professor Jacques Renaud and Leandro C. Coelho, who inspired me in many ways. I want to thank them for all the effort they make to provide their teams with a great research environment, precious guidance, and financial support. I appreciate their open-mindedness, their attention to details, their scientific rigor, and their non-stop quest for challenges. First, I thank Jacques for creating an atmosphere, which helps us to produce high quality scientific research while developing our own autonomy and scientific vision. Second, I would like to thank my co-advisor, Professor Leandro C. Coelho, for offering me the right assistance, sharing his knowledge with me, and supporting me both scientifically and professionally. Both Jacques and Leandro were always supportive and encouraging me to strive beyond my limits. Thanks to both of you for all your riveting discussions, feedback, guidance, and trust in my choices throughout this research work.

I would also like to express my gratitude to the professors who participated in this thesis, the thesis project, the Ph.D exam committees, and the doctoral courses: Gilbert Laporte, Fayez Boctor, Monia Rekik, and Daniel Pascot.

My deepest appreciation is extended to Laval University, the Faculty of Business Administration and, beyond them, all the wonderful people that work hard to make our doctoral experience memorable. I must mention Judy-Anne Hélie, Carole Lalonde, Johanne Nadeau, Catherine Vézina, Dominique Bernier, as well as many others who work behind the scenes.

A huge thanks are due to Benoit Montreuil and Sehl Mellouli for enabling me to begin my doctoral studies at Laval University.

I would also like to express my gratitude to Professor Pascal Pallé for administrative assistance.

Furthermore, I would like to extend my sincere gratitude to the institutions that provided support for projects developed in this doctoral thesis: the Natural Sciences and Engineering Research Council of Canada (NSERC), Centre d'Innovation en Logistique et Chaîne d'Approvisionnement Durable (CILCAD) and Canada Research Chair on Integrated Logistics. I also profoundly thank Ameublements Tanguay Canada and Logix Operations Inc for both their financial support and their proactive collaboration.

Within our Interuniversity Research Centre on Enterprise Networks, Logistics and Transportation (CIRRELT), I would like to thank all of my colleagues, those who left and those who are still with us. The support and administrative staff: Pierre Marchand, Olivier Duval-Montminy, Martine L'Heureux, Mireille Leclerc, Louise Doyon and Alexis Roy.

Furthermore, I am happy to have met many graduate and undergraduate students during my studies with whom I have not only shared similar interests, exchanged cutting edge ideas, and offered unwavering support to each other, but also developed important friendships: Sergine Arona Diop, Rabie Jaballah, Khaled Belhassine, Patrick Walther, Maryam Darvish, Thomas Chabot, Salma Naccache, Muhammad Mohiuddin, Moez Charfeddine, Salman Kimiagari, Helia Sohrabi, Sidi-Mahmoud Aidara Mbibi, Hamza El Fassi, Bala Diop, Parfait Aïhounhin, Roubila Lilya Kadri and Michel David Nebnoma Sawadogo, and many others.

I also want to express my sincere gratitude to all of my friends in Canada, France and Tunisia, who have become my extended family, for always being there when I need them, for supporting me, and for shedding happiness and joy on my life: Akrem, Najib, Chaker and Amal; Driss and Lois; Marwene and Wiem; Nidhal and Maha; Maher and Raja; Hichem and Sana; Louis and Anne; Lotfi and Kalthoum; Jamel, Zied, Emmanuel, Martin, Mourad, Mohammed, Amin, Issam, Sami, Nabil, and Mondher.

My great appreciation and thanks to my dearest wife Intissar for her never-ending unconditional support and understanding during my busy and long doctorate journey.

My deepest gratitude goes to my family for their patience and love throughout all of my studies and my life. Thanks to my wonderful parents Oumar and Sadiya who always encouraged us to study and who made our achievements their priority in life. Thank you for your unconditional love, for your unlimited support, for your endless devotion through every step I did in this world, and for brightening my universe all the time. Thanks to my amazing sisters Olfa, Nesrine, and Aycha, who are always soothing me, caring about me, and reminding me how lucky and honored I am to have them in.

To all of those I may have left out, thank you.

Preface

This thesis presents my work as a Ph.D. student developed at the Centre Interuniversitaire de recherche sur les Reseaux d'Entreprise, la Logistique et le Transport (CIRRELT) at the Faculty of Business Administration of Laval University. The thesis consists of three papers, each of which is written in collaboration with other researchers of the CILCAD and the Canada Research Chair in Integrated Logistics, mainly my directors Jacques Renaud and Leandro Callegari Coelho. Revision of one of these papers was received and the others have been submitted to the corresponding journals. In all three papers, I remain the first author and have played the principal role of setting up and conducting the research, description and modeling of the problems, implementation of algorithms, analyzing the results, preparing and writing the papers.

The first paper entitled *Time-Dependent Quickest Path Problem with Emission Minimization* is written in collaboration with Leandro C. Coelho and Jacques Renaud. The paper has been submitted for publication in Transportation Science in September 2017 and a revision was received in February 2018.

The second paper entitled *Time-dependent Vehicle Routing Problem with Emission and Cost Minimization considering Dynamic Paths* is written in collaboration with Jacques Renaud and Leandro C. Coelho. The paper has been submitted for publication in Transportation Research Part B: Methodological in February 2018.

The third paper entitled *Measuring emissions in vehicle routing: new emission estimation models using supervised learning* is written in collaboration with S. Arona Diop, Leandro C. Coelho and Jacques Renaud. The paper has been submitted for publication in Production Operations Management (POMS) in March 2018.

Chapter 1

Introduction

In recent years, freight transportation has evolved into a multi-faceted logistics challenge. The immense volume of freight has considerably increased the flow of commodities in all transport modes. Despite the vital role of freight transportation in the economic development, it also negatively impacts both the environment and human health. Nowadays freight transportation by truck is one of the most challenging sectors facing environment pollution and climate changes due to increasing energy demand and to its high dependence on diesel and fuel.

The distribution of goods between a set of geographically scattered customers through urban area networks is a central activity in vehicle routing and scheduling. Third-party logistics (3PL) service providers, transport operators as well as trucking companies are looking for effective ways to enhance goods distribution, dispatching and delivery efficiency, to maximize the operational profits and benefits from the economic perspective. They also try to reduce the environmental impacts of freight transportation activities by reducing energy usage. For example, Transports Canada has introduced the *ecoFREIGHT* program to deploy efficient business models and operating policies that enhance the use of information and decision technologies and industrial practices by enterprises operating in the logistics sector in order to reduce fuel consumption and emissions, and achieve sustainable levels of transportation energy use (Transports Canada 2011).

The first chapter of this thesis is organized as follows. In Section 1.1 the main trade-offs between road freight transportation and environmental awareness are discussed. Subsequently, routing and scheduling issues of green road freight transportation are briefly presented. Section 1.2 presents the scope of machine learning in green logistics field. The main problem that will be studied, the time-dependent routing problem with dynamic paths, is introduced in Section 1.3. The objectives of this thesis are presented in Section 1.4. Finally, the overall structure and conceptual organization of this thesis are explained in Section 1.5.

1.1 Road freight transportation and environment

Over the past half century, the demand for goods has grown significantly, so that today a vital component of a more competitive economy is a cost-effective freight transportation system (Zenghelis 2006). Road transportation plays a central position in the economy and is by far the most prominent among the various modes of freight transportation (Bektaş, Demir, and Laporte 2016).

Freight transportation is a key element of the economic and logistics of the supply chain that is designed to provide efficient distribution and timely availability of manufactured goods to meet client requirements at minimum cost (Crainic 2000, 2003). Considering the multiple decision levels of freight transportation networks, it can be viewed as a complex activity that includes various players with many objectives interrelated with a number of human, technological and operational costs factors and resources (Crainic and Roy 1988).

In the remainder of this section, the growth of freight transportation flows is discussed as well as freight transportation greenhouse gas (GHG) emissions trends in Canada and Québec. Additionally, the effects of congestion on distribution costs are briefly presented. Finally, in the last part of this section, we take a closer look at distribution operations and how their level of efficiency affects environmental performance.

1.1.1 Freight traffic growth

Road or trucking transportation provides mobility for passengers and facilitates the distribution of goods. As Canada's largest freight transportation subsector among rail, marine, and air transportation, it is particularly crucial for the transport of manufactured goods and merchandises in terms of freight volume, flow and value (Transports Canada 2017). In 2014, 72% of the total freight was transported between provinces by for-hire trucking, representing about $168 billion of interprovincial merchandise trade (Transports Canada 2017). Major trucking companies were centralized in four provinces: Ontario (41.5%), Alberta (16.2%), Québec (15.1%), and British Columbia (14.2%) (Transports Canada 2017). In the United States (U.S.) the annual gross domestic product (GDP) spending on freight transport approached 9.5% and U.S. reliance on the freight transportation system has steadily grown in scale (United States Department of Transportation 2017). In this subject, in European union countries about 45.8% of total freight was transported via road transportation in 2010 (Europeia 2012).

The increase of population and goods flow causes an increase in transportation costs due to the growth of congestion. Medium and heavy-duty trucks carrying freight share the same streets and arteries with private and public vehicles transporting people (Lahyani, Khemakhem, and Semet 2015, Crainic, Gendreau, and Potvin 2009). All these vehicles contribute to the growth of congestion and environmental nuisances, such as GHG emissions, accidents and environmental damage that negatively affect the quality of life and human health in urban areas

(Southworth and Peterson 2000, Patier et al. 2002, Figliozzi 2007).

1.1.2 Greenhouse gas emissions trends in the freight transportation sector

Road freight transportation is a major contributor to GHG emissions and to fuel consumption (Demir, Bektaş, and Laporte 2014b). At the local and regional areas, a significant portion of goods delivery is transported by truck, which emits a large amount of pollutants. Concern has been growing over the environmental effect of freight transportation operations. Thus, attention of business organizations and governments has moved to the growth in GHG emissions from the freight transportation sector (Piecyk and McKinnon 2010).

Freight transportation in urban areas is among the largest sources of GHG emissions in most countries (Laporte 2016). With increasing road transportation activity within city limits and the expected growth of freight volumes at a fast rate, GHG is expected to continue to increase at a similar pace (Crainic, Gendreau, and Potvin 2009, Transports Canada 2017). Energy use and emissions from freight transportation are increasing at a more rapid rate than from other modes of transportation. It is estimated that freight transportation in countries of the Organization for Economic Co-operation and Development (OECD) is responsible for a third of the CO_2 emissions belonging to the transportation sector (Short 2008). In the U.S. in 2005, freight transportation accounted for approximately 6800 trillion BTU (British Thermal Unit) of energy consumption, representing 25.7% of total non-military transportation energy use (Winebrake et al. 2008). Globally, according to the Stern report, transport accounts for 14% of total greenhouse gas emissions, with three quarters of these emissions originating from road transport (Stern 2007). In 2012, the transportation sector (including passenger, freight and off-road emissions) in Canada was the second-largest source of GHG, reaching 24% of total global GHG emissions (Environment Canada 2014). In 2014, the GHG emissions from road transportation sectors were responsible for 142.6 Mt of CO_2, approximately 83.2% of transportation related GHG emissions and accounted for 19.5% of Canada's total GHG emissions (Transports Canada 2017). GHG emissions from on-road freight vehicles have increased by almost 14% from 2005 to 2014, raising to 55 Mt compared with 48 Mt. Road freight activity, measured in tonne-kilometers, has increased by almost 25% over the same time period (Transports Canada 2017).

GHG emissions vary significantly across provinces, depending on various factors such as population size, manufacturing activities, economic growth and energy price (Environment Canada 2014). Concerning the province of Québec, the transportation sector accounted for the largest share of the overall GHG emissions with 44% in 2014 (MDDELCC 2016). Emissions from road transportation were responsible for 82% of downstream transportation emissions, which accounts for about 33.6% of total emissions in Québec. This explains why reducing GHG emissions in the transportation sector is a challenging task on account of the fast growth in both passenger and shipping activity that could overtake all performance measures.

In general, GHG emissions are directly proportional to the amount of fuel consumed which in turn, depends on speed, distance, acceleration, weight of the vehicle, fleet size and mix, backhauls and roadway gradients (Figliozzi 2011, Demir, Bektaş, and Laporte 2011, 2014b, Franceschetti et al. 2013, Ehmke, Campbell, and Thomas 2016b). Optimization of routing decisions related to these factors, notably average speed, as is often the case in the academic literature, may not always be easy, particularly in dynamic urban areas (Ehmke, Campbell, and Thomas 2016a).

1.1.3 High cost of congestion

In large urban areas, trucks must often travel at the speed imposed by traffic, and traffic congestion has major adverse consequences on speed level and travel time particularly at certain periods of day. This variability in speed has a significant impact on transport reliability, GHG emissions and energy consumption (Vanek and Morlok 2000, Demir, Bektaş, and Laporte 2011, Eglese and Bektas 2014).

It is widely recognized that congestion seriously affects logistics operations and causes undesirable effects to the road freight transportation systems in major cities (Figliozzi 2010, Verbeeck 2016). Traffic congestion occurs when the capacity of a particular transportation link is insufficient to accommodate an incoming flow at a particular point in time. Increased travel times as well as delay, queuing and reduced mobility caused by congestion impact the efficiency of logistics operations. Congestion has a number of adverse consequences on both economic, social and environmental dimensions, including longer travel times and variations in trip duration which results in decreased transport reliability, increased fuel consumption and large amount of emissions. In addition, the driver's inefficiency caused by congestion significantly increases the cost of goods movements and affects the just-in-time delivery expected by most customers (Jula, Dessouky, and Ioannou 2008).

The effects of congestion on vehicle GHG emissions are prominent but difficult to forecast since it is shown that it is possible to create routes for which distance or duration increases but fuel consumption or emissions decrease (Figliozzi 2011). To reduce the significant impact of freight transportation emissions on the environment, new alternative planning and coordination strategies directly related to routing and scheduling operations are required at operational, environmental and temporal dimensions.

Congestion occurs when many vehicles travel along the same path link at the same time period. Nowadays, with the information and communication technologies advances it is possible for several vehicles with a given set of origins and destinations, to coordinate shipping routes and travel times along each arc of the road networks (Speranza 2018). It is well-known that congestion has recurring patterns for different periods of the planning horizon, so one can use historical traffic data to approximate and forecast time-dependent travel times and congestion

ratios related to each link of the considered urban network (Ehmke, Meisel, and Mattfeld 2012).

In this thesis, to generate paths between scattered clients we assume that vehicles must travel at the speed imposed by traffic conditions and do not have the ability to fully control their speed in a way that minimizes GHG emissions as well as fuel consumption. Fuel consumption depends on multiple factors that can be divided into four categories: i) vehicle related such as curb weight and engine type, ii) drivers related like idle time, iii) environmental conditions (roadway gradient, wind conditions, etc.) and iv) traffic conditions including speed and acceleration, among others (Demir, Bektaş, and Laporte 2011, 2014b).

1.1.4 Efficiency of distribution operations and environmental performance

Road freight transportation is responsible for a large portion of GHG emissions, of which manufactured goods transport constitutes a sizable portion (Jabali, Van Woensel, and de Kok 2012). Thus, there is a need to address both operational and environmental factors in the context of freight transportation. 3PL and carrier companies may voluntarily adopt green policies if this is aligned with cost reduction. This could be in the form of GHG greedy procedures, or when CO_2 emissions become taxable. As a largest contributor to GHG emissions, road freight transportation has been an important focus of these initiatives (Piecyk and McKinnon 2010, Ehmke, Campbell, and Thomas 2016b). Given current concerns about environment and energy issues, numerous strategies and approaches have been established to reduce GHG emissions in the field of green transportation logistics, which aims to involve the incorporation of environmental dimension into distribution logistics (Psaraftis et al. 2016). Green transportation logistics tries to achieve an acceptable level of environmental performance and sustainability in transportation systems, while at the same time respecting traditional economic performance criteria (Psaraftis et al. 2016).

Operations research has long concentrated in improving operations. Traditional routing models and policies for distribution of goods have focused on minimizing costs under various operational constraints (Crainic 2000, Sbihi and Eglese 2010, Dekker, Bloemhof, and Mallidis 2012). Most works that addressed routing issues are focused on the resolution of the classical Vehicle Routing Problem (VRP) which consists of determining best routes through a set of geographically scattered customers, subject to various operational constraints (Laporte 2016). The common standard objective is the minimization of routing costs (or distance). However, the consideration of the several objectives and factors concerned with the Green VRP (GVRP) leads to new schemes of delivery and efficient distribution methods, some of which pose interesting new applications for logistics models (Sbihi and Eglese 2010, Dekker, Bloemhof, and Mallidis 2012, Demir, Bektaş, and Laporte 2014b, Lin et al. 2014). With an increasing concern for the environment impact in large cities, logistics providers and freight transportation companies have started paying more attention to the negative effects of their

distribution operations on human life.

Furthermore, consideration of various routes between a pair of nodes for distribution planning is not well studied in the literature. A sustainable model for the logistics of distribution ought to choose the routes which minimize the fuel consumption or GHG emissions. A variety of alternative paths can exist between a pair of nodes and each path is taken as a distinct arc connecting the two nodes (Gajanand and Narendran 2013, Ehmke, Campbell, and Thomas 2016b, Qian and Eglese 2016, Huang et al. 2017). If each lane of a highway is considered as an alternative path, the length is the same but the speed will be different. Another possibility is the existence of multiple paths with different lengths, different road types and different average speeds. The availability of multiple paths between two clients can be observed in large urban networks.

The rapid penetration of modern technology, such as the cellular technology, in our daily habits, has allowed travelers to act as moving sources of real-traffic information. Therefore, vehicle navigation and route planning vendors are nowadays in position to acquire in real-time instantaneous live-traffic reports (e.g., road blockages due to car accidents), as well as periodic speed-probes that allow the maintenance of historic traffic data about this time-varying behavior of each and every road segment in a network.

1.2 Machine learning in green logistics

The availability of traffic data can allow new approaches to be applied in green logistics field for producing high prediction accuracy and better routing models. Ultimately, machine learning could be used to model complex relationships by learning from the field data (Choi, Wallace, and Wang 2018). In fact, machine learning provides well-established supervised learning methods, namely Neural Networks (NN), Support Vector Machines (SVM), and Gradient Boosting Machines (GBM), to fit complex relationship and design flexible nonlinear models (Kuhn and Johnson 2013). Supervised learning schemes can enhance the estimation accuracy of different types of predictor variables such as speed and emission observations.

In this thesis, the importance of time-dependent setting and environmental dimension are highlighted and the pertinence of extending the scope of distribution logistics management from the tactical and operational levels to the temporal and environmental levels is addressed. Such issues will be presented from various theoretical and practical facets related to distribution and logistics using time-dependent models, in which traffic congestion patterns are considered. Further, we employ supervised learning methods to model emissions and improve the prediction accuracy in green logistics field.

1.3 Stating the research problem

In the next chapter we present a literature review on time-dependent shortest path problems and on green routing problems. We describe the terminology, the major concepts and introduce the main studied problems. In this thesis we address two important Time-dependent Distribution Problems (TDDPs) induced by time-dependent setting and environmental dimension. We also study the accuracy of emission estimation according to new scope in green logistics, namely big data and machine learning techniques. These are described next.

To begin, the main goal of the first part of this thesis is to introduce and solve a new variant of the classical time-dependent quickest path problem (Calogiuri, Ghiani, and Guerriero 2015), entitled the **Time-Dependent Quickest Path Problem with Emission Minimization** (TDQPP-EM). The TDQPP-EM combines decisions based on economic and environmental dimensions to evaluate alternative paths between nodes on the underlying physical road network. The objective is to minimize the total cost considering a comprehensive objective function composed by GHG emissions, fuel consumption, drivers and time-dependent congestion-induced costs.

Thereafter, in the second part of this thesis we will focus on the analysis of the trade-offs that occur in the total cost, time, distance, fuel consumption and GHG emissions in large time-dependent road networks when optimizing these different measures. The problem of optimizing the schedule for a fleet of vehicles given time-dependent travel times and taking into account environmental factors is entitled the **Time-dependent Vehicle Routing Problem with Emission and Cost Minimization considering Dynamic Paths** (TDVRP-ECMDP). The TDVRP-ECMDP is an extension of the Pollution Routing Problem (Bektaş and Laporte 2011). The TDVRP-ECMDP is concerned with the routing of a fleet of heterogeneous vehicles each with a finite capacity, in order to serve a set of customers across a time-dependent network modeled as a multigraph in which the traveling speed of each arc changes over time. Each customer has a certain demand and must be served within a pre-defined time window. The TDVRP-ECMDP aims at minimizing an objective function comprising the fuel and duration costs of all routes involving dynamic path choice decisions. The fuel consumption along a route and its duration depend on the traveling speed. The cost function includes emissions and driver costs, taking into account traffic congestion which, at peak periods, significantly affects vehicle speeds and increases GHG emissions.

The main contribution of the third part of the thesis, named **Measuring emissions in vehicle routing: new emission estimation models using supervised learning**, is the analysis of the accuracy of emission estimations considering different input variables and large sets of speed observations, that aims to enhance the prediction accuracy of emissions in time-dependent road networks. From a machine learning point of view, a number of opportunities may exist with the availability of time-varying speeds observations, instantaneous fuel con-

sumption, roadway gradient, vehicle load, and stop-and-go traffic data related to vehicle trips of logistics and freight companies across large cities. GPS and on-board real-time emission measurement devices provide real-world observations of emissions of micro scale events under real-world traffic congestion. In this work, the objective is to perform a large-scale empirical analysis of historical fuel consumption data on the underlying road network. Therefore, using supervised learning methods we aim to build nonlinear emission models considering time-varying speeds, vehicle load fluctuations, stop-and-go driving patterns, acceleration, and breaking events.

1.4 Objectives

The research described throughout this thesis aims to study the trade-offs that occur in total road freight transportation costs, travel time, distance, GHG emissions and fuel consumption by analyzing and optimizing a variety of real-world time-dependent distribution problems. The objectives of this thesis are to provide efficient heuristics and exact optimization methods for three important time-dependent distribution problems:

1. the TDQPP-EM addressing direct routing between two clients, finding a least cost path between two nodes on a discrete time-dependent and first-in, first-out (FIFO) network,
2. the TDVRP-ECMDP which consists of routing a fleet of vehicles to serve a set of scattered customers on a FIFO network with time-dependent speed flow, minimizing the total travel cost function encompassing driver and GHG emissions costs,
3. and the emissions prediction problem.

We will develop efficient routing algorithms and optimization methods used to assist online vehicle routing and scheduling, yielding high-cost savings, low fuel consumption and GHG emissions. In order to achieve these goals, the following objectives are considered:

- Present a literature review that highlights the contribution of operations research concerning the time-dependent shortest path and pollution routing problems;
- Define and mathematically model the cost functions of the TDQPP-EM and the TDVRP-ECMDP on a time-dependent network with FIFO consistency;
- Create benchmark instances that allow for a realistic way of testing time-varying speeds and congestion patterns in large time-dependent road networks;
- Develop speed-up algorithms to update the least cost paths in time-dependent network or multigraph when the link travel costs change over time;

- Design and implement efficient heuristics and optimization methods to solve the studied TDQPP-EM and TDVRP-ECMDP;
- Perform a large-scale empirical study of historical traffic and emissions data;
- Develop nonlinear emission models using supervised learning methods.

1.5 Outline of the thesis

The remainder of this thesis is organized as follows. In Chapter 2, a literature review of time-dependent quickest path problems and pollution routing problems is presented.

In the first part of Chapter 3, the properties of TDQPP-EM are mathematically defined and discussed, including least travel cost upper and lower bounds, among others. In the second part of Chapter 3, efficient algorithms are proposed to solve the problem. More importantly, realistic problem instances that originate from a large road network with available time-dependent speed profiles will be solved by the proposed solution methods.

In Chapter 4, the TDVRP-ECMDP is addressed using data-driven approaches, time-dependent quickest path optimization, and a multi-neighborhood local search improvement heuristic is presented.

In Chapter 5, the challenge of emissions modeling and estimation in vehicle routing is studied through machine learning approaches that allows previously developed heuristics to handle time-dependent emissions prediction based on a large set of speed and fuel consumption observations.

Chapter 6 discusses the conclusions of this research as well as meaningful extensions to this thesis.

Chapter 2

Literature Review

2.1 Introduction

In recent years there has been a considerable resurgence in the area of time-dependent routing. In practical transportation applications like Route Guidance System (RGS) and Fleet Management Software (FMS), link traversal costs may vary significantly over time due to traffic congestion and environmental conditions, or when the speed flow is defined by decision makers (Gendreau, Ghiani, and Guerriero 2015). Broadly speaking, the research on this field can be divided into four principal broad areas (Ghiani and Guerriero 2014b, Cordeau, Ghiani, and Guerriero 2014):

(i) travel time modeling and estimation;

(ii) the time-dependent shortest path problem (TDSPP);

(iii) the time-dependent traveling salesman problem (TDTSP) and its variants;

(iv) and the time-dependent vehicle-routing problem (TDVRP).

New technological advances on road transportation applications and the growing branch of green logistics, and in particular green vehicle routing, have stimulated a renewed interest in the study of time-dependent routing problems with new insights. On the one hand, time-dependent routing problems have been studied on time-dependent networks where arc travel times change over time. On the other hand, time-dependent routing problems have been restated with the aim of minimizing a total cost function encompassing GHG emissions and fuel consumption costs. In such a context, the purpose of this chapter is to present a comprehensive survey of relevant works that have addressed the TDSPP, Green VRP (GVRP), TDVRP and their extensions. Emphasis will be placed on time-dependent models, efficient heuristics and exact methods used for solving the TDSSP, GVRP and TDGVRP arising in road freight transportation.

More precisely, the remainder of the chapter is organized as follows. Section 2.2 defines the classical SPP and Section 2.3 the TDSSP and its variants. Section 2.4 presents relevant work on the GVRP and its meaningful extensions.

2.2 The shortest path problem

The SPP in road networks has been the subject of extensive research for many years in diverse fields such as transportation of goods and computer science (Ahuja et al. 2003). Freight distribution management, real-time vehicle routing operations, web-based travel information services and logistics planning are among several application areas involving the determination of optimal shortest paths (Chabini 1998, Ghiani and Guerriero 2014b, Cordeau, Ghiani, and Guerriero 2014, Gendreau, Ghiani, and Guerriero 2015).

In the basic version of SPP the arc travel costs, usually interpreted as an arc traversal time, arc length or weight are static and deterministic. Hence, the information required to formulate the problem is time-invariant.

We first start by presenting the notation as well as the basic problem. Let $G = (V, A)$ be a graph, where V is a node (road junction) or vertex set and A is an arc (traffic link) set. Denote the numbers of nodes $|V| = n$ and the number of arcs $|A| = m$. Each arc denoted by (i, j) is represented as an ordered pair of nodes. Let $c : A \rightarrow \mathbb{R}$ be a function which assigns a numerical value for the cost c_{ij} of each arc. A path from an origin to a destination can be defined as sequential list of nodes from the origin o to the destination d and the travel cost of the path $p = (o = v_1, v_2, ..., v_k = d)$ is the sum of travel costs of its individual arcs. The SPP consist of finding a least cost path from the origin node $o \in V$ to the destination node d. For simplicity, we will assume that:

- V and A are invariant.
- G does not contain any directed cycle with negative costs, thus guaranteeing a finite solution to the SPP.
- G is strongly connected and does not include parallel arcs.
- All nodes are reachable from o.

Using a linear programming notation, the classical SPP can be formulated as follows:

$$(SPP)\min \sum_{(i,j)\in A} c_{ij}x_{ij} \tag{2.1}$$

subject to

$$\sum_{j\in\Gamma^+(i)} x_{ij} - \sum_{j\in\Gamma^-(i)} x_{ji} = \begin{cases} 1 & \text{for } i = o \\ 0 & \text{for } i \in V \setminus \{o, d\} \\ -1 & \text{for } i = d \end{cases} \tag{2.2}$$

$$x_{ij} \geq 0, \forall (i,j) \in A \tag{2.3}$$

$$x \in \mathbb{Z}^{|A|} \tag{2.4}$$

where

$x_{ij} = 1$ if (i, j) is in the shortest path p.

$\Gamma^+(i)$ and $\Gamma^-(i)$ denote the arc sets leaving i and incident to i, respectively:

$\Gamma^+(i) = \{(u, v) \in A : u = i\}$,

and $\Gamma^-(i) = \{(u, v) \in A : v = i\}$.

Typically, the function c refers to distance or cost, but any other measures of interest can be used such as time or any function modeling the problem on hand.

2.3 The time-dependent shortest path problem and its variants

In many transportation applications, travel times, speed profiles and costs on some arcs may change over time. Based on real-time or historical traffic information, a new shortest path problem can be defined in which only the travel time along a set of arcs of the network differs from that of the original problem. In time-dependent road networks, also known as time-varying or dynamic networks, the problem is called the Time-Dependent SPP (TDSPP). This problem is also known as the minimum cost path problem or the dynamic SPP (DSPP). It has been first considered by Cooke and Halsey (1966).

In Section 2.3.1 we review the TDSPP. This is done by presenting the mathematical formulation and describing its properties including time-dependent network types, among others. The FIFO property is presented in Section 2.3.2. In Section 2.3.3 we present the existing models of time-dependent transportation model. Section 2.3.4 is devoted to concisely summarize the major contributions of TDSPP, exploring their variants and summarizing the algorithmic approaches and optimization methods that have been proposed for solving it.

2.3.1 Basic definitions, mathematical models and properties

In general, the TDSPP is an SPP applied on a time-dependent network (Orda and Rom 1990, Kaufman and Smith 1993, Ziliaskopoulos and Mahmassani 1993, Chabini 1998). The

TDSPP can be defined as follows. Let $G = (V, A, C, D)$ be a graph, where $V = \{1, ..., n\}$ is the set of nodes, $|V| = n$, and $A = \{(i, j) \in V \times V\}$ the set of directed arcs connecting the nodes, $|A| = m$. We denote by $D = \{\tau_{ij}(t)|(i, j) \in A\}$ the set of time-dependent arc travel times and by $C = \{c_{ij}(t)|(i, j) \in A\}$ the set of time-dependent arc travel costs. Let $T = t_0 + K\delta$, where $\delta > 0$ is the smallest increment over which a perceptible change in the travel time will take place and K a finite number of discrete time slots considered. For each arc $(i, j) \in A$, the time horizon $[0, T]$ is then composed by discrete time slots $Z_k = [z_k, z_{k+1}[$ where $0 \leq k \leq K - 1$, $z_0 = t_0$ and $z_K = T$. For each $t \in [0, T]$ and each arc $(i, j) \in A$, the function $\tau_{ij}(t)$ assigns a positive, real-valued travel time incurred when traversing arc (i, j) departing node i at starting time $t \in [z_k, z_{k+1}[$. Thus, $\tau_{ij}(t)$ is a discrete and time-dependent function that takes a constant value after a finite number of time slots K. Function $c_{ij}(t)$ has real-valued range and real-valued domain. Note that $c_{ij}(t)$ has fixed value when the departure time is greater than or equal to T. Let $\Gamma^+(i)$ denotes the set of successor nodes of node i, thus, $j \in \Gamma^+(i)$ implies $(i, j) \in A$. Likewise, $\Gamma^-(i)$ denotes the set of predecessor nodes of node i, hence $j \in \Gamma^-(i)$ implies $(j, i) \in A$. G is also called a discrete time-dependent or dynamic network. It is assumed that:

- arc traversal times for each starting time $t \in [0, T]$,
- arc traversal times are known, and are at least as large as the discretization interval,
- waiting at the nodes is forbidden,
- cycle back through a previously visited node is not allowed.

The general TDSPP consists of finding a least cost path from an origin node to selected destination nodes in the defined time-varying networks. Let $\varphi_i(t)$ denote the minimum total cost from an origin node $o \in V$ to a destination node $d \in V$ departing at time $t \in [0, T]$. The least-cost path is then formulated using the following recursion:

$$\begin{cases} \min_{j \in \Gamma^+(o)}(c_{oj}(t) + \varphi_j(t + \tau_{oj}(t))) & \text{if } o \neq d \\ 0 & \text{if } o = d \end{cases} \tag{2.5}$$

Formally, a time-dependent network is a quintuple $G = (V, A, \tau, c)$, where V is the set of nodes, $|V| = n$, A the set of directed arcs connecting the nodes, $\tau : A \times \mathbb{R} \to \mathbb{R}_0^+$ the arc travel time functions, and $c : A \times \mathbb{R} \to \mathbb{R}$ the travel cost function.

In TDSPP, the time-dependent network can be dynamic, stochastic or both of them. Based on extensive literature survey related to TDSPP, time-varying networks, dynamic networks and dynamic time-dependent networks have the same conceptual and practical meanings. In these

types of network, the travel arc costs are time-dependent (Orda and Rom 1990, Kaufman and Smith 1993, Ziliaskopoulos and Mahmassani 1993, Chabini 1998).

In the case of deterministic discrete time-dependent networks, the TDSPP can be analyzed and solved by defining a space-time network $R = (N, E)$ as follows:

$$N = \{i_k : i \in V, 0 \leq k \leq K-1, \}, |N| = nK \tag{2.6}$$

and

$$E = \{(i_k, j_h) : (i,j) \in A, t_k + \tau_{ij}(t_k) = t_h, 0 \leq k < h \leq K-1\}, |E| \leq (m+n)K. \tag{2.7}$$

Furthermore, each vehicle that leaves node i_h at time $t_h \in [z_h, z_{h+1}[$, will arrive at node j_k at time $t_k \in [z_k, z_{k+1}[$. With each arc is associated a tuple of the form $\langle (i,j), z_0, z_K, (\tau_{ij}(t_1), \tau_{ij}(t_2), ..., \tau_{ij}(t_K))\rangle$ that gives the values of travel time $\tau_{ij}(t_k)$ incurred when traversing arc (i,j) departing from node i at time $t_k \in [z_k, z_{k+1}[$. Alternatively, because the flow of speed along each arc (i,j) depends on the time period, then road speed pattern is defined as tuple of the form $\langle (i,j), z_0, z_K, (\tau_{ij}(t_1), \tau_{ij}(t_2), ..., \tau_{ij}(t_K))\rangle$, where s_k^{ij} is the speed in a given arc $(i,j) \in A$, which is assumed to be equal to a constant during each time interval $Z_k = [z_k, z_{k+1}[$.

In real road networks, two vehicles traveling at the same speed along the same arc (i,j) will arrive at the terminating node of the arc in the same order as they leave the node i, even with multiple levels of traffic congestion during the trip (Sung et al. 2000). Hence, inside time-dependent network, arc travel times possess some fundamental properties that need to be integrated in the design of time-dependent point-to-point routing models and optimization methods. To manage the effect of passing and ensure consistency with the requirements of real-time transportation applications, first-in-first-out (FIFO) and cost consistency properties are considered in numerous studies. They may be formulated in various mathematical forms. Details about these properties are given in the next sections.

2.3.2 FIFO property

The FIFO property was first introduced by Ford Jr (1956), Bellman (1958) and Moore (1959). Provided that FIFO property holds, the arrival time is a strictly monotonic (non-decreasing) function of the departure time (Calogiuri, Ghiani, and Guerriero 2015). The FIFO property is also called the non-passing property (Sung et al. 2000) or the no overtaking property (Carey 1986, Delling and Nannicini 2012, Nannicini et al. 2012). The satisfaction of FIFO dynamics is ensured by arc travel time or arrival time functions, which results to be strictly monotonic and piecewise linear function of the starting time.

More formally, let $\gamma_{ij}(t)$ denote the arrival time function for every arc $(i,j) \in A$. The function $\gamma_{ij}(t)$ gives the arrival time at node j if one departs from i at time $t \in [0, T]$. Given a start

time t and a path $p = (o = v_1, v_2, ..., v_k = d)$, arrival time at the destination node d is defined recursively as $\gamma_p(t) = \gamma_{v_{k-1}v_k}(\gamma_{v_{k-2}v_{k-1}}(...\gamma_{v_1v_2}(t)))$, with the initialization $\gamma_{v_1v_2}(t) = r+\tau_{ij}(t)$. The value given by the function $\gamma_{ij}(t) - 1$ corresponds to the travel time $\tau_{ij}(t)$ along the arc (i, j) if one leaves node i at time t. The inverse arc arrival time function $\gamma_{ij}^{-1}(t)$ provides the latest time one may start to move from node i to node j at time t. We also have $\gamma_{ij}^{-1}(t) \leq t$ (Dean 2004b). Thus, FIFO assumptions can be defined as follows:

FIFO assumption in the case of a deterministic time-dependent network (Orda and Rom 1990, Kaufman and Smith 1993) The FIFO property states that if two vehicles starting at the departure node u of an edge respectively at time t' and $t \geq t'$ are arriving at the end node v of the edge at times $\gamma_{uv}(t')$ and $\gamma_{uv}(t)$, respectively, then $\gamma_{uv}(t') \leq \gamma_{uv}(t)$.

For any arc $(u, v) \in A$, $t' + \gamma_{uv}(t') \leq t + \gamma_{uv}(t)$ for all $t, t' \in [0, T]$, if $t' \leq t$.

In the case of classical SSP, Dijkstra's algorithm is able to find an optimal shortest path between a pair of nodes (Dijkstra 1959). Nevertheless, when the objective is to minimize travel costs in time-varying network rather than travel time, the classical Dijkstra's algorithm cannot guarantee finding an optimal path even if the FIFO condition is respected (Wen, Çatay, and Eglese 2014).

When the FIFO condition holds for each arc of the network, then the time-dependent network is FIFO (Chabini 1998). Thus, the arrival time $\gamma_{ij}(t)$ is non-decreasing for all arcs $(i, j) \in A$. In this way, all arc travel times satisfy the FIFO property and the Bellman's principle of optimality (Bellman 1958) can also be applied. The TDSPP in FIFO networks is polynomially solvable (Kaufman and Smith 1993, Dean 2004b). In this context, Kim et al. (2014) have demonstrated that a least travel time path can be optimally found in FIFO network by generalizing the classical shortest path algorithms using time-dependent algorithmic approaches.

In the case of non-FIFO networks, the TDSPP is NP-hard (Orda and Rom 1990). Even with a single non-FIFO arc the TDSPP is no longer polynomially solvable, but NP-Hard (Sherali, Hobeika, and Kangwalklai 2003). Non-FIFO networks may contain cycles and waiting at the nodes are either allowed or disallowed (Orda and Rom 1990, Chabini 1998). The aim of the next section is to present the relevant models for time-dependent networks.

2.3.3 Existing models for time-dependent networks

Sung et al. (2000) distinguishes between two types of models for time-dependent networks:

1. flow speed model (FSM) where it is the speed of each arc, and not the travel time, which depends on the time period. In this case solution obtained by FSM models are consistent with the FIFO dynamics and are stable to the variance of the time period length.

2. link travel time model (LTM) where arc travel times depend on the time period. LTM models may not satisfy the FIFO property.

These two kinds of models a discussed hereafter.

2.3.3.1 Flow speed model

In the FSM, introduced by Sung et al. (2000), the speed on each arc depends on the time interval. So, it is the flow speed on each arc and not the travel time which changes over time. For each arc $(i,j) \in A$ let the set of speed flows s_k^{ij} at time t_k and the set of time slots $[z_k, z_{k+1}[$ be denoted by S_{ij} and Γ_{ij}, respectively, and $S = \cup_{\forall (i,j) \in A} S_{ij}$ and $\Gamma = \cup_{\forall (i,j) \in A} \Gamma_{ij}$. With each arc is associated a non-negative travel distance L_{ij}, which is assumed to be constant. Let l_{ij}^k denote the portion of the length L_{ij} covered during time periods Z_k. For the FSM the graph is represented by $G = (V, A, \Gamma, S)$.

Sung et al. (2000) have proved that with FSM, the arrival times $\gamma_{ij}(t)$ are consistent with the FIFO assumption. It is easy to understand because all vehicles travel at the same speed whatever the time at which they entered the arc. Assuming that $\omega \in [z_1, z_2[$ the arrival time $\gamma_{ij}(\omega)$ is calculated using the following relationships proposed by (Sung et al. 2000):

$$\gamma_{ij}(\omega) = L_{ij}/s_0^{ij} + \omega \text{ if } L_{ij}/s_0^{ij} < z_1 - w \tag{2.8}$$

$$\text{else } \gamma_{ij}(\omega) = (L_{ij} - l_{ij}^0)/s_1^{ij} + z_1 \text{ if } (L_{ij} - l_{ij}^0)/s_1^{ij} < z_2 - z_1 \tag{2.9}$$

$$\text{else } \gamma_{ij}(\omega) = (L_{ij} - l_{ij}^{k-1})/s_k^{ij} + z_k \text{ if } (L_{ij} - l_{ij}^{k-1})/s_k^{ij} < z_{k+1} - z_k \tag{2.10}$$

where

$$l_{ij}^k = \begin{cases} s_0^{ij}(z_1 - w) & \text{if } k = 0 \\ l_{ij}^{k-1} + s_k^{ij}(z_{k+1} - z_k) & \text{if } k > 0. \end{cases} \tag{2.11}$$

Moreover, given a set of speeds, the arc travel time function $\tau_{ij}(t)$ can be computed using Ichoua, Gendreau, and Potvin (2003) travel time calculation or derivation algorithms (Cordeau, Ghiani, and Guerriero 2014, Ghiani and Guerriero 2014b). The main idea behind this algorithm is that when a vehicle travels across a specific arc, speed is not a constant over the entire length of L_{ij}, but it changes when the boundary between two consecutive time slots is crossed (Ichoua, Gendreau, and Potvin 2003) (see Figure 2.6). Thus for a given starting time, it is easy to calculate when the link will be exited.

Let us assume that the start time t and the arrival time $t + \tau_{ij}(t)$ belong respectively to the time slots Z_{h_1} and Z_h, with $h_1 \in \{0, ..., K-1\}$ and $h \in \{h_1, ..., K\}$. The travel time on arc (i,j) can be expressed as proposed by Cordeau, Ghiani, and Guerriero (2014):

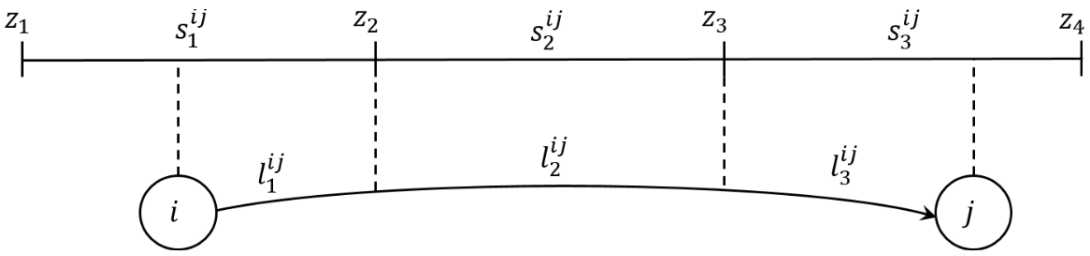

Figure 2.1: Illustrations of a link traversing three time periods

$$\tau_{ij}(t) = \sum_{k=h_1}^{h} l_{ij}^k / s_k^{ij}. \tag{2.12}$$

2.3.3.2 Link travel time model

Another approach used in TDSPP is the LTM, first proposed by Cooke and Halsey (1966). In the LTM the shortest paths may or may not satisfy the FIFO condition (Miller-Hooks and Yang 2005). Hence, the shortest path is very unstable to the change on the time interval length. In the LTM, the arc travel time function $\tau_{ij}(t)$ is equal to the time needed by a vehicle to travel across arc (i, j), where t denotes the departure time from i. Hence, arc travel times are specified upon entrance on the head node of the arc and are assumed to be fixed for that particular vehicle until it leaves the terminal node (Miller-Hooks and Yang 2005). In that case, it is assumed that for each departure time t and each arc, $\tau_{ij}(t+\varepsilon) = \tau_{ij}(t)$ where $0 < \varepsilon < \delta$. So, the arc traversal speed remains unchanged until a vehicle arrives at the next arc.

The travel time $\tau_{ij}(t)$ is known for several breakpoints z_k, with $0 \leq z_k \leq T$, $k \in \mathbb{N}$, $0 \leq k \leq K-1$, $z_0 = t_0$ and $z_K = T$. In that case, $\tau_{ij}(t)$ is considered to be a continuous piecewise linear function of time. Thus, to avoid undesired and unrealistic effect of passing and satisfy the FIFO condition, Fleischmann, Gietz, and Gnutzmann (2004) have constructed the following travel time function:

$$\tau_{ij}(t) = \begin{cases} \tau_{ijk} & \text{for } z_{k-1} + \delta_{ij,k-1} \leq t \leq z_k - \delta_{ijk} \\ \tau_{ijk} + (t - z_k + \delta_{ijk})\rho_{ijk} & \text{for } z_k - \delta_{ijk} < t < z_k - \delta_{ijk} \end{cases} \tag{2.13}$$

where

$k = 1, ..., K-1$,

δ_{ijk} is an appropriate parameter used to define the slope ρ_{ijk}, such that: $\delta_{ij0} = \delta_{ijK} = 0$,

$\delta_{ijk} \leq \frac{1}{2}(z_k - z_{k-1})$ and $\delta_{ijk} \leq \frac{1}{2}(z_{k+1} - z_k)$,

and $\rho_{ijk} = \frac{\tau_{ij,k} - \tau_{ijk}}{2\delta_{ijk}}$.

Furthermore, the arrival time function $\gamma_{ij}(t) = t + \tau_{ij}(t)$ is continuous and strictly monotonic over the interval, which satisfies the FIFO property.

The LTM was applied in several papers, such as Fleischmann, Gietz, and Gnutzmann (2004), Nannicini et al. (2012) and Delling and Nannicini (2012).

2.3.4 Major contributions on the TDSPP and typologies of the problem

The TDSPP has been first introduced by Cooke and Halsey (1966). They solved the problem with a recursion function, which is an extension of the Bellman (1958) principle of optimality, that takes into account inter-nodal time requirements which are time-dependent. Dreyfus (1969) generalized the Dijkstra's algorithm (Dijkstra 1959), to find the fastest path between two nodes where the travel time on an arc depends on the departure time from the origin node.

Many variants of the TDSPP have been described over the past 50 years. There does not exist a standard version of the problem. We will, therefore refer to basic versions of the TDSPP, in which most of the research effort has been concentrated, and to variations of the basic versions, which are more elaborate. Depending on the type of network, how time is treated and involved constraints, time-dependent shortest path problems can be categorized in several types:

(a) the basic TDSPP;

(b) the time-dependent quickest path problem (TDQPP);

(c) and other extensions of the TDSPP such as the time-dependent emissions minimizing path problem.

Throughout the following sections we present a comprehensive review of the related TDSPP literature. Specifically, we review the major contributions on the basic or dynamic TDSPP, some relevant studies on the time-dependent quickest path problem (TDQPP) and the main extensions of the TDSPP.

2.3.4.1 The basic time-dependent shortest path problem

The basic or dynamic TDSPP extends the classical SPP to the dynamic or time-dependent scenario where arc costs are updated at regular periods (Delling and Wagner 2007, Delling and Nannicini 2012). Obviously, the basic idea behind the TDSPP is to study the SPP in time-dependent networks through a more realistic scenario that takes into consideration traffic jams during rush hours (Delling and Wagner 2007).

Kaufman and Smith (1993) have principally considered the problem of individual route guidance in an intelligent vehicle-highway system, which corresponds to identifying the shortest paths in time-dependent networks. Under the FIFO consistency the time-dependent shortest path can be computed with exactly the same computational complexity as the SPP.

Based on the general Bellman's principle of optimality (Bellman 1958), Ziliaskopoulos and Mahmassani (1993) developed an efficient label-correcting shortest path algorithm that calculates a least time path from all nodes to a specific destination node in a time-dependent network. Their model does not satisfy the FIFO condition. With the aim of ensuring the FIFO dynamics, Sung et al. (2000) designed the FSM model where the flow speed of each arc dependent on the time slots. They showed that the computation of an optimal solution using FSM is easier than one based on LTM models.

Chabini (1998) studied three types of TDSPPs: the one-to-all fastest path problem departing from an origin node at a given time interval, the all-to-one shortest paths for all departure time intervals, and the one-to-all shortest path for all departure time intervals. In these problems, the cost of an arc is the travel time related to it. In addition, the components of arc costs can be of general form. An algorithm based on the concept of decreasing order of time was developed to solve these problems.

An alternative method for finding the shortest path in a time-dependent network is the A* goal-directed search algorithm (Hart, 1968). A* organizes the search toward the target by avoiding scans that are not in the direction of the target node. They either use a potential function $\pi : V \to \mathbb{R}$ on the arcs, which corresponds to a lower bound on the arc travel cost c_{ij} when traveling from node i to j. The classical A* search algorithm was extended by Chabini and Lan (2002) to find the shortest paths in time-dependent networks, in which arc travel costs are time-dependent.

Miller-Hooks and Yang (2005) extended the work of Pallottino and Scutella (2003) to case of the reoptimization of a least time path where future travel times in time-dependent networks change. Two reoptimization algorithms were developed. The first one is called the time-dependent least time path (TDLTP) that determines a minimum time path tree from all origins to a single destination for each departure time in a specific time period. The second one is called the Reverse Chrono-Shortest Path Tree (SPT) reoptimization algorithm, which can be viewed as a modified version of the original Chrono-SPT algorithm developed by Pallottino and Scutella (1998).

In Huang, Wu, and Zhan (2007), to solve the TDSPP the authors have proposed the Lifelong Planning A* (LPA*) algorithm to consider both the changing locations of the driver and changing traffic conditions in the road network. It is an incremental version of A* algorithm that can share the results in previous search levels (Koenig, Likhachev, and Furcy 2004).

Considering several related contributions on the TDSPP and its variants, we further summarize the main characteristics of the reviewed papers in Table 2.1, which presents the criteria used to classify them, namely, time-dependency, cost components, mathematical models, algorithmic methods and the type of benchmark instances. Time-dependency refers to the setting of the studied problem. Under a time-dependent network travel costs (TC) are time-dependent. Objective function can encompass several components such as distance (D), travel time (TT), carried load (CL) and emissions (E) or fuel consumption (FC). The benchmark instances can either be constructed randomly or using road network and traffic information.

As seen in Table 2.1 the TDSPP has been the subject of extensive research over the past years. An overview of the major variants of the TDSPP is given in the following sections.

2.3.4.2 The time-dependent quickest path problem

The time-dependent quickest (fastest) path problem (TDQPP) is a specific form of the TDSPP. It can be formulated as follows (Calogiuri, Ghiani, and Guerriero 2015).

Let $G = (V, A)$ be a graph, where V is the set of nodes and A is the set of arcs. Let $\tau_{ij}(t)$ denote a function designing the time that a vehicle takes to traverse an arc $(i, j) \in A$ when leaving at a specific starting time t. Assume that the travel time functions satisfies the FIFO condition. If the vehicle leaves an origin $o \in V$ to a destination $d \in V$ at time t then the traversal time $z_p(t)$ of a given path $p = (o = i_1, i_2..., i_k = d)$ can be defined recursively as below:

$$z_p(t) = z(p, t) = z((i_1, ..., i_{k-1}), t) + \tau_{ij}(t + z((i_1, ..., i_{k-1}), t)) \tag{2.14}$$

such that $z((i_1, i_2), t) = \tau_{i_1,i_2}(t)$.

The TDQPP aims to find a path p such that the traversal time $z_p(t)$ is minimum.

Solutions for determining quickest paths are crucial for the coordination and the planning of routing in dynamic time-varying road networks, where detailed and reliable real-time traffic information are available for some big cities (Calogiuri, Ghiani, and Guerriero 2015). This stimulated the design of multiple speedup techniques for the dynamic scenarios where the piecewise linear functions that are used to model time-dependent arc travel times or generalized cost variations over time.

Table 2.1: Classification of the papers on the TDQPP based on the solution methods

Reference	Time dependency	Cost components	Mathematical models	Algorithmic methods	Benchmarks (traffic on road networks)		
					Based on historical traffic data	GIS or real-life network	Randomly generated
Cooke and Halsey (1966)		TT		Adapted form of Bellman's (1959) iteration scheme using dynamic programming approach			
Dreyfus (1969)		D/TT/TC		Extensions of Dijkstra method			
Orda and Rom (1990)		D/TT/TC/W		Minimum-delay algorithms		✓	✓
Ziliaskopoulos and Mahmassani (1993)		D/TT/TC		Algorithm based on the Bellman's principle of optimality		✓	✓
Fu and Rilett (1998)		D/TC	Probability-based approximation models	Heuristic algorithm based on shortest path algorithm		✓	✓
Chabini (1998)		D/TT/W		Decreasing order of time (DOT) algorithm Three dynamic adaptations of label-correcting algorithms		✓	✓
Cheung (1998)		D/TT/TC		Variations of iterative label-correcting methods including Bellman's algorithm, the d-queue method, the two-queue method, the threshold methods and small-label-first principle			✓
Miller-Hooks and Mahmassani (2000)		D	Least expected travel time paths mathematical formulation	Label-correcting expected value (EV) algorithm			✓
Desaulniers and Villeneuve (2000)		TT/TC/W/TW	Nonlinear integer programming model Two-resource generalized SPP with resource constraints model	Adaptation of the dynamic programming algorithm of Ioachim et al. (1998)		✓	✓
Sung et al. (2000)	✓	TT		Modified Djikstra's label-setting shortest path algorithm			✓
Bander and White (2002)		D/TT/TC	Finite-horizon Markov decision process model	Dynamic programming approach using AO* (AND/OR) search heuristic		✓	✓
Chabini and Lan (2002)		D/TT/TC		Dynamic adaptation of the A* algorithm			✓
Pallottino and Scutella (2003)		TC	Linear programming model	Reoptimization algorithm using dual feasibility conditions and Dijkstrable subgraph			
Miller-Hooks and Yang (2005)	✓	D/TT/TC	Time-dependent dynamic Flow mathematical model	Time-dependent least time path (TDLTP) algorithm Reverse Chrono-SPT (Shortest Path Tree) Reoptimization algorithm		✓	✓
Kim, Lewis, and White (2005)		D/TT/TC/TW	Discrete time, finite horizon Markov decision processes mathematical model		✓	✓	✓
Huang, Wu, and Zhan (2007)		D/TT/TC		A*-algorithm-Lifelong Planning A* (A*-LPA*) Minimum bounded rectangle (MBR) constrained shortest path search		✓	✓

Table 2.1 (Continued)

Reference	Time dependency	Cost components	Mathematical models	Algorithmic methods	Benchmarks (traffic on road networks)		
					Based on historical traffic data	GIS or real-life network	Randomly generated
Nie and Wu (2009)		D/TT	Adaptive and a priori path model based on Frank (1969) optimal path formulation	Algorithm SPP with on-time arrival reliability (SPORTAR-LC)		✓	✓
Ziliaskopoulos, Mandanas, and Mahmassani (2009)		TT		Denardo and Fox label setting algorithm Hybrid shortest path (HPS) algorithm			✓
Bauer et al. (2010)		D/TT		Adaptation of Dijkstra's algorithm using hierarchical and goal-directed speed-up techniques			✓
Nannicini et al. (2012)	✓	D/TT/TC		Bidirectional search with A* using lower bounds on arc costs		✓	✓
Delling and Nannicini (2012)	✓	D/TT/TC		Core routing method combined with bidirectional goal-directed search with A*		✓	✓
Huang and Gao (2012)		D/TT	Multistage adaptive feedback control process formulation	Picard's method of successive approximation		✓	✓
Yang and Zhou (2014)		TT/TC	IOptimal path model based on disutility functions (linear or nonlinear)	Exact label-correcting complete dependency-path (CD-path) algorithm using minimum expected disutility (MED)			✓
Wen, Çatay, and Eglese (2014)	✓	D/TT/FC/TC		Modified Dijkstra's algorithm	✓	✓	✓
Qian and Eglese (2014)	✓	D/TT/FC/TC		DP method	✓	✓	✓
Calogiuri, Ghiani, and Guerriero (2015)	✓	TT		Unidirectional A* algorithm embedding a static and time-dependent lower bound		✓	✓
Ehmke, Campbell, and Thomas (2016a)	✓	D/TT/CL/E		Path-based sampling A*-based algorithm Arc-averaging time-dependent label setting algorithm	✓	✓	
Sun et al. (2017)		D/TT/TC		Heap-based Bellman-Ford algorithm for the Query FiST Extended Bellman-ford algorithm for Query BeST	✓	✓	
Di Bartolomeo et al. (2017)	✓	TT/TC		Branch-and-Bound Time Expanded Network			✓
Behnke and Kirschstein (2017)		D/TT/CL/E	Linear program	Dijkstra's algorithm Multigraph approach		✓	✓

Furthermore, efficient time-dependent hierarchical speedup techniques have been successfully applied to solve the static shortest path problems. These techniques were evolved to the time-dependent setting; such is the case of the works of Nannicini et al. (2008, 2012) which use A* bidirectional search as a speed-up technique for fast computation of point-to-point shortest paths on time-dependent road networks.

In Delling and Nannicini (2012) a core routing approach was combined with bidirectional goal-directed search to find a quickest path in large-scale time-dependent road networks. The insight behind core routing is to split the original network to generate new subnetwork (core graph) with a smaller number of nodes, thus reducing the search space.

To handle spatial travel time correlations in time-dependent network Yang and Zhou (2014) applied a Lagrangian relaxation-based solution approach. They also developed a modified label-setting algorithm and a branch and bound method to solve the TDQPP.

On the other hand, Calogiuri, Ghiani, and Guerriero (2015) studied the properties and bounds of time-dependent quickest path problems on a very large time-dependent road network. Using the FIFO travel time model proposed by Ichoua, Gendreau, and Potvin (2003), they prove that, if the congestion factors of all links are set to the lightest congestion factor during all time slots of the planning horizon, the TDQPP can be solved as a static QPP. A time-dependent lower bound on the time-to-target was developed which is both accurate and fast to compute. To efficiently solve the TDQPP Calogiuri, Ghiani, and Guerriero (2015) incorporated these bounds into an unidirectional A* algorithm.

Recently, Sun et al. (2017) generated time-dependent networks using traffic data to predict the travel times and to dynamically find a quickest path. By analyzing traffic networks characteristics of sparsity and hierarchy, they developed two algorithms to determine a quickest path: heap-based Bellman–Ford algorithms and extended Bellman (1958) label correcting algorithms.

2.3.4.3 The time-dependent emissions minimizing path problem

Green road freight transportation, aiming at reducing the harmful effects of transportation on the environment, has gained importance in recent years. In particular, an explicit consideration is given to reducing GHG emissions through better operational level of planning and decision-making (Eglese and Bektas 2014). In their work Wen, Çatay, and Eglese (2014) studied the minimum cost path in time-dependent network. The travel cost incorporates three components: congestion, fuel and driver costs. The speed is defined according to real traffic information and is not a decision variable. Two adaptations of the Dijkstra algorithm were proposed to solve the problem. These authors have also demonstrated that minimum cost paths may differ significantly from shortest paths in peak periods.

Ehmke, Campbell, and Thomas (2016a) studied the emissions-minimizing shortest paths in urban networks under congestion. Only emissions have been considered in their works and load assumptions for the case of full and empty truck load were used to find the emissions minimizing shortest paths reducing congestion charge. They proposed efficient adaptations of A* heuristic and label-setting algorithm to compute least emission paths.

Recently, Behnke and Kirschstein (2017) studied the impact of path selection in road networks depending on vehicle specifications and payload. In particular, they adjust Dijkstra's algorithm to calculate all emission minimizing paths for a given vehicle.

2.4 The green routing problem and its variants

Over the last decade numerous works have addressed VRP problems in the broader context of green logistics, and in particular the green vehicle routing (GVRP). By considering both operational and environmental constraints a new extension of the VRP with Time Windows (VRPTW) was introduced by Bektaş and Laporte (2011), the pollution routing problem (PRP).

Demir, Bektaş, and Laporte (2014b) have presented a review on the green road freight transportation focusing on factors affecting GHG emissions as well as microscopic and macroscopic models of fuel consumption. A study by Lin et al. (2014) provides a state of the art review on the GRVP in order to identify future research trends. Eglese and Bektas (2014) and Bektaş, Demir, and Laporte (2016) presented a review of the GVRP, focused mainly on the PRP which is a founding pillar of this new growing line of research. The main concern of this part of the chapter is to build on previous reviews on GVRP by focusing on the cost functions incorporated into the PRP models, routing decisions and resolution approaches. Section 2.4.1 presents a mathematical formulation for the PRP. Section 2.4.2 is devoted to review the major contributions on the GVRP and its variants. Specifically, we summarize heuristics and optimization methods applied to solve the GVRP.

2.4.1 Mathematical model for the pollution routing problem

The primary objective of PRP is to plan the trips of a fleet of vehicles while explicitly considering GHG emissions (Bektaş and Laporte 2011). The aim of this problem is to route a fleet of vehicles in order to serve a set of customers under time windows restrictions, and determining their speed along each route segment, so as to minimize a total cost function encompassing fuel, GHG emissions, and driver costs.

The PRP is defined on complete graph $G = (N, A)$ where $N = \{0, 1, 2, ..., n\}$ is the set of nodes and $A = \{(i, j)|i, j \in N, i \neq j\}$ is the set of arcs between each pair of nodes. The relevant notation used in the formulation of the PRP is listed below:

- 0, the depot;
- $N_0 = N \backslash \{0\}$, the set of customers;
- m, number of homogeneous vehicles based at the depot to serve the customers;
- d_{ij}, the distance from i to j;
- q_i, a non-negative demand of customer i;
- Q, the capacity limit of each vehicle;
- $[a_i, b_i]$, the time windows of service associated to customers i, arriving early at the nodes are allowed but vehicle has to wait until time a_i before service can start;
- t_i, the service time of customer i.

The approach taken in Bektaş and Laporte (2011) assumes that all parameters related to each arc inside a route will remain constant, except speed and load that can vary along each arc in a vehicle trip. When traveling across an arc (i, j) over a specific route each vehicle emits a certain amount of GHG. The amount of GHG emissions of vehicles is proportional to the amount of fuel consumed and is affected by a variety of key factors including load and speed, among others. In their comparative analysis of several emissions models Demir, Bektaş, and Laporte (2011) have shown that the rate of fuel consumption of heavy-duty vehicles is affected significantly by the payload or carried loads. The load of a vehicle is made up of empty load and carried loads.

Furthermore, along each arc (i, j) in the network the travel speed is constrained by a lower bound and an upper bound, denoted l_{ij} and u_{ij} respectively, often speed limits are imposed by road traffic regulations depending on the geographical area and the period of the day.

The PRP consists of designing a set R ($|R| \leq m$) of routes to serve a set of customers within preset time windows such that all vehicles depart from and return to the depot 0, and determining the speeds along each arc of the routes and departure times from each node so as to minimize an objective function encompassing fuel consumption, GHG emissions, and driver costs. In PRP each customer is visited once by a single vehicle that doesn't carry loads more than its capacity Q.

More specifically, Bektaş and Laporte (2011) have addressed four problems, all of which involve constructing routes for a homogeneous fleet of vehicles that must depart from and return to the depot 0, such that each vehicle serves a quantity of demand that does not exceed its capacity Q. Each problem has a different objective function. They are defined as follows:

(i) $\mathcal{C}_D$: a distance-minimizing objective function assuming constant speed on all arcs of the road network, which is the case of the classical VRPTW;

(ii) $\mathcal{C}_L$: a weighted load-minimizing objective function assuming constant speed on all arcs of the road network, which corresponds to the delivery problem with variable payload;

(iii) $\mathcal{C}_E$: an energy-minimizing objective function assuming speed as a decision variable;

(iv) $\mathcal{C}_C$: a cost-minimizing objective function comprising fuel, GHG emissions and driver's costs assuming variable speed and loads along each arc of the trips.

The objective function defined by Bektaş and Laporte (2011) is based on the Comprehensive Modal Emissions Model (CMEM) of Barth, Younglove, and Scora (2005), Scora and Barth (2006), Barth and Boriboonsomsin (2008), and Barth and Boriboonsomsin (2009) to estimate fuel consumption and GHG emissions for a given time instant. The CMEM is an extension of the model of Ross (1994) comprising three modules, namely engine power, engine speed and fuel rates. Further, the CMEM has two main characteristics (Bektaş and Laporte 2011, Demir, Bektaş, and Laporte 2014b, Bektaş, Demir, and Laporte 2016):

(i) it is one of the few microscopic models that take into account the change in the vehicle load as it travels;

(ii) it is also suitable to the GVRP when estimating heavy-duty vehicle GHG emissions as well as fuel consumption.

In their modeling approach Bektaş and Laporte (2011) assume that a vehicle carrying a total load $M = w + f_{ij}$ will travel at a constant speed v_{ij} on a given arc (i, j) of length d_{ij} with a road angle θ_{ij}. They propose to estimate GHG emissions according to the CMEM model using the following instantaneous fuel consumption or fuel use rate function (liter/second):

$$FR = \xi(kSV + P/\eta)/\varpi \tag{2.15}$$

where ξ is fuel-to-air mass ratio, k is the engine friction factor, S is the engine speed, V is the engine displacement, and a η and ϖ are constants. The parameter P represents the second-by-second engine power output (in kilowatt), and is determined by the following formula:

$$P = P_{tract}/\varepsilon + P_{acc} \tag{2.16}$$

where ε is the vehicle drive train efficiency, and P_{acc} is the engine power demand associated with running losses of the engine and the operation of vehicle accessories such as air conditioning. P_{acc} is assumed to be zero. The total tractive power requirements P_{tract} (in kilowatt) placed on the vehicle at the wheels is given by:

$$P_{tract} = (Ma + Mg\sin\theta + 0.5C_dA\rho v^2 + MgC_r\cos\theta)v/1000. \tag{2.17}$$

In the above expression M is the total vehicle weight (kilogram), v is the vehicle average speed (meter/second), a is the acceleration (m/s^2), θ is the road angle, g is the gravitational constant, and C_d and C_r are the coefficients of the aerodynamic drag and rolling resistance, respectively, ρ is the air density and A is the frontal surface area of the vehicle.

Recently, Dabia, Demir, and Van Woensel (2017) proposed a new mathematical formulation of the PRR using a set partitioning formulation as well as a branching rules. They describe the PRP as follows. Let Ω denote the set of feasible routes. A route is feasible if it satisfies both capacity constraint and time window restrictions. Each vehicle must depart from and return to the depot. Each customer is visited once by a single vehicle. A route is composed by the sequence of customers visited, the departure time at the depot D and the traveling speed v. For each route $p \in \Omega$, the parameters s_p and v_p denote the departure time at the depot and the traveling speed that lead to a least-cost route, respectively. Additionally, $e_p = \delta^p_{n+1}(s_p, v_p)$ represents the arrival time at the end depot. Furthermore, $c_p = c_d(e_p - s_p)_F(v_p)$ calculates the path's cost induced by the route duration and fuel consumption costs. The parameter σ_p indicates if node i is visited by route p is used. Finally, y_p is a binary variable equal to 1 if and only if route p is used in the solution. Thus, the PRP is formulated as a set partitioning problem:

$$\text{Minimize} \sum_{p\in\Omega} c_p y_p \tag{2.18}$$

subject to

$$\sum_{p\in\Omega} \sigma_{ip} y_p = 1,\ \forall i \in N \tag{2.19}$$

$$y_p \in \{0,1\},\ \forall p \in \Omega \tag{2.20}$$

where the objective function (2.18) minimizes the cost of the chosen routes. Constraints (2.19) guarantee that each node is visited exactly once. The authors propose to use a column generation method to solve the LP-relaxation of (2.18)-(2.20).

2.4.2 Contributions on the GVRP and its extensions

In this section, we concentrate our review on the major contributions on the GVRP and classify its extensions. The contributions are presented in chronological order. A detailed classification

of GVRP is presented on Table 2.2. Additionally, solution methods are summarized in Table 2.3.

In Table 2.2, time-dependency refers to the setting of the studied GVRP. It can either be static or time-dependent. Under a static network travel cost is fixed along each arc. Under a time-dependent network, the link travel cost is time-varying. Road network information can be used to explicitly consider path flexibility. Different cost structure can be used to better model the problem on hand, namely, distance, travel time, emissions, fuel consumption and driver costs. Finally, more classical VRP considerations can be included such as fleet composition which can be either homogeneous or heterogeneous, and the number of vehicles available may be fixed or unconstrained.

2.4.2.1 The bi-objective PRP

The PRP is a single-objective optimization problem where each component of the travel cost function is expressed in dollars and computed as a single objective metric. The reduction of time spent on a specific route can be achieved by traveling at a higher speed, at the expense of an increased fuel consumption and GHG emissions. Considering that the two objectives of minimizing fuel and driving time are conflicting, the PRP can be viewed as a multi-objective optimization problem. Hence, to address such an issue the bi-objective PRP was introduced by Demir, Bektaş, and Laporte (2014a).

The two conflicting objectives in the bi-objective PRP are fuel consumption and total driving time. The first one is similar to the fuel consumption objective modeled by Bektaş and Laporte (2011) and Demir, Bektaş, and Laporte (2012). The second one corresponds to the sum of the travel time across all routes starting and ending at the depot. To solve the bi-objective PRP, Demir, Bektaş, and Laporte (2014a) have developed an enhanced version of the ALNS algorithm as a search engine to determine a set of non-dominated solutions.

2.4.2.2 The fleet size and mix PRP

Available research on GHG emission and fuel consumption models (Demir, Bektaş, and Laporte 2011, 2014b) shows the significant impact that the vehicle type has on fuel consumption. Sometimes, routing smaller light-duty vehicles can increase the total distance traveled and may also increase GHG emissions. In their study Kopfer, Schönberger, and Kopfer (2014) point out that using multiple vehicles of different types may reduce in some case the amount of GHG emissions.

Table 2.2: Classification of contributions on GVRP and its variants

Reference	Problem	Objectives	Time-dependency	Path flexibility	Fleet composition	Routing decisions	Cost components	Mathematical modeling approaches
Bektaş and Laporte (2011)	PRP	- Distance-minimization - weighted-load minimization - energy minimization - cost minimization			Homogeneous	- speed - payload - time windows - service time - number of vehicles	- distance - GHG emissions - fuel consumption - driver	- Analytical model - Integer linear programming model
Demir, Bektaş, and Laporte (2012)	PRP	- Distance minimization - weighted-load minimization - energy minimization - cost minimization - speed optimization			Homogeneous	- speed - payload - time windows - service time, - number of vehicles	- distance - GHG emissions - fuel consumption - driver	- Analytical model - Integer linear programming model
Franceschetti et al. (2013)	TDPRP	- Distance minimization - weighted-load minimization - energy minimization - cost minimization - speed optimization - departure time optimization	✓		Homogeneous	- speed - payload - time windows - service time, - number of vehicles - congestion profiles - driver wages/waiting	- distance - GHG emissions - fuel consumption - driver - congestion	- Analytical model - Integer linear programming model
Demir, Bektaş, and Laporte (2014a)	Bi-objective PRP	- minimization of fuel consumption - minimization of driving time			Homogeneous	- speed - payload - time windows - service time, - number of vehicles	- distance - GHG emissions - fuel consumption - driver	- Analytical model - Integer linear programming model
Tajik et al. (2014)	PRP-PD	- Distance minimization - weighted-load minimization - energy minimization - cost minimization			Homogeneous	- speed (more than 20 km/h) - payload - time windows - service time, - number of vehicles - driver wages - pickup and delivery	- distance - GHG emissions - fuel consumption - driver	- Analytical model - Integer linear programming model
Koç et al. (2014)	Fleet size/mix PRP	- Distance minimization - weighted-load minimization - energy minimization - cost minimization			Heterogeneous	- speed (more than 20 km/h) - payload - time windows - service time, - number of vehicles - driver wages - type of vehicles (size/mix)	- distance - GHG emissions - fuel consumption - driver	- Analytical model - Integer linear programming model
Kramer et al. (2015b,a)	PRP with flexible departure times	- cost minimization - speed optimization - departure time optimization			Homogeneous	- speed (more than 20 km/h) - payload - time windows - service time, - driver wages - departure time/waiting	- distance - GHG emissions - fuel consumption - driver	- Analytical model - Set partitioning model
Xiao and Konak (2016)	HGVRSP	- Distance minimization - weighted-load minimization - energy minimization - cost minimizing	✓		Heterogeneous	- speed - payload - time windows - service time, - number of vehicles - type of vehicles (size and mix) - driver wages - congestion profiles - departure time/waiting	- distance - GHG emissions - fuel consumption - driver - congestion	- Analytical model - Mixed-integer programming model

Table 2.2 (Continued)

Reference	Problem	Objectives	Time-dependency	Path flexibility	Fleet composition	Routing decisions	Cost components	Mathematical modeling approaches
Suzuki (2016)	Practical PRP	- weighted-load minimizing objective - energy minimization			- Homogeneous - HDV	- payload - number of vehicles - driver wages	- distance - GHG emissions - fuel consumption - driver	- Analytical model - Mixed-integer programming model
Qian and Eglese (2016)	TDVRP-EM	- Distance minimization - energy minimization	✓	✓	Homogeneous	- speed - payload - time windows - service time, - number of vehicles - driver wages/arrival times	- distance - GHG emissions - fuel consumption - driver	- Analytical model - Set partitioning model
Ehmke, Campbell, and Thomas (2016b)	TDVRP-EM	- weighted-load minimization - energy minimization - cost minimization	✓	✓	Homogeneous	- speed - payload - time windows - service time, - number of vehicles - driver wages/arrival times	- distance - GHG emissions - fuel consumption - driver	- Analytical model
Dabia, Demir, and Van Woensel (2017)	PRP	- Distance minimization - weighted-load minimization - energy minimization - cost minimization			Homogeneous	- speed (more than 20 km/h) - payload - time windows - service time, - number of vehicles - driver wages/arrival times	- distance - GHG emissions - fuel consumption - driver	- Analytical model - Set partitioning model
Franceschetti et al. (2017a)	TDPRP	- Distance minimization - weighted-load minimization - energy minimization - cost minimization	✓		Homogeneous	- speed - payload - time windows - service time, - number of vehicles - driver wages/arrival times	- distance - GHG emissions - fuel consumption - driver	- Analytical model
Huang et al. (2017)	TDVRP-PF	- Distance minimization - weighted-load minimization - energy minimization - cost minimization	✓	✓	Homogeneous	- speed - payload - time windows - service time, - number of vehicles - driver wages/arrival times	- distance - GHG emissions - fuel consumption - driver	- Mixed integer program - Stochastic mixed integer program
Androutsopoulos and Zografos (2017)	BTL-VRPTW	- Distance minimization - weighted-load minimization - energy minimization - cost minimization	✓	✓	Homogeneous	- speed - payload - time windows - service time, - number of vehicles - driver wages/arrival times	- distance - GHG emissions - fuel consumption - driver	- Analytical model - Set partitioning model

Table 2.3: Organization of contributions on the GVRP based on solution methods

Reference	Branch-and-cut	Branch and price	Set partitioning	RVND	ALNS	ILS	INS	SOA	DSOP	SD-TOA	Column generation	Label-setting algorithm	Multigraph
Bektaş and Laporte (2011)	✓												
Demir, Bektaş, and Laporte (2012)	✓				✓			✓					
Franceschetti et al. (2013)	✓								✓				
Demir, Bektaş, and Laporte (2014a)					✓			✓					
Tajik et al. (2014)	✓				✓			✓					
Koç et al. (2014)					✓			✓					
Kramer et al. (2015a)			✓	✓		✓		✓					
Kramer et al. (2015b)				✓		✓				✓			
Suzuki (2016)							✓						
Xiao and Konak (2016)							✓						
Qian and Eglese (2016)			✓								✓		
Ehmke, Campbell, and Thomas (2016b)												✓	
Dabia, Demir, and Van Woensel (2017)		✓	✓								✓		
Franceschetti et al. (2017a)					✓				✓				
Huang et al. (2017)												✓	✓
Androutsopoulos and Zografos (2017)												✓	✓

ALNS: *Adaptive Large Neighborhood Search*; DSOP: *Departure Time and Speed Optimization Problem*; ILS: *Iterated Local Search*; INS: *Iterated Neighborhood Search*; RVND: *Randomized Variable Neighborhood Descent*; SD-TOA: *Speed and Departure-time Optimization Algorithm*; SOA: *Speed Optimization Algorithm.*

Koç et al. (2014) have introduced the fleet size and mix PRP which extends the PRP by considering the decision of the choice of the vehicle to use within a heterogeneous fleet of vehicles. The aim of the FSMPRP is to determine a set of routes for a heterogeneous fleet of vehicles that meet the demands of all customers within their respective time window restrictions. Thus, the objective is to minimize a total cost function incorporating vehicle, driver, fuel and GHG emissions costs. Koç et al. (2014) have studied three types of vehicles, namely light duty, medium duty and heavy-duty.

2.4.2.3 The time-dependent green vehicle routing problem

The TDPRP was introduced first by Franceschetti et al. (2013). The objective of the TDPRP is to construct a set of routes that meet the demands of all customers within their respective predefined time windows, starting and ending at the depot, and determine the speeds on each arc of the routes as well as the departure times from each node so as to minimize a total cost function encompassing vehicles, driver fuel, emissions and congestion costs (Franceschetti et al. 2013). Recently, Xiao and Konak (2016) considered a heterogeneous fleet of vehicles in the context of Green VRSP with time-dependent traffic congestion schemes.

Time-dependent routing considering dynamic paths and GHG emissions amounts to design optimal routes in a large road network in which link traversal times may vary over time. The incorporation of time-dependent optimization approaches into the Quickest Path Problem (QPP) and the Pollution Routing Problem (PRP) makes them more realistic and effective, because they account for speed variability and congestion patterns which are almost always present in urban areas. Slightly different from the classical GVRP, some have worked on the paths connecting two customers. Many studies have dealt with emission-minimizing paths between customers in vehicle routing (Ehmke, Campbell, and Thomas 2016a, Qian and Eglese 2016, Wen, Çatay, and Eglese 2014). These applied the Methodology for Estimating Emissions from Transport (MEET) (Hickman et al. 1999) to calculate GHG emissions which does not explicitly take the changing weight of the carried load into account. Ehmke, Campbell, and Thomas (2016b) proposed an emissions-minimizing model that explicitly accounts for the path finding problem between stops. The majority of paths between customers are pre-computed in advance using path averaging and approximation method. However, none of these works considered the effects of flexible departure times or waiting at depot and traffic conditions on both emissions and costs.

Androutsopoulos and Zografos (2017) deal explicitly with the trade-offs between travel time and emissions considering time-varying traffic conditions. Focusing on a bi-objective time, load and path dependent vehicle routing problem, they proposed an Ant Colony System algorithm to enhance capacity-feasible routes with a routing method that considers simultaneously routing and path finding decisions on multigraph (Garaix et al. 2010).

2.5 Discussion and direction for future research

The results of the previous works show that the traditional objectives consisting of only travel times do not necessarily imply the minimization of either fuel or driver costs, and that least cost solutions do not imply a GHG emissions-optimal solution. Indeed, there is a gap in the PRP research area related to the integration of GHG emissions models into TDQPP. Few papers have addressed path flexibility and GHG emissions-minimized paths. The exceptions are the works of Wen, Çatay, and Eglese (2014), Ehmke, Campbell, and Thomas (2016a,b), Qian and Eglese (2016) and Huang et al. (2017). As a direction for future research, more comprehensive objective functions can be considered to capture and minimize the cost of GHG emissions and fuel consumption along with operational costs considering time-varying speeds on the underlying road network. Based on the above reasoning, future work could model a more comprehensive cost objective function which measures and minimizes the cost of GHG emissions along with the operational costs of drivers and fuel consumption, and perform the analysis of time-dependent travel cost lower and upper bounds on time to destination. Also, finding the path with the overall minimum cost can be considered as an additional issue to the above-mentioned class of papers and take into account a time-dependent cost associated to each arc which depends on the arrival time at each visited nodes.

Considering that vehicle speeds vary according to time-dependent congestion patterns, the objective is to minimize the total travel cost function encompassing driver and GHG emissions costs while respecting capacity constraints and service time windows. Costs are based on driver wages, GHG emissions and fuel consumption, which in turn depends on multiple factors, such as travel distance, load carried and speed variations. Further, the underlying physical sub-network between two clients for each shipment is explicitly considered to determine road paths between any pair of customers (Qian and Eglese 2016, Huang et al. 2017). Nowadays, with the availability of historical traffic data obtained from real-world transportation applications and shipments data provided by the supply chain partners, more comprehensive routing constraints can be embedded, such as traffic congestion schemes, speed variability and environmental impacts. Path choice decisions complement routing ones, impacting the overall cost, GHG emissions, the travel time between nodes, and thus the set of a feasible time-dependent least cost (cheapest) path. Therefore, accounting for and avoiding congested road paths is possible as the required traffic data is easily available and, at the same time, has a great potential for both energy and cost savings (Kok, Hans, and Schutten 2012, Ehmke, Campbell, and Thomas 2016a). Omitting time-dependent settings and paths flexibility in routing decisions might lead to overtime and missed deliveries (Kok, Hans, and Schutten 2012, Dabia et al. 2013, Ehmke, Campbell, and Thomas 2016b, Huang et al. 2017). In particular, methods like multigraph (Ben Ticha et al. 2018) would seem appropriate for the case of the time-dependent version with dynamic paths.

With the real-time traffic information collected as well as the historical data provided by

traffic systems, numerous studies have been conducted mainly on routing through a time-independent road networks (Calogiuri, Ghiani, and Guerriero 2015). This stimulated the design of a number of efficient solution algorithms for the time-dependent scenarios where piecewise linear functions are used to model time-dependent arc traveling speed or generalized cost variations over time. Solutions for determining the expected quickest paths are crucial for the coordination and the planning of routing and could be enhanced with the availability of real-time traffic information for some big cities. Further, there have been a few works that explicitly address the question of emission estimations in time-dependent routing with road network information. A promising extension is to study and design effective emission models using big data analytic techniques such as machine learning may uncover additional potential for enhancing scheduling in time-dependent routing.

Chapter 3

Time-Dependent Quickest Path Problem with Emission Minimization

Résumé

En tant que principal contributeur aux émissions de gaz à effet de serre (GES) dans le secteur du transport, le transport routier de marchandises est au centre de nombreuses stratégies pour lutter contre la pollution accrue. Une façon de réduire les émissions est de considérer la congestion et d'être en mesure d'acheminer le trafic autour d'elle. Dans ce chapitre, nous avons étudié le problème du chemin le plus rapide dépendant du temps avec la minimisation des émissions (TDQPP-EM), dans lequel la fonction objectif prend en compte les coûts des émissions de GES, du conducteur et de congestion. Les coûts de déplacement sont affectés par le trafic en raison de la variation des niveaux de congestion en fonction de l'heure de la journée, des types de véhicules et de la charge transportée. Nous avons développé également des bornes inférieures et supérieures dépendant du temps, qui sont à la fois précises et rapides à calculer. Des expérimentations numériques ont été effectuées sur des instances qui intègrent la variation du trafic tout au long de la journée, en utilisant trois adaptations de l'algorithme de Dijkstra. Nous avons montré que la prise en compte des vitesses variables dans le temps apporte des améliorations substantielles par rapport à des vitesses fixes. Nos résultats de calcul démontrent que contrairement au TDQPP, l'obtention de la solution optimale se fait plus difficilement dans le cas du TDQPP-EM, mais les algorithmes proposés sont robustes et efficaces pour réduire le coût total même pour les grandes instances.

Chapter information A research paper based on this chapter, named *Time-Dependent Quickest Path Problem with Emission Minimization*, has been submitted to the journal Transportation Science by Heni H., Coelho L. C., and Renaud J. in September 2017.

Abstract

As the largest contributor to greenhouse gas (GHG) emissions in the transportation sector, road freight transportation is the focus of numerous strategies to tackle increased pollution. One way to reduce emissions is to consider congestion and being able to route traffic around it. In this paper we study the time-dependent quickest path problem with emission minimization (TDQPP-EM), in which the objective function comprises GHG emissions, driver and congestion costs. Travel costs are impacted by traffic due to changing congestion levels depending on the time of the day, vehicle types and carried load. We also develop time-dependent lower and upper bounds, which are both accurate and fast to compute. Computational experiments are performed on real-life instances that incorporate the variation of traffic throughout the day, by using three adaptations of the Dijkstra's label-setting algorithm. We show that considering time-varying speeds provides substantial improvements over the one based only on fixed speeds. Our computational results demonstrate that contrary to the TDQPP, the TDQPP-EM is more difficult to solve to optimality but the proposed algorithms are shown to be robust and efficient in reducing the total cost even for large instances.

Keywords: time-dependent networks; congestion; emission; quickest path; label-setting algorithm.

3.1 Introduction

Road freight transportation is a significant contributor to greenhouse gas (GHG) emissions (Demir, Bektaş, and Laporte 2014b). This is mostly driven by increased traffic congestion due to the high number of vehicles on urban areas. When traveling in cities, fuel consumption and GHG emissions are highly affected by speed levels depending on paths used by vehicles. To reduce the emissions intensity and environmental pollution caused by road freight transportation activities, new alternative planning and coordination strategies directly related to routing and scheduling operations are required for both operational and environmental considerations (Savelsbergh and Van Woensel 2016, Franceschetti et al. 2017b).

Many works have demonstrated the importance of speed in minimizing travel costs. Most of the existing research assumes that trucks can travel at the emissions-minimizing speed, which largely ignores the effect of congestion, notably in urban areas. In this work we introduce and solve a new variant of both the classical time-dependent quickest path problem (TDQPP) of Calogiuri, Ghiani, and Guerriero (2015) and the time-dependent emissions-minimizing path problem of Ehmke, Campbell, and Thomas (2016a) which we call the Time-Dependent Quickest Path Problem with Emission Minimization (TDQPP-EM). Here, the cost of an arc depends not only on distance but also on fuel consumption (the rate of GHG emissions) and on driver costs, which are all affected by speed variation. The overall objective is to determine a least cost path based on a time-dependent network with time-varying speeds. With data obtained for Québec City, we test our algorithms on a large road network with real traffic data. We adapt Dijkstra's label-setting algorithm to account for time-dependent traffic and our comprehensive objective function, and we compute lower and upper bounds on the overall cost taking into account the time-dependent context.

By conducting extensive experiments, we show that GHG emissions, fuel consumption as well as cost savings can be achieved through the fast computation of point-to-point least cost paths using a comprehensive objective function composed of GHG emissions, fuel and driver costs, instead of the traditional distance-minimizing and least time path objectives of the TDQPP.

This paper makes several important contributions to the literature:

- we introduce the TDQPP-EM a variant of the minimum-cost path across time-dependent network, where arc costs are time-dependent and are evaluated by explicitly considering GHG emissions and fuel consumption as parts of the cost components. It takes into account the variability of both emissions and costs considering time-varying speeds across each arc of the underlying road network;
- we prove that, under the first-in, first-out (FIFO) property, a least cost path obtained by ignoring traffic congestion can be no worse than an optimal path cost according to the heaviest congestion factor applied to all arcs at each time interval;

- we propose an efficient method to obtain tight time-dependent bounds, reducing the computational burden, and investigate when it is important to incorporate the load carried by the vehicle and traffic congestion factors into the lower and upper bounding algorithms;
- we propose an effective approach for computing travel cost and GHG emissions in time-dependent networks under the FIFO dynamic. This ensures that our solution methods account for the impact of speed variations on the optimization of a chosen path;
- finally, we adapt Dijkstra's time-dependent label-setting algorithm to solve the TDQPP-EM.

The remainder of the paper is organized as follows. Section 4.2 provides a literature review of the TDQPP and closely related problems. In Section 3.3, we provide a formal description of TDQPP-EM, and present some properties of the TDQPP-EM. Section 3.4 describes the proposed lower and upper bounds on the cost. Section 3.5 is devoted to extending the dynamic Dijkstra's label-setting algorithm, incorporating our lower and upper bounds on that algorithm. In Section 4.5, we give details on the benchmarks created from the Québec metropolitan area and validate the performance of our algorithms providing a detailed experimental evaluation. Our conclusions are presented in Section 4.6.

3.2 Literature review

The TDQPP-EM is a problem in the field of green road freight transportation (Demir, Bektaş, and Laporte 2014b), and more specifically close to the pollution-routing problem (PRP) (Bektaş and Laporte 2011). A number of recent contributions on the PRP have addressed both operational and GHG emissions-related objectives (Demir, Bektaş, and Laporte 2014a, Franceschetti et al. 2017b).

Most of these contributions consider the shortest path between each pair of customers as fixed. Time-dependent shortest path problems (TDSPPs) have been studied in most cases in the context of other objectives, such as determining Quickest Path (QP) (Delling and Nannicini 2012, Calogiuri, Ghiani, and Guerriero 2015), least emissions path (LEP) (Ehmke, Campbell, and Thomas 2016a,b) and least cost path (LCP) (Di Bartolomeo et al. 2017). The TDQPP-EM is an extension of the TDQPP considering a time-dependent travel cost and can be seen as a variant of the minimum-cost path problem (MCPP) over time-dependent networks, which is NP-hard as stated in Orda and Rom (1991) and Dean (2004b) and demonstrated by Di Bartolomeo et al. (2017). Since the TDQPP-EM is a special case of the MCP which aims to find the least travel cost path over time-dependent networks considering a cost function encompassing GHG emissions and driver costs, then it is also $\mathcal{NP}$-hard. Polynomial-time

algorithms for the TDQPP can be adapted to solve MCP (Dean 2004b, Brodal and Jacob 2004, Dehne, Omran, and Sack 2012).

In what follows, we review contributions on the TDQPP in Section 3.2.1 and on the time-dependent emissions-minimizing path problem in Section 3.2.2.

3.2.1 The time-dependent quickest path problem

A large part of the literature dealing with shortest paths on time-dependent networks aims at finding a path with the least travel time, also known as the TDQPP. This problem has been first introduced by Cooke and Halsey (1966). The classical Dijkstra's label-setting algorithm can be used to determine quickest paths in time-dependent networks, in which the FIFO property was implicitly considered as it is consistent with the requirements imposed by real transportation networks. Under FIFO dynamics the TDQPP can be solved optimally and efficiently in polynomial time by adapting any label-setting shortest path algorithm (Dean 2004a).

Moreover, many existing works have not explicitly considered whether the FIFO assumption holds (Miller-Hooks and Yang 2005, Ehmke, Campbell, and Thomas 2016a), making shortest path algorithms very unstable. Sherali, Hobeika, and Kangwalklai (2003) show that a network with a single non-FIFO arc yields a TDQPP algorithm which can no longer be solved in polynomial time.

With the aim of ensuring that the time-dependent network is consistent with the FIFO dynamics, Sung et al. (2000) proposed the flow speed model (FSM) in which the flow speed of each arc depends on the time period. They developed a solution method based on Dijkstra's label-setting algorithm and showed that the computation of an optimal solution using the FSM is easier than the one based on the link travel time model (LTM). In fact, the LTM does not guarantee the FIFO rule as the arc travel time changes as the period changes. The determination of quickest paths with LTM requires some additional steps to ensure the FIFO dynamics by eliminating potential cycles if waiting at nodes is not allowed (Miller-Hooks and Yang 2005) and deriving a travel time function satisfying the non-passing consistency (Fleischmann, Gietz, and Gnutzmann 2004). Recently, Yang and Zhou (2014) proposed a branch and bound method to solve the TDQPP in a space-time network by defining time-dependent nodes based on the departure and arrival times at each physical node.

Ichoua, Gendreau, and Potvin (2003) proposed a time-dependent speed model that respects the FIFO dynamics. The main point of their model is that the speed of each arc depends on the period. Hence, the speed across each arc changes when the boundary between two consecutive time intervals is crossed. Later, Van Woensel et al. (2008) proposed a queuing approach to capture traffic congestion and model travel times. A study by Kok, Hans, and Schutten (2012) proposed a speed model that satisfies the FIFO property to reflect traffic

congestion in real road networks.

A best-first search heuristic for the fast computation of quickest path in a time-dependent network is the A* goal-directed search algorithm (Hart, Nilsson, and Raphael 1968). A* can be seen as an efficient adaptation of Dijkstra's algorithm that determines a quickest path on time-dependent networks using time-to-destination lower bounds satisfying the FIFO property.

Ghiani and Guerriero (2014a) proposed an effective lower bound for the quickest path problem, which was embedded into an A* algorithm. Calogiuri, Ghiani, and Guerriero (2015) studied the properties and bounds of TDQPP. Using the time-dependent speed model of Ichoua, Gendreau, and Potvin (2003), they prove that under the FIFO assumption, if the congestion factors of all links are set to the lightest congestion factor, the TDQPP can be solved as a QPP with suitable-defined fixed travel times. We extend this development to the context of our paper.

3.2.2 Time-dependent pollution-routing and emissions-minimized paths

Demir, Bektaş, and Laporte (2014b) provided a review of several fuel consumption models including the MEET (Methodology for Calculating Transportation Emissions and Energy Consumption) developed by (Hickman et al. 1999) and the CMEM (Comprehensive Modal Emissions Model) designed by Barth and Boriboonsomsin (2008) and Barth and Boriboonsomsin (2009), among others. Note that, CMEM considers the impact of vehicle load on fuel consumption. However, MEET uses a load correction factor to take the vehicle load into account when computing fuel consumption.

Bektaş and Laporte (2011) introduced the pollution-routing problem. Based on the comprehensive modal emissions model (CMEM), they minimize GHG emissions by determining the optimal speed with respect to the load carried by the vehicle, fuel consumption and driver induced costs. Later, Demir, Bektaş, and Laporte (2012) extend it by applying a speed optimization algorithm, identifying the optimal speed on each arc in order to minimize the expected costs of fuel consumption and driver wages.

Jabali, Van Woensel, and de Kok (2012) studied the Emission Vehicle Routing Problem (EVRP), which uses the MEET to derive the GHG emissions. However, this study ignores the load when calculating the emissions. Focusing on the analysis of time-dependent costs as a function of speed, load and fuel consumption, Franceschetti et al. (2013) extended the PRP to a time-dependent setting using the time-dependent travel time model of Jabali, Van Woensel, and de Kok (2012). Recently, Franceschetti et al. (2017b) developed a metaheuristic approach to solve the PRP under congestion, which integrates departure time and speed optimization procedures.

In Wen and Eglese (2015), the authors solve the vehicle routing problem (VRP) with time-

dependent speeds, where the total cost involves fuel cost, driver cost and congestion charge. Their model is based on MEET and the impact of vehicle load is not considered. In their work, fixed congestion charges are applied once per day for each vehicle.

The results of the previous works show that the traditional objectives consisting of only travel times do not necessarily imply the minimization of either fuel or driver costs, and that least cost solutions do not imply an GHG emissions-optimal solution. Indeed, there is a gap in the PRP research area related to the integration of GHG emissions models into TDQPP. Few papers have addressed path flexibility and GHG emissions-minimized paths. The exceptions are the works of Wen, Çatay, and Eglese (2014), Ehmke, Campbell, and Thomas (2016a,b), Qian and Eglese (2016) and Huang et al. (2017). Following these works, we assume that vehicles must travel at the speed of traffic and do not have the ability to control their speed in a way that minimizes costs. Additionally, we consider that in time-dependent networks, congestion patterns are variable across each segment. Our goal is to model a more comprehensive objective function which captures and minimizes the cost of GHG emissions and fuel consumption along with operational costs considering time-varying speeds on the underlying road network.

3.3 Formal description and problem statement

In this section, we introduce our notation, give a formal definition for the TDQPP-EM and describe some of its properties. Let $\mathcal{G} = (\mathcal{V}, \mathcal{A}, \mathcal{Z}, \mathcal{S})$ be a directed time-dependent network, where $\mathcal{V}$ is the set of nodes, and $\mathcal{A} \subseteq \{(i,j) \in \mathcal{V} \times \mathcal{V}, i \neq j\}$ is a set of arcs. The number of nodes and arcs are $|\mathcal{V}| = n$ and $|\mathcal{A}| = m$. We assume that $\mathcal{G}$ is strongly connected, thus, there is a path from every node to all other nodes. The time-dependent network is considered at a set of discrete times $\mathcal{Z} = \{t_0, t_0 + \delta ..., t_0 + H\delta\}$, with $\delta > 0$ being the smallest increment of time over which a change in the congestion pattern occurs. The time horizon T is divided into H time slots $Z_h = [z_h, z_{h+1}[$, such that $z_h = t_0 + h\delta$, where $h = 0, 1, 2, ..., H-1$. Let $\mathcal{S} = \{s_{ij}^h\}$ represent the set of time-dependent arc travel speeds, where for each arc $(i,j) \in \mathcal{A}$ s_{ij}^h represents the travel speed value during the time slot Z_h. Hence, the travel speed of each arc is assumed to be dynamic for a particular traveler across any arc. We denote the distance between two nodes i, j as L_{ij}. Time-dependent travel times as well as costs vary for each departure time $t \in T$. With each arc (i,j) are associated two time-dependent functions which assign, respectively, travel time $\tau_{ij}(t)$ and travel cost $c_{ij}(t)$ related to the time at which a vehicle leaves node i. Travel time functions $\tau_{ij}(t)$ are piecewise linear and satisfy the FIFO property.

The speed at which a vehicle travels on arc (i,j) is constrained by a lower bound and an upper bound, denoted $\mathcal{L}_{ij}$ and $\mathcal{U}_{ij}$, respectively, usually imposed by traffic. A unit of GHG emitted (usually in kilograms) has an estimated cost c_e.

Given a starting time t the TDQPP-EM aims to determine a path $p = (o = v_0, ..., v_i, ..., v_j, ..., v_k =$

d) such that the time-dependent total cost $\varphi_p(t)$ between source $o \in \mathcal{V}$ and destination $d \in \mathcal{V}$ is minimum.

Following the FSM, when a vehicle traverses arc (i,j) of length L_{ij}, speed may change when the boundary between two consecutive time slots is crossed before reaching j. The arc travel time is then obtained by summing up the travel times used for each section traversed at different speeds. Hence, with FSM we assume that speed s_{ij}^h on arc (i,j) depends on time interval:

$$s_{ij}^h = \sigma_{ijh} u_{ij}, \tag{3.1}$$

where $\sigma_{ijh} \in [0,1]$ represents the congestion ratio of arc (i,j) in the time interval Z_h, and u_{ij} is the maximum speed of arc $(i,j) \in \mathcal{A}$ during the horizon T.

For a given arc (i,j) let l_{ij}^h denote the portion of the length L_{ij} traveled during time slot Z_h. Let h_t and h_γ be the indices of time slots where the start time $\gamma_i^p(t)$ at node i and the arrival time $\gamma_j^p(t)$ at node j belong to, respectively, with $h_t \in \{0, ..., H-1\}$ and $h_\gamma \in \{h_t, ..., H-1\}$. The travel time along an arc is the sum of three portions of time:

(i) The time associated with the first interval h_t: $z_{h_t+1} - \gamma_i^p(t)$.

(ii) The duration of the $(h_\gamma - h_t - 1)$ intermediate time intervals crossed when travelling along arc (i,j): $\sum_{h=h_t+1}^{h_\gamma - 1} (z_{h+1} - z_h)$, where $h = h_t + 1, ..., h_\gamma - 1$.

(iii) The time related to the last time slot when leaving the arc: $\gamma_j^p(t) - z_{h_\gamma}$.

Therefore, we can express the travel time of each arc as follows:

$$\tau_{ij}(\gamma_i^p(t)) = \begin{cases} L_{ij}/(\sigma_{ijh_t} u_{ij}) & \text{if } h_\gamma = h_t \\ \gamma_j^p(t) - \gamma_i^p(t) & \text{if } h_\gamma = h_t + 1 \\ (z_{h_t+1} - \gamma_i^p(t)) + (h_\gamma - h_t - 1)\,\delta + \left(\gamma_j^p(t) - z_{h_\gamma}\right) & \text{if } h_\gamma > h_t + 1. \end{cases} \tag{3.2}$$

The arrival time γ_j^p at node j is expressed as follows:

$$\gamma_j^p(t) = \begin{cases} L_{ij}/s^{h-1} + \gamma_i^p(t) & \text{if } L_{ij}/s^h < z_h - \gamma_i^p(t), h = h_t \\ (L_{ij} - l^{h-1})/s^h + z_h & \text{if } (L_{ij} - l^{h-1})/s^h < z_{h+1} - z_h, h \in \{h_t + 1, ..., h_\gamma\}, \end{cases} \tag{3.3}$$

where $l^{h_t - 1} = s^{h_t}(z_{h_t} - t)$ and $l^h = l^{h-1} + s^h(z_{h+1} - z_h)$ if $h \in \{h_t + 1, ..., h_\gamma\}$, and $L_{ij} = \sum_{h=h_t}^{h_\gamma} l^h$. Note that the traversal time $\Gamma_p(t)$ of a path p can be induced from the arrival time at the destination node d. Therefore, it is given by:

$$\Gamma_p(t) = \gamma_d^p(t) - t. \tag{3.4}$$

3.3.1 Time-dependent GHG emission and fuel consumption functions

Our modeling for emissions and fuel consumption follows the same approach applied in some relevant works, namely Bektaş and Laporte (2011), Demir, Bektaş, and Laporte (2012), Franceschetti et al. (2013, 2017b), Dabia, Demir, and Van Woensel (2017) and Huang et al. (2017), among others. According to these works GHG emissions are directly proportional to fuel consumption. We also use the CMEM to estimate the amount of fuel consumption and GHG emissions. The CMEM is a microscopic model that allows the consideration of vehicle specific parameters, such as engine speed, traffic related parameters, and environment related factors (Barth and Boriboonsomsin 2008, 2009). According to the CMEM the fuel use rate ($liter/s$) for a given time instant is a function encompassing travel speed, vehicle load and road gradient:

$$e_r = \frac{\zeta}{\varpi\psi}\left(kN_eV + \frac{1}{\varepsilon}\left(\frac{((w+q)(a+g\sin\theta+gC_r\cos\theta)+0.5C_dA\rho s^2)s}{1000\eta_{tf}} + P_{acc}\right)\right). \quad (3.5)$$

All required parameters with their typical values are described in Table 3.1. P_{acc} is the engine power demand for vehicle accessories in hp. We consider the default value of P_{acc}, which is zero. Using $\alpha = a + g\sin\theta + gC_r\cos\theta$, $\beta = 0.5C_dA\rho$, $\varsigma = \frac{1}{(1000\varepsilon\eta_{tf})}$ and $\lambda = \frac{\zeta}{\varpi\psi}$, and based on the assumption associated with values of used parameters, expression (3.5) can be rewritten as:

$$e_r = \lambda(kN_eV + \varsigma\alpha(w+q)s + \varsigma\beta s^3). \quad (3.6)$$

Table 3.1: Parameters used in the CMEM

Notation	Description	Typical values
w	Curb-weight (kg)	15000
q	Carried load (kg)	0-10000
ζ	Fuel-to-air mass ratio	1
k	Engine friction factor ($kJ/rev/liter$)	0.25
N_e	Engine speed (rev/s)	60
V	Engine displacement ($liter$)	7
g	Gravitational constant (m/s^2)	9.81
ρ	Air density (k/m^3)	1.2041
C_d	Coefficient of aerodynamic drag	0.7
A	Frontal surface area (m^2)	5
C_r	Coefficient of rolling resistance	0.01
η_{tf}	Vehicle drive train efficiency	0.4
η	Efficiency parameter for diesel engines	0.9
c_f	Fuel and GHG emissions cost per liter (\$CAD/$liter$)	1.05
c_d	Driver wage (\$CAD/s)	0.0085
ϖ	Heating value of a typical diesel fuel (kJ/g)	44
ψ	Conversion factor (g/s to $liter/s$)	737
s^l	Lower speed limit (m/s)	11.111
s^u	Upper speed limit (m/s)	19.444
s	Average speed at a portion of segment (m/s)	
a	Acceleration (m/s^2)	0
θ	Roadway gradient (degree)	0

Using only average speeds may not capture the average GHG emissions on a particular arc. In fact, CMEM computations taking into account only fixed speed are not often enough

accurate to reflect GHG emissions at peak hour traffic congestion considering fluctuating speed (Turkensteen 2017, Franceschetti et al. 2016). For example, if the travel speed on a path often drops far below the average speed, then the actual emissions may be much higher than if the trip occurs consistently at the average speed. Thus, to optimize GHG emissions in an urban area, one must explicitly consider the variability of the speed at different times of the day. Moreover, for a given arc (i, j) along a path p starting at time t (time slot Z_{h_t}), the corresponding fuel consumption can be expressed based on a combination of equations (3.6) and (3.2):

$$\mathcal{F}_{ij}(t) = f_{ij}(t) + g_{ij}(t), \tag{3.7}$$

where

$$f_{ij}(t) = \sum_{h=h_t}^{h_\gamma} \left[\left(\frac{l_{ij}^h}{s_{ij}^h} \right) \lambda \varsigma \alpha (w+q) s_{ij}^h \right] = \lambda \varsigma \alpha (w+q) \sum_{h=h_t}^{h_\gamma} l_{ij}^h = \lambda \varsigma \alpha (w+q) L_{ij}, \tag{3.8}$$

and

$$g_{ij}(t) = \sum_{h=h_t}^{h_\gamma} \left[\left(\frac{l_{ij}^h}{s_{ij}^h} \right) \lambda (k N_e V + \varsigma \beta (s_{ij}^h)^3) \right] = \lambda k N_e V \tau_{ij}(t) + \lambda \varsigma \beta \sum_{h=h_t}^{h_\gamma} l_{ij}^h (s_{ij}^h)^2. \tag{3.9}$$

For a departure time t and a path p, the total amount of fuel consumed can be calculated as follows based on equation (3.7):

$$\mathcal{F}_p(t) = \sum_{(i,j) \in p} \mathcal{F}_{ij}(\gamma_i^p(t)). \tag{3.10}$$

3.3.2 Time-dependent travel cost function

Given a departure time t, the driver cost incurred from path p can be calculated as the cost of the traversal time according to (3.4):

$$\varphi(\Gamma_p(t)) = c_d \Gamma_p(t). \tag{3.11}$$

On the basis of (3.8) the cost of GHG emissions on a given arc (i, j) across a path p can be calculated as $c_f \mathcal{F}_{ij}(t)$. Thus, fuel consumption cost (in \$) of path p is given by:

$$\varphi(\mathcal{F}_p(t)) = c_f \mathcal{F}_p(t). \tag{3.12}$$

As we know that the path's cost encompasses the traversal duration and fuel costs, the total cost of a path from o to d starting at time t can be expressed by combining equations (3.11) and (3.12) as follows:

$$\varphi_p(t) = \varphi(\Gamma_p(t)) + \varphi(\mathcal{F}_p(t)) = \sum_{(i,j) \in p} c_{ij}(\gamma_i^p(t)), \tag{3.13}$$

where

$$c_{ij}(\gamma_i^p(t)) = c_d\tau_{ij}(\gamma_i^p(t)) + c_f\mathcal{F}_{ij}(\gamma_i^p(t)). \tag{3.14}$$

Note that the cost $c_{ij}(\gamma_i^p(t))$ of traveling across arc (i,j) is expressed by combining equations (3.2) and (3.7).

An optimal path from source o to destination d given the starting time t is the path p_c^* with the least travel cost, denoted by $\varphi_{p_c^*}(t)$.

A mathematical programming formulation for the TDQPP-EM is presented in the Appendix A.

3.4 Time-dependent lower and upper bounds for the TDQPP-EM

When dealing with the TDQPP-EM, it is useful to compute the least cost lower and upper bounds. These bounds are useful to validate the accuracy of designed TDQPP-EM algorithms. Additionally, they can be embedded into a time-dependent search heuristics as best-first search that associate to each node i a label equal to the known travel cost at arrival time $\gamma_{v_i}^p(t)$ at the current node i plus a lower bound on the cost to the destination.

This section presents time-dependent lower and upper bounds for the TDQPP-EM that can be computed by ignoring the network-wide traffic congestion. Let $\mathcal{P}_\varphi$ be the set of all feasible paths of the TDQPP-EM on $\mathcal{G}$. Given a path $p \in \mathcal{P}_\varphi$, let $\Gamma(p)$ be the traversal time of p assuming (3.1) holds. We also denote by $\underline{\Gamma}(p)$ the traversal time of p if the congestion ratios of all arcs are set to the lightest congestion factor $\sigma_h = \max_{(i,j)\in\mathcal{A}}(\sigma_{ijh})$ for each time slot Z_h. Let $\Delta = \min_{ijh}(\frac{s_{ij}^h}{\sigma_h u_{ij}})$ be the heaviest degradation of congestion ratio of any arc (i,j) over the time horizon T. Finally, let $\underline{\underline{\Gamma}}(p)$ denote the duration of p if all s_{ij}^h are set to the speed limit u_{ij}. This is equivalent to assuming that all arc speeds become constant and the TDQPP and the TDQPP-EM are reduced to the QPP and to the QPP-EM, respectively. Let p^*, $\underline{p}^*$ and $\underline{\underline{p}}^*$ be optimal solutions of the TDQPP under the assumptions previously defined, i.e., $p^* = \arg\min_{p\in\mathcal{P}_\varphi}\{\Gamma(p)\}$, $\underline{p}^* = \arg\min_{p\in\mathcal{P}_\varphi}\{\underline{\Gamma}(p)\}$, and $\underline{\underline{p}}^* = \arg\min_{p\in\mathcal{P}_\varphi}\{\underline{\underline{\Gamma}}(p)\}$.

Given a path $p \in \mathcal{P}_\varphi$, let $\varphi(p)$ be its traversal cost, starting at time t. We also denote $\underline{\underline{\varphi}}(p)$ the traversal cost of p if all s_{ij}^h are set to the speed limit u_{ij}. Let p_c^* and $\underline{\underline{p_c}}^*$ be optimal solutions of the TDQPP-EM and QPP-EM, respectively, thus, $p_c^* = \arg\min_{p\in\mathcal{P}_\varphi}\{\varphi(p)\}$, and $\underline{\underline{p_c}}^* = \arg\min_{p\in\mathcal{P}_\varphi}\{\underline{\underline{\varphi}}(p)\}$.

Adopting $\underline{\underline{p}}^*$ as a heuristic solution of the TDQPP-EM under the speed variation relationship (3.1) presents multiple advantages. Firstly, efficient algorithms designed for the QPP can be

immediately applied to solve the TDQPP-EM. Secondly, if all arc speeds are set according to the maximum speed u_{ij}, then $\underline{\underline{p}}^*$ is a near-optimal solution for the TDQPP-EM. Indeed, in the following subsections we prove that $\varphi(\underline{\Gamma}(\underline{\underline{p}}^*)) + \varphi(\mathcal{F}(\underline{\underline{p}}^*, q_0, s^*)) \leq \varphi(p_c^*)$ is a lower bound on $\varphi(p_c^*)$ and that $\min\{\varphi(\underline{\underline{p_c}}^*), \varphi(p^*), \varphi(\underline{p}^*), \varphi(\underline{\underline{p}}^*)\} \leq \varphi(\underline{\underline{p}}^*)$ is its upper bound:

$$\varphi(\underline{\Gamma}(\underline{\underline{p}}^*)) + \varphi(\mathcal{F}(\underline{\underline{p}}^*, q_0, s^*)) \leq \varphi(\Gamma(p^*)) + \varphi(\mathcal{F}(\underline{\underline{p}}^*, q_0, s^*)) \leq \varphi(p_c^*) \leq \min\{\varphi(\underline{\underline{p_c}}^*), \varphi(p^*), \varphi(\underline{p}^*), \varphi(\underline{\underline{p}}^*)\} \leq \varphi(\underline{\underline{p}}^*) \leq \tfrac{1}{\Delta}\varphi(\Gamma(p_c^*)) + \varphi(\mathcal{F}(\underline{\underline{p}}^*)) \tag{3.15}$$

where $q_0 = 0$ is used to indicate empty load and $s^* = (\frac{kNV}{2\beta\varsigma})^{1/3}$ is the optimal speed which minimizes fuel consumption cost for any arc, which results from $\frac{\partial \mathcal{F}_{ij}}{\partial s_{ij}}(s^*) = 0$.

3.4.1 A lower bound on the cost $\varphi(p_c^*)$

We now demonstrate that $\varphi(\underline{\Gamma}(\underline{\underline{p}}^*)) + \varphi(\mathcal{F}(\underline{\underline{p}}^*, q_0, s^*)) \leq \varphi(p_c^*)$ is a lower bound on $\varphi(p_c^*)$ and that if the vehicle travels with the same load q at speed s^* that minimizes fuel consumption across all arcs, then $\underline{\underline{p}}^*$ is optimal for TDQPP-EM, that is, $\underline{\underline{p}}^* = \underline{\underline{p_c}}^*$.

Theorem 1 *Path $\underline{\underline{p}}^*$ is an optimal solution for the TDQPP-EM when the vehicle travels with constant load, and the speed for all arcs $(i,j) \in \mathcal{A}$ is set to $s^* = (\frac{kNV}{2\beta\varsigma})^{1/3}$, minimizing fuel consumption.*

Proof. Given a solution path $p_c \in \mathcal{P}_\varphi$ it follows from (3.13) that:

$$\varphi(p_c, q, s^*) = \varphi(\Gamma(p_c, s^*)) + \varphi(\mathcal{F}(p_c, q, s^*)). \tag{3.16}$$

From (3.11) it results that the travel time can be expressed as (3.17) and fuel consumption and GHG emissions cost can be defined as (3.18), based on (3.8), (3.9) and (3.13):

$$\varphi(\Gamma(p_c, s^*)) = c_d \Gamma(p_c, s^*), \tag{3.17}$$

$$\varphi(\mathcal{F}(p_c, q, s^*)) = c_f e_r(q, s^*) \Gamma(p_c, s^*), \tag{3.18}$$

where $e_r(q, s^*)$ is constant across all arcs of path p_c and represents the minimum fuel consumption rate. Combining (3.17) and (3.18) results in:

$$\varphi(p_c, q, s^*) = [c_d + c_f e_r(q, s^*)]\, \Gamma(p_c, s^*). \tag{3.19}$$

As the vehicle travels with load q at speed s^* across all arcs, the first part of the equation (3.19) $c_d + c_f e_r(q, s^*)$ is constant. Hence, the overall cost is minimum if the total travel time $\Gamma(p_c, s^*)$ of the path p_c is minimum. The minimum travel time is given by an optimal solution for the TDQPP, i.e., $\underline{\underline{p}}^*$. Hence, an implication of (3.19) is that the optimal path $p_c^* = \underline{\underline{p}}^*$, which completes the proof of Theorem 1.

Corollary 1.1 *Given two optimal paths $\underline{\underline{p}}^*$ and p_c^* (with respect to $\varphi(\underline{\underline{p}}^*)$ and $\varphi(p_c^*)$, respectively) for the TDQPP and the TDQPP-EM, respectively, the following relationship is satisfied:*

$$\varphi(\underline{\Gamma}(\underline{\underline{p}}^*)) + \varphi(\mathcal{F}(\underline{\underline{p}}^*, q_0, s^*)) \leq \varphi(p_c^*). \tag{3.20}$$

Proof. By observing that when the congestion ratios of all arcs are set to their lightest values $\sigma_h = \max_{(i,j)\in\mathcal{A}} (\sigma_{ijh})$ for each time interval Z_h it follows that the traversal time of a given path $p = (o = v_0, v_2, ..., v_k = d)$ starting a time $t = 0$ is

$$\underline{\underline{\Gamma}}(p) = \sum_{l=1}^{k} \frac{L_{v_{l-1}v_l}}{u_{v_{l-1}v_l}} = \sum_{l=1}^{k} \int_{t}^{t+\tau_{v_{l-1}v_l}(t)} \sigma(\gamma)d\gamma = \int_{t_0}^{\underline{\Gamma}(p)} \sigma(\gamma)d\gamma \tag{3.21}$$

where $\sigma(\gamma) = \sigma_h$. Furthermore, if we consider another path $p' \in \mathcal{P}_\varphi$, from (3.21) it follows that:

$$\underline{\underline{\Gamma}}(p') \leq \underline{\underline{\Gamma}}(p) \Leftrightarrow \underline{\Gamma}(p') \leq \underline{\Gamma}(p), \tag{3.22}$$

which implies that:

$$\underline{\Gamma}(\underline{\underline{p}}^*) = \underline{\Gamma}(\underline{p}^*). \tag{3.23}$$

As $\underline{p}^* = \arg\min_{p\in\mathcal{P}_\varphi} \{\underline{\Gamma}(p)\}$ and $\underline{\Gamma}(p_c^*) \leq \Gamma(p_c^*)$, from (3.23) it results that:

$$\underline{\Gamma}(\underline{\underline{p}}^*) \leq \Gamma(p_c^*). \tag{3.24}$$

Hence,

$$\varphi(\underline{\Gamma}(\underline{\underline{p}}^*)) \leq \varphi(\Gamma(p_c^*)). \tag{3.25}$$

If we consider the case of fixed speed s^* which minimizes the fuel consumption we may assert that:

$$\mathcal{F}(\underline{\underline{p}}^*, q_0, s^*) \leq \mathcal{F}(p_c^*). \tag{3.26}$$

Then the following relationship also holds:

$$\varphi(\mathcal{F}(\underline{\underline{p}}^*, q_0, s^*)) \leq \varphi(\mathcal{F}(p_c^*)). \tag{3.27}$$

Combining (3.26) and (3.27) yields:

$$\varphi(\underline{\Gamma}(\underline{\underline{p}}^*)) + \varphi(\mathcal{F}(\underline{\underline{p}}^*, q_0, s^*)) \leq \varphi(p_c^*), \tag{3.28}$$

which completes the proof of Corollary 1.1.

3.4.2 A worst-case analysis

In this subsection, we provide a worst case analysis on the cost $\varphi(\underline{\underline{p}}^*)$.

Theorem 2 *The value $\varphi(\underline{\underline{p_c}}^*)$ is an upper bound not greater than $\frac{1}{\Delta}\varphi(\Gamma(p^*)) + \varphi(\mathcal{F}(\underline{\underline{p}}^*))$.*

Proof. As p^*, $\underline{p}^*$, and $\underline{\underline{p}}^*$ are optimal solutions for the TDQPP, they are also feasible solutions for the TDQPP-EM. Additionally, $\underline{\underline{p_c}}^*$ is a feasible solution for the TDQPP-EM, then:

$$\varphi(p_c^*) \leq \varphi(p^*) \tag{3.29}$$

$$\varphi(p_c^*) \leq \varphi(\underline{p}^*) \tag{3.30}$$

$$\varphi(p_c^*) \leq \varphi(\underline{\underline{p}}^*) \tag{3.31}$$

$$\varphi(p_c^*) \leq \varphi(\underline{\underline{p_c}}^*). \tag{3.32}$$

By combining (3.29), (3.30), (3.31) and (3.32) we obtain the proof of the first part of the upper bound inequality:

$$\varphi(p_c^*) \leq \min\{\varphi(\underline{\underline{p_c}}^*), \varphi(p^*), \varphi(\underline{p}^*), \varphi(\underline{\underline{p}}^*)\} \leq \varphi(\underline{\underline{p}}^*) \tag{3.33}$$

Furthermore, if the congestion ratio σ_{ijh} takes a value in the interval $[\Delta\sigma_h, \sigma_h]$, then it results that for a given path p:

$$\underline{\Gamma}(p) \leq \Gamma(p) \leq \frac{1}{\Delta}\underline{\Gamma}(p). \tag{3.34}$$

Combining (3.33) and (3.34) yields:

$$\Gamma(\underline{\underline{p}}^*) \leq \frac{1}{\Delta}\Gamma(p^*) \leq \frac{1}{\Delta}\Gamma(p_c^*), \tag{3.35}$$

which implies that:

$$\varphi(\Gamma(\underline{\underline{p}}^*)) \leq \frac{1}{\Delta}\varphi(\Gamma(p^*)) \leq \frac{1}{\Delta}\varphi(\Gamma(p_c^*)). \tag{3.36}$$

Since $\varphi(\underline{\underline{p}}*) = \varphi(\Gamma(\underline{\underline{p}}^*)) + \varphi(\mathcal{F}(\underline{\underline{p}}^*))$, it follows that:

$$\varphi(\Gamma(\underline{\underline{p}}^*)) + \varphi(\mathcal{F}(\underline{\underline{p}}^*)) \leq \frac{1}{\Delta}\varphi(\Gamma(p_c^*)) + \varphi(\mathcal{F}(\underline{\underline{p}}^*)). \tag{3.37}$$

An implication of (3.37) is that $\varphi(\underline{\underline{p}}*)) \leq \frac{1}{\Delta}\varphi(\Gamma(p_c^*)) + \varphi(\mathcal{F}(\underline{\underline{p}}^*))$, which completes the proof of Theorem 2.

3.5 Design of efficient TDQPP-EM algorithms

In this section, we propose several heuristic algorithms that will be applied to efficiently solve the TDQPP-EM in polynomial time based on the FSM and the LTM. First, we present the algorithms used to compute arrival times, travel times and travel costs. Second, we present the time-dependent Dijkstra algorithm. Lastly, we describe speed-up methods for the fast computation of lower and upper bounds on path traversal costs.

3.5.1 Time-dependent arrival time and travel time computation

In the case of the FSM, during each time period Z_h the flow speed on each arc (i, j) is assumed to be constant. Given the set of speeds and a starting time $\gamma_i^p(t)$ at node i, both arrival time and travel time across arc (i, j) can be computed through Algorithm 3.1.

Algorithm 3.1 Computing the travel time $\tau_{ij}(\gamma_i^p(t))$ across a given arc (i, j) based on the FSM

function TRAVEL_TIME_FSM($\gamma_i^p(t)$, $(i, j), \mathcal{Z}, \mathcal{S}$)
  $h|\gamma_i^p(t) \in Z_h = [z_h, z_{h+1}[$
  $k \leftarrow h$
  $d \leftarrow L_{ij} - \left[s_{ij}^k(z_{k+1} - \gamma_i^p(t))\right]$
  while $d > 0$ **do**
    $k \leftarrow k + 1$
    $d \leftarrow d - \left[s_{ij}^k(z_{k+1} - z_k)\right]$
  end while
  $\gamma_j^p(t) \leftarrow z_{k+1} + d/s_{ij}^k$
  $\tau_{ij}(\gamma_i^p(t)) \leftarrow \gamma_j^p(t) - \gamma_i^p(t)$
  return $\tau_{ij}(\gamma_i^p(t))$
end function

In the case of the LTM the travel time of arc (i, j) is specified when departing from node i at given time period Z_h and is assumed to be constant until exiting at the node j. The calculation of arrival and travel times across arc (i, j) are summarized in Algorithm 3.2.

3.5.2 Time-dependent fuel consumption and travel cost computation

Given a starting time $\gamma_i^p(t)$ at node i, the fuel consumption, GHG emissions and travel costs across arc (i, j) are computed using the FSM and the LTM models based on Algorithms 3.3 and 3.4, respectively.

Algorithm 3.2 Computing the travel time $\tau_{ij}(\gamma_i^p(t))$ across a given arc (i,j) based on the LTM

function TRAVEL_TIME_LTM($\gamma_i^p(t)$, (i,j), $\mathcal{Z}$, $\mathcal{S}$)
  $h|\gamma_i^p(t) \in Z_h = [z_h, z_{h+1}[$
  $\tau_{ij}(\gamma_i^p(t)) \leftarrow L_{ij}/s_{ij}^h$
  return $\tau_{ij}(\gamma_i^p(t))$
end function

In Algorithm 3.3, we identify all speed changes according to the time periods crossed when traversing arc (i,j) and consider the associated portions of distance covered. Hence, at every iteration the time-dependent travel cost and energy consumption are induced, including the amount of GHG emissions and fuel consumption computed using CMEM. The algorithm stops when node j is reached.

Algorithm 3.3 Computing the travel cost $c_{ij}(\gamma_i^p(t))$ across a given arc (i,j) based on the FSM

function TRAVEL_COST_FSM($\gamma_i^p(t)$, (i,j), $\mathcal{Z}$, $\mathcal{S}$)
  $h|\gamma_i^p(t) \in Z_h = [z_h, z_{h+1}[$
  $k \leftarrow h$
  $l \leftarrow s_{ij}^k(z_{k+1} - \gamma_i^p(t))$
  $d \leftarrow L_{ij} - l$
  $g \leftarrow \lambda k N_e V \left(\frac{l}{s_{ij}^k}\right) + l\lambda\varsigma\beta(s_{ij}^k)^2$
  while $d > 0$ **do**
    $k \leftarrow k + 1$
    $l \leftarrow s_{ij}^k(z_{k+1} - z_k)$
    $g \leftarrow g + \lambda k N_e V \left(\frac{l}{s_{ij}^k}\right) + l\lambda\varsigma\beta(s_{ij}^k)^2$
    $d \leftarrow d - \left[s_{ij}^k(z_{k+1} - z_k)\right]$
  end while
  $\gamma_j^p(t) \leftarrow z_{k+1} + d/s_{ij}^k$
  if $k > h$ **then**
    $l \leftarrow s_{ij}^k(\gamma_j^p(t) - z_k)$
    $g \leftarrow g + \lambda k N_e V \left(\frac{l}{s_{ij}^k}\right) + l\lambda\varsigma\beta(s_{ij}^k)^2$
  else
    $g \leftarrow \lambda k N_e V \left(\frac{L_{ij}}{s_{ij}^h}\right) + L_{ij}\lambda\varsigma\beta(s_{ij}^h)^2$
  end if
  $\tau_{ij}(\gamma_i^p(t)) \leftarrow \gamma_j^p(t) - \gamma_i^p(t)$
  $\mathcal{F}_{ij}(\gamma_i^p(t)) \leftarrow \lambda\varsigma\alpha(w+q)L_{ij} + g$
  $c_{ij}(\gamma_i^p(t)) \leftarrow c_d\tau_{ij}(\gamma_i^p(t)) + c_f\mathcal{F}_{ij}(\gamma_i^p(t)$
  return $c_{ij}(\gamma_i^p(t))$
end function

Algorithm 3.4 Computing the travel cost $c_{ij}(\gamma_i^p(t))$ across a given arc (i,j) based on the LTM

function TRAVEL_COST_LTM($\gamma_i^p(t)$, (i,j), $\mathcal{Z}$, $\mathcal{S}$)
  $h|\gamma_i^p(t) \in Z_h = [z_h, z_{h+1}[$
  $\tau_{ij}(\gamma_i^p(t)) \leftarrow s_{ij}^h / L_{ij}$
  $\gamma_j^p(t) = \gamma_i^p(t) + \tau_{ij}(\gamma_i^p(t))$
  $\mathcal{F}_{ij}(\gamma_i^p(t)) \leftarrow \lambda(kN_eV + \varsigma\alpha(w+q)s_{ij}^h + \varsigma\beta(s_{ij}^h)^3)\frac{L_{ij}}{s_{ij}^h}$
  $c_{ij}(\gamma_i^p(t)) \leftarrow c_d\tau_{ij}(\gamma_i^p(t)) + c_f\mathcal{F}_{ij}(\gamma_i^p(t))$
  return $c_{ij}(\gamma_i^p(t))$
end function

3.5.3 Time-dependent Dijkstra algorithms

In this section we propose new solution methods based on two adaptations of Dijkstra's label-setting algorithm. The travel cost across each arc is computed according to the set of flow speeds obtained at the time of traversing the arc. Therefore, FSM and LTM models for the computation of time-dependent arc arrival time and travel costs are integrated at every iteration of the main label-setting algorithm when choosing the next connecting node. We call these modified versions the time-dependent Dijkstra's (TD-Dijkstra) FSM and LTM algorithms.

The TD-Dijkstra-FSM and TD-Dijkstra-LTM algorithms work by examining all temporarily labeled nodes in the network starting with the source node o. At the beginning, the priority queue N contains all nodes and their status are initialized to unlabeled except the source o. Hence, c_o is set to 0 and for each unlabeled node i the cost c_i is set to ∞. At each iteration of node expansion, the algorithm selects a labeled but not examined node i with the least labeled time-dependent cost from the set of temporarily labeled nodes $E^+(i)$, updates its cost label, and puts the node into a set of examined and permanently labeled nodes E, and each arc leaving from it is evaluated. If the labeled cost of node i plus the cost of arc (i,j) is smaller than the labeled cost of node j, then the cost from the source node to node j is updated with a value equal to the sum of the labeled cost of node i plus the cost of arc (i,j). Then, the algorithm continues the node examination process and takes the next node to be examined. The algorithm terminates when the destination node d is reached or when the priority queue becomes empty. In the node-examination process, a tree connecting all examined nodes is created, and the permanently labeled time-dependent travel cost associated with each examined node represents the least cost path from the origin node to that one.

Let $Travel\_Cost\_*()$ be the method that computes the travel cost at node j when starting from node i at time $\gamma_i^p(t)$, where the symbol $*$ represents the appropriate model for time-dependent networks (FSM or LTM). Let o denote the origin node and $predecessor(i)$ be the predecessor of node i. Therefore, the TD-Dijkstra-* label-setting algorithms are designed as in Algorithm 3.5.

Algorithm 3.5 Determination of a near-optimal least cost path by adapting Dijkstra label-setting algorithm (TD-Dijkstra-*)

function TD_DIJKSTRA($o, d, \mathcal{G}$)
  $E \leftarrow \varnothing$
  $N \leftarrow \mathcal{V}$
  $c_i \leftarrow \infty$, $\forall i \in V$
  $c_o \leftarrow 0$ and $predecessor(o) \leftarrow o$
  while $|E| < n$ **do**
    let $i \in N$ be a node for which $c_i \leftarrow \min\{c_j : j \in N\}$
    $E \leftarrow E \cup \{i\}$
    $N \leftarrow N \backslash \{i\}$
    if $i = d$ **then**
      Stop
    end if
    for each $(i, j) \in E^+(i)$ **do**
      if $c_j > Travel\_Cost\_*(\gamma_i^p(t), (i, j), \mathcal{Z}, \mathcal{S})$ **then**
        $c_j \leftarrow c_i + Travel\_Cost\_*(\gamma_i^p(t), (i, j), \mathcal{Z}, \mathcal{S}))$
        $predecessor(j) \leftarrow i$
      end if
    end for
  end while
end function

The original Dijkstra's algorithm has a computational complexity of $O(m \log(n))$. However, the TD-Dijkstra-LTM has a computational complexity of $O(m \log(n) + n)$, where n and m are the number of nodes and arcs in the time-dependent network, respectively. For every arc and departure time at node i the arc travel cost is computed in $O(1)$. As each node label remembers the index of the time period, we reduce the scanning time from $O(m)$ to $O(n)$. Similarly, the TD-Dijkstra-FSM algorithm solves the TDQPP-EM with $O(m \log(n) + nK)$ time complexity, where K denotes the maximum number of time periods scanned by the function Travel_Cost_FSM.

3.5.4 Dijkstra-SL and fast computation of time-dependent least cost upper and lower bounds

We now propose an effective speed-up technique to ensure the fast computation of time-dependent lower and upper bounds for the TDQPP-EM. First, we run the classical Dijkstra to solve the TDQPP-EM to optimality where the network-wide traffic congestion is ignored and travel speeds become constant. We call this version the Dijkstra algorithm with speed limits (Dijkstra-SL). In this case, all arc travel speeds s_{ij}^h are set according to the speed limit u_{ij}. Second, we compute the lower bound by applying Algorithms 3.6 and 3.7 in order to obtain travel cost across each arc of the QPP-EM optimal solution considering time-varying speeds. Algorithm 3.6 computes driver costs considering the heaviest congestion ratio for all

arcs over time interval Z_h. Algorithm 3.7 computes fuel cost considering optimal speeds (see Section 3.4). Next, we compute upper bounds by evaluating the travel cost across each arc using Algorithm 3.3.

Algorithm 3.6 Computing the driver cost across a given arc (i, j) according to the heaviest congestion ratios

function DRIVER_COST_HEAVIEST($\gamma_i^p(t)$, $(i, j), \mathcal{Z}, \mathcal{S}, \sigma_h$)
  $h|\gamma_i^p(t) \in Z_h = [z_h, z_{h+1}[$
  $\tau_{ij}(\gamma_i^p(t)) \leftarrow (\sigma_h u_{ij})/L_{ij}$
  return $c_d \tau_{ij}(\gamma_i^p(t))$
end function

Algorithm 3.7 Computing the fuel cost across a given arc (i, j) based on optimal speeds

function FUEL_COST_OPTIMAL_SPEED($\gamma_i^p(t)$, $(i, j), \mathcal{Z}, \mathcal{S}, s^*$)
  $h|\gamma_i^p(t) \in Z_h = [z_h, z_{h+1}[$
  $\tau_{ij}(\gamma_i^p(t)) \leftarrow L_{ij}/s^*$
  $\mathcal{F}_{ij}(\gamma_i^p(t)) \leftarrow \lambda(kN_eV + \varsigma\alpha(w+q)s^* + \varsigma\beta(s^*)^3)\tau_{ij}(\gamma_i^p(t))$
  return $c_f \mathcal{F}_{ij}(\gamma_i^p(t))$
end function

3.6 Computational experiments

In this section, the experimental design and methodology for generating networks with their arc information are provided. Then, detailed computational results of our TDQPP-EM algorithms are presented and analyzed.

3.6.1 Benchmarks set

Our experiments are conducted on a real large road network generated from the geographical information of Québec City. The obtained network contains 50,367 arcs and 17,431 nodes, and is composed by a set of physical nodes, and a set of arcs of different types, such as arterial streets, ramps and highway segments. Figure 3.1 shows a portion of the geographical area. We have considered 60 time periods of 15 minutes from 6h00 to 21h00, which covers a typical workday. For each arc and each time period the time-dependent flow speeds are computed based on a large set of real-world data including more than 24 million of GPS observations provided by the city administration and logistic partners (Belhassine et al. 2018). Relevant speed observations were extracted, consolidated and stored to obtain historical congestion patterns in this network.

As shown in Table 3.2 we have designed 80 test instances divided into four sets:

1. large networks considering a fixed departure time,

2. medium networks considering a fixed departure time,

3. small networks considering a fixed departure time,

4. and large networks with different departure times.

For each instance we generate a pair of source and destination which corresponds to real historical shipment data provided by one of our logistic partners. Further, each instance is solved with different carried loads: empty (15 – tons), less-than-truck load (LTL – 17.5, 20, and 22.5 tons) and full truck load (TL – 25 tons).

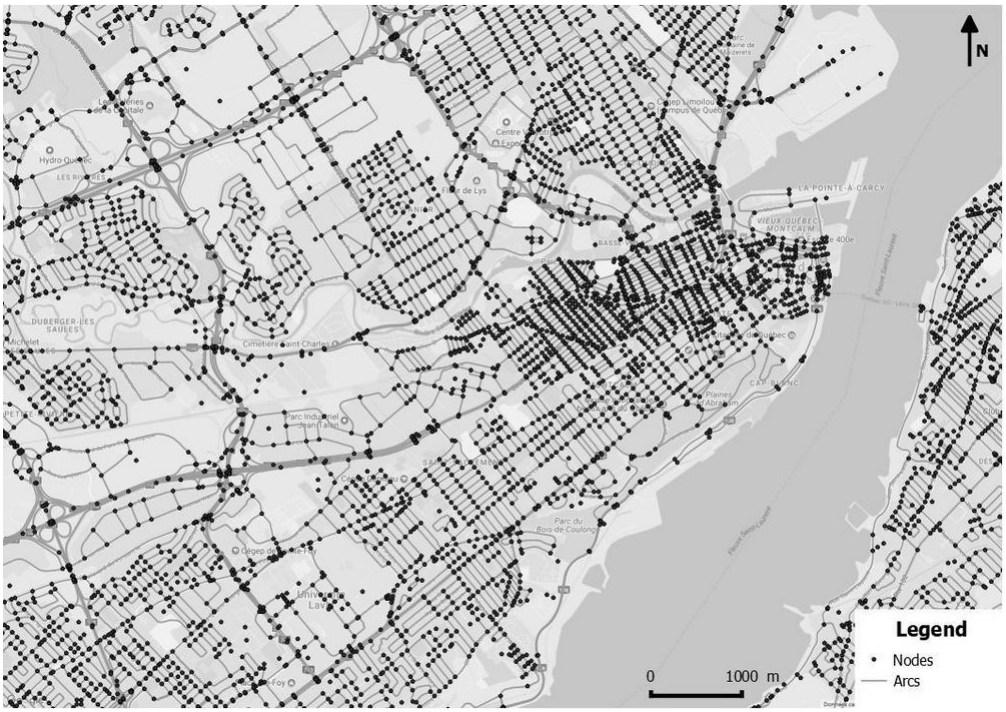

Figure 3.1: Portion of the geographical area

3.6.2 Experimental design

Table 3.3 summarizes our experimental design. All the instances were solved using three different optimization objectives, namely travel time, fuel consumption, and travel cost. We observe that minimizing fuel consumption is equivalent to minimizing GHG emissions as one liter of diesel generates 0.00279 $t\ CO_2\ e$ (Ministère de l'Énergie et des Ressources Naturelles 2014). For each set of instances and objective functions, we apply the developed algorithms by adjusting their objective function accordingly, namely classical Dijkstra with speed limits (Dijkstra-SL), TD-Dijkstra-LTM, TD-Dijkstra-FSM, LB and UB. Then, the exact value of each solution is recalculated with Algorithms 3.1 and 3.3 according to FSM and CMEM to reflect the key elements of real road network considering time-varying speeds.

Table 3.2: Test instances

Instances	Networks	Number of nodes	Number of arcs	Speed observations	Departure time	Carried load
L1-L20	Large	17431	50367	613485	08h15	LT/LTL/Empty
M1-M20	Medium	3859	5388	266280		
S1-S20	Small	1612	2810	78709		
D1	Large	17431	50367	613485	07h30	
D2					08h00	
D3					08h30	
D4					09h00	
D5					09h30	
D6					10h00	
D7					10h30	
D8					11h00	
D9					11h30	
D10					12h00	
D11					12h30	
D12					13h00	
D13					13h30	
D14					14h00	
D15					14h30	
D16					15h00	
D17					15h30	
D18					16h00	
D19					16h30	
D20					17h00	

All algorithms are implemented in C++ 17 using Jetbrains CLion C++ 2017 release 2 with cmake C++ compiler and were run on a ThinkCenter professional workstation with 32-gigabyte RAM and Intel core i7 vPro, running Ubuntu Linux 16.05 LTS x86 operating system.

Table 3.3: Overview of experimental design

Optimization criteria	Related Routing problems	Algorithms	Solution evaluation criteria
Travel time Fuel (GHG emission) Cost	TDQPP TDLEPP TDQPP-EM	Dijkstra-SL TD-Dijkstra-LTM TD-Dijkstra-FSM LB/UB	Distance (m) Travel time (s) Fuel consumption ($liter$) Cost ($)

3.6.3 Computational results and analysis

In this section we assess the effectiveness and robustness of the proposed algorithms. Table 3.4 shows the average results of the proposed algorithms for each of the three optimization criteria over the four sets of instances. For each combination we present the average distance in meters (Dist), the travel time in seconds (TT), the fuel consumption in liters (Fuel), the total cost in dollars (Cost) and the required computing time in seconds (Sec). For these results we assume the case of full truck load (25 t).

As shown in Table 3.4, the results indicate that the proposed algorithms run quickly even for very large size instances. Such fast solution is critical for providing real-time routing to drivers. When looking at the cost optimization criterion, the average computation time of Dijkstra-

SL, TD-Dijkstra-LTM and TD-Dijkstra-FSM is 0.15, 0.43 and 0.33 seconds, respectively. Note that the computation time of the proposed algorithms is less than one second for all instances. To further assess the performance and the scalability of the algorithms various experiments have been made with road networks provided by the 9th DIMACS challenge for the classical SPP. The average computation time for each core instance and over 1000 random node pairs were collected. As an example, the full USA road network instance includes 23.947 million nodes and 58.333 million arcs. The average runtime of TD-Dijkstra-FSM algorithm is 4.8 seconds for 20 DIMACS instances with the full USA road network.

Regarding the quality of the obtained solutions, we first observe that the TD-Dijkstra-FSM generates the best solutions for each optimization criterion. More specifically, when we minimize the travel time TD-Dijkstra-FSM yields an optimal solution for each instance under FIFO networks using time-varying speeds. For the travel time optimization criterion, we can see from Table 3.4 that over our 80 instances TD-Dijkstra-FSM produces an average travel time of 1,338.59 seconds, which is 0.9% lower than TD-Dijkstra-LTM (1,350.79 seconds) and 6.67% lower than Dijkstra-SL (1,434.25 seconds). This exposes the error margin associated with using the LTM or the speed limit instead of using exact calculations with the FMS. The fuel consumption reported by the TD-Dijkstra-FSM (under the travel time objective) is 9.9 liters of fuel for a distance of 20.82 km which corresponds to 47.54 liters per 100 km. This value is remarkably close to the annual average consumption of 46.9 reported by Transports Canada (2017) in their annual statistical report.

When looking at the Fuel Consumption optimization criterion, the TD-Dijkstra-FSM algorithm minimizes the travel time and the fuel consumption, as expected. When Fuel Consumption is minimized instead of Travel Time, for TD-Dijkstra-FSM, the distance decreases, on average, by 10.69% from 20.82 to 18.60 km yielding a reduced amount of emissions of 5.68% for all instances. More specifically, for all D* instances the distance decreases, on average, by 13.13% to create 7.80% savings in emissions. The distance decreases by 8.69% to create 3.98% savings in emissions for medium network instances M*, and the distance decreases by 11.86% to create 4.36% savings in emissions for small network instances S*. These results clearly show that for TD-Dijkstra-FMS, minimizing the travel time does not minimize the fuel consumption. In fact, even if the travel time increased globally by 7.08% (from 1338 to 1440 seconds), the consumption decreases 5.68% (from 9.89 to 9.34 liters). The same observation holds for TD-Dijkstra-LTM and Dijkstra-LS. We can conclude that when minimizing fuel consumption, our algorithms successfully manage the traffic congestion to find better paths.

The third part of Table 3.4 considers the cost-minimizing objective. Again, the TD-Dijkstra-FMS produces the best results with an average path cost of 22.45$ compared to 22.50$ and 24.08$ with TD-Dijkstra-LTM and Dijkstra-SL. Minimizing the cost implies a compromise between the travel time (cost) of the drivers and the fuel cost. As the driver costs are the largest component of the total cost, the TD-Dijkstra-FMS solution obtained under the cost

Table 3.4: Algorithm performances under different optimization criteria

Optimization criteria	Instances	Dijkstra-SL					TD-Dijkstra-LTM					TD-Dijkstra-FSM				
		Dist	TT	Fuel	Cost	Sec	Dist	TT	Fuel	Cost	Sec	Dist	TT	Fuel	Cost	Sec
Travel Time	***L1-L20***	24310.27	1770.60	12.08	28.95	0.19	24845.29	1687.35	11.98	28.12	0.44	24901.75	**1658.10**	11.90	27.78	0.39
	L1-M20	10397.11	990.20	5.79	15.07	0.11	10886.42	875.90	5.57	13.85	0.26	10946.48	**867.05**	5.57	13.78	0.24
	S1-S20	6216.59	664.05	3.68	9.87	0.06	6910.06	569.85	3.57	8.95	0.15	6846.87	**565.45**	3.53	8.87	0.13
	D1-D20	42174.18	2312.15	19.28	41.83	0.24	39288.77	2270.05	18.13	40.14	0.56	40593.86	**2263.75**	18.59	40.62	0.50
	Average	20774.54	1434.25	10.21	23.93	0.15	20482.64	1350.79	9.81	22.76	0.35	20822.24	**1338.59**	9.90	22.76	0.32
Fuel Consumption	***L1-L20***	22321.74	2016.95	12.01	30.95	0.19	23072.33	1747.90	11.52	28.10	0.50	23094.44	1734.90	**11.49**	27.95	0.40
	M1-M20	9416.36	1110.45	5.80	16.11	0.11	9992.72	919.20	5.38	13.99	0.29	9994.84	910.95	**5.35**	13.90	0.23
	S1-S20	5701.79	715.25	3.64	10.26	0.06	6022.40	621.05	3.42	9.22	0.15	6034.97	605.80	**3.38**	9.03	0.12
	D1-D20	34468.35	2854.00	17.84	44.77	0.26	35092.44	2546.15	17.17	41.39	0.66	35265.19	2510.85	**17.14**	41.05	0.52
	Average	17977.06	1674.16	9.82	25.53	0.16	18544.97	1458.58	9.37	23.17	0.40	18597.36	1440.63	**9.34**	22.98	0.32
Cost	***L1-L20***	23208.80	1834.30	11.89	29.26	0.19	23970.88	1681.00	11.67	27.70	0.54	23935.03	1672.30	11.64	**27.59**	0.42
	M1-M20	9783.68	1052.75	5.79	15.60	0.11	10664.25	873.15	5.49	13.74	0.31	10669.63	870.20	5.48	**13.70**	0.24
	S1-S20	5784.21	702.65	3.64	10.15	0.06	6651.81	572.50	3.50	8.89	0.17	6668.82	568.75	3.49	**8.85**	0.13
	D1-D20	35977.58	2483.40	17.57	41.31	0.25	37154.89	2305.50	17.47	39.68	0.70	36925.96	2313.10	17.40	**39.67**	0.55
	Average	18688.57	1518.28	9.72	24.08	0.15	19610.46	1358.04	9.531	22.50	0.43	19549.86	1356.09	9.50	**22.45**	0.33

minimization criteria uses less travel time that when minimizing the fuel (1356.01 instead of 1440.63 seconds) but a little more fuel (9.50 instead of 9.34 liters). Therefore, our savings in travel time are up to 5.87% combined with a small increase in fuel consumption of up to 1.74%, leading to a reduction in the overall cost, on average, by 2.31% from 22.98 to 22.45 dollars. Further, we see from Table 3.4 that our TD-Dijkstra-FSM yields a global saving on GHG emissions and overall costs of 1.36% (22.45 versus 22.76 dollars) and 4.01% (9.50 versus 9.90 liters), respectively, between cost-minimizing and travel time minimizing paths.

We note that both TD-Dijkstra-LTM and TD-Dijkstra-FSM produce coherent results with respect to the optimization criterion used. Thus, when the travel time criterion is used, the TT is effectively lower with respects to its value under the other optimization criteria. This pattern is not respected by the Dijkstra-SL as the minimum cost (23.93) is obtained under the travel time optimization criterion. Finally, it is remarkable that our TD-Dijkstra-FSM algorithm provides the best solutions for all optimization criteria: 1,338.59 seconds for travel time, 9.34 liters for fuel consumption, and 22.45 dollars for costs. Finally, Table 3.4 clearly shows that in the presence of traffic congestion, using a time-dependent algorithm (TD-Dijkstra-LTM or TD-Dijkstra-FMS) significantly enhances the quality of solutions with respect to a time-independent one (Dijkstra-SL).

Additional experiments were conducted to assess the variations of cost and GHG emissions incurred as a consequence of traffic congestion during rush hours, such as at 16h00. Table 3.5 presents additional experiments conducted to assess the impact of traffic congestion on the travel time, fuel consumption and total cost. To this end, we now used the average results over the 60 instances L*, M* and S* with departure times ranging from 07h30 to 08h30, before the morning congestion, and between 15h30 and 16h30 during the afternoon traffic. In the following, results of the time-independent Dijkstra-SL are not reported as it uses a fixed speed which is incoherent with this analysis.

If we look at the TD-Dijkstra-FSM with fuel consumption as the optimization criterion, we see that it increases from 6.37 to 6.81 liters (6.91%) when the path departure times are changed from 7h30 to 16h30. Similarly, the travel time increased, on average, by 14.66% induced by changes from 983.13 to 1,127.30 seconds. We observe the same pattern for the overall costs, which is increased, on average, by 11.10% induced by changes from 15.68 to 17.42 dollars. Overall, all algorithms produced expected results with respect to traffic conditions.

Figure 3.2 analyses in more details the impact of departure time on average path travel time and total cost for instances D1 to D20 (see Table 3.4). In Figure 3.2, the results of the TD-Dijkstra-FMS replicate the traffic pattern of Québec City with a moderate morning congestion between 7h30 and 9h00; low traffic between 10h00 and 14h30 results in lower travel times and costs. Then, as expected, congestion rapidly increases between 15h00 and 15h30 to reach a peak between 16h00 and 17h30. Interestingly, allowing delayed or flexible departures can lead

Table 3.5: Impacts of departure time

Departure Time	Optimization criteria	TD-Dijkstra-LTM				TD-Dijkstra-FSM			
		Avg Dist	Avg TT	Avg Fuel	Avg Cost	Avg Dist	Avg TT	Avg Fuel	Avg Cost
07h30	***Travel Time***	13695.50	938.67	6.57	15.45	13663.22	935.43	6.55	15.48
	Fuel consumption	12754.75	989.78	6.38	15.75	12762.90	983.13	6.37	15.68
	Cost	13449.36	943.28	6.50	15.49	13410.70	939.78	6.47	15.43
07h45	***Travel Time***	14343.47	1005.68	6.9648	16.51	14314.26	996.77	6.93	16.44
	Fuel consumption	12931.19	1028.83	6.54	16.26	12955.70	1022.32	6.53	16.20
	Cost	13316.18	1003.78	6.60	16.13	13307.89	997.72	6.59	16.05
08h00	***Travel Time***	13816.95	991.14	6.74	16.13	13776.51	986.06	6.72	16.15
	Fuel consumption	13074.91	1058.21	6.68	16.68	13083.87	1044.64	6.65	16.52
	Cost	13667.57	1012.77	6.76	16.38	13769.62	1004.20	6.77	16.32
08h15	***Travel Time***	14213.93	1044.37	7.04	16.95	14231.70	1030.20	7.00	16.81
	Fuel consumption	13029.15	1096.05	6.77	17.10	13041.42	1083.88	6.74	16.96
	Cost	13762.31	1042.22	6.89	16.78	13757.83	1037.08	6.87	16.72
08h30	***Travel Time***	14139.83	983.61	6.83	16.17	14155.14	977.76	6.82	16.15
	Fuel consumption	13071.85	1035.03	6.60	16.39	13079.92	1031.15	6.59	16.34
	Cost	13653.33	994.92	6.69	16.15	13713.31	988.58	6.70	16.10
15h30	***Travel Time***	14296.88	1024.13	6.99	16.56	14205.08	1005.31	6.91	16.49
	Fuel consumption	13116.88	1058.94	6.70	16.70	13233.37	1038.92	6.67	16.51
	Cost	13595.96	1029.03	6.78	16.54	13541.31	1022	6.73	16.42
15h45	***Travel Time***	14355.48	1042.26	7.04	16.94	14302.52	1032.83	7.00	16.83
	Fuel consumption	13107.03	1093.23	6.78	17.09	13126.18	1088.15	6.77	17.03
	Cost	13706.53	1052.32	6.86	16.83	13824.59	1044.07	6.88	16.78
16h00	***Travel Time***	14387.18	1063.75	7.10	17.11	14501.99	1054.90	7.11	17.14
	Fuel consumption	13135.97	1122.06	6.84	17.40	13133.05	1107.13	6.81	17.24
	Cost	13666.95	1075.03	6.89	17.06	13720.86	1068.59	6.88	16.99
16h15	***Travel Time***	14425.41	1073.80	7.14	17.37	14320.00	1061.42	7.07	17.16
	Fuel consumption	13168.82	1128.38	6.87	17.50	13208.30	1117.80	6.85	17.38
	Cost	13878.132	1073.02	6.97	17.14	13926.41	1067.25	6.97	17.09
16h30	***Travel Time***	14529.90	1072.42	7.18	17.34	14374.23	1067.22	7.11	17.25
	Fuel consumption	12987.398	1141.72	6.85	17.58	13055.88	1127.30	6.81	17.42
	Cost	13879.06	1070.81	6.96	17.11	13924.58	1065.17	6.97	17.07

to better alternative paths yielding significant reduction of both GHG emissions and overall costs.

The results shown in Table 3.6 further presents average results when the cost minimization objective is used for the TD Lower Bound, TD Upper Bound, Dijkstra-SL, TD-Dijkstra-LTM and TD-Dijkstra-FSM algorithms. It shows that both TD-Dijkstra algorithms consistently provide average solution costs bounded by the lower and upper bounds. Indeed, for the TD-Dijkstra-FSM the average gap between the lower bound value and the cost minimizing paths ranges from 3.77 to 7.07%, which are lower than those of the Dijkstra-SL ranging from 9.65 to 24.25%. For example, when the departure time is 08h00 the results of the time-independent Dijkstra-SL for L* (29.68), M* (15.15) and S* (10.06) always exceed the corresponding upper bounds of 29.22, 14.72 and 9.61 dollars. These results clearly show that the effectiveness of paths strongly increase if we consider time-varying speeds using TD-Dijkstra algorithms compared to those generated with Dijkstra-SL algorithm that uses fixed speeds.

Table 3.6: Average results under the total cost optimization criterion

Departure time	Instances	TD Lower Bounds		TD Upper Bounds		Dijkstra-SL			TD-Dijkstra-LTM			TD-Dijkstra-FSM		
		Cost	Sec	Cost	Sec	Cost	Gap (%)	Sec	Cost	Gap (%)	Sec	Cost	Gap (%)	Sec
07h30	***L1-L20***	25.90	0.30	28.21	0.20	28.40	9.64	0.20	27.17	4.88	0.56	27.03	4.33	0.43
	M1-M20	11.65	0.17	13.21	0.11	13.22	13.43	0.11	12.27	5.27	0.33	12.22	4.92	0.25
	S1-S20	6.77	0.09	7.29	0.06	7.30	7.80	0.06	7.04	3.98	0.15	7.04	3.98	0.12
	Average	14.87	0.19	16.24	0.13	16.30	9.65	0.12	15.49	4.18	0.35	15.43	3.77	0.27
07h45	***L1-L20***	26.03	0.29	28.58	0.19	28.87	10.92	0.19	27.35	5.10	0.55	27.24	4.67	0.42
	M1-M20	12.31	0.16	15.09	0.11	15.21	23.54	0.12	13.22	7.39	0.34	13.12	6.57	0.26
	S1-S20	7.38	0.09	9.46	0.06	9.12	23.59	0.07	7.80	5.64	0.17	7.80	5.64	0.13
	Average	15.35	0.18	17.71	0.12	17.73	15.57	0.13	16.13	5.08	0.35	16.05	4.61	0.27
08h00	***L1-L20***	26.15	0.29	29.22	0.19	29.68	13.52	0.19	27.68	5.85	0.54	27.53	5.29	0.41
	M1-M20	12.28	0.16	14.72	0.11	15.15	23.44	0.11	13.33	8.61	0.30	13.29	8.23	0.24
	S1-S20	7.46	0.09	9.61	0.06	10.06	34.81	0.06	8.14	9.11	0.16	8.14	9.10	0.12
	Average	15.43	0.18	17.85	0.12	18.30	18.56	0.12	16.38	6.15	0.33	16.32	5.73	0.26
08h15	***L1-L20***	26.25	0.29	28.95	0.19	29.26	11.48	0.19	27.70	5.55	0.55	27.59	5.14	0.42
	M1-M20	12.57	0.17	15.61	0.12	15.60	24.10	0.11	13.74	9.27	0.31	13.70	8.98	0.24
	S1-S20	7.90	0.09	9.87	0.07	10.15	28.45	0.06	8.89	12.45	0.17	8.85	11.95	0.13
	Average	15.69	0.18	17.92	0.12	18.34	16.86	0.12	16.78	6.91	0.34	16.72	6.51	0.27
08h30	***L1-L20***	25.94	0.31	28.37	0.21	28.60	10.24	0.19	27.32	5.31	0.55	27.20	4.85	0.42
	M1-M20	11.99	0.18	14.41	0.12	15.06	25.65	0.11	12.94	7.92	0.30	12.90	7.64	0.23
	S1-S20	7.53	0.10	9.80	0.07	10.10	34.16	0.06	8.21	9.02	0.16	8.21	9.00	0.26
	Average	15.26	0.19	17.53	0.13	17.92	17.40	0.12	16.15	5.83	0.33	16.10	5.49	0.26
15h30	***L1-L20***	26.08	0.30	29.56	0.20	29.38	12.66	0.19	27.49	5.42	0.55	27.33	4.80	0.43
	M1-M20	12.41	0.17	14.71	0.11	15.57	25.46	0.11	13.61	9.63	0.32	16.66	34.21	0.24
	S1-S20	7.71	0.09	9.74	0.06	10.47	35.81	0.06	8.52	10.45	0.17	8.51	10.43	0.13
	Average	15.51	0.19	18.00	0.12	18.47	19.12	0.12	16.54	6.64	0.34	16.42	5.89	0.27
15h45	***L1-L20***	26.60	0.30	30.19	0.20	30.09	13.10	0.20	28.28	6.29	0.57	28.15	5.80	0.44
	M1-M20	12.45	0.18	14.63	0.12	14.86	19.31	0.11	13.49	8.37	0.31	13.49	8.33	0.24
	S1-S20	7.83	0.09	9.61	0.06	9.98	27.41	0.06	8.71	11.21	0.18	8.71	11.17	0.14
	Average	15.70	0.19	18.14	0.13	18.31	16.64	0.12	16.83	7.21	0.35	16.78	6.91	0.27
16h00	***L1-L20***	26.81	0.30	30.78	0.20	30.84	15.05	0.20	28.53	6.40	0.58	28.46	6.17	0.45
	M1-M20	12.70	0.16	16.47	0.11	17.48	37.63	0.12	14.45	13.81	0.33	14.34	12.92	0.25
	S1-S20	7.98	0.09	11.35	0.06	11.16	39.89	0.06	8.90	11.60	0.18	8.90	11.58	0.14
	Average	15.89	0.18	19.53	0.12	19.60	23.39	0.13	17.06	7.38	0.36	17.00	7.00	0.28
16h15	***L1-L20***	26.88	0.30	31.90	0.20	31.86	18.52	0.20	28.59	6.35	0.59	28.52	6.11	0.45
	M1-M20	12.81	0.17	16.08	0.11	16.25	26.81	0.11	14.05	9.69	0.32	13.98	9.13	0.25
	S1-S20	7.90	0.09	11.12	0.06	11.16	41.35	0.06	8.77	11.02	0.17	8.76	11.00	0.13
	Average	15.90	0.18	19.70	0.12	19.76	24.25	0.13	17.14	7.78	0.36	17.09	7.49	0.28
16h30	***L1-L20***	27.19	0.29	31.80	0.19	31.86	17.19	0.20	28.59	5.15	0.59	28.52	4.92	0.45
	M1-M20	12.71	0.19	16.39	0.13	16.89	32.81	0.12	14.67	15.41	0.33	14.60	14.87	0.26
	S1-S20	7.84	0.09	10.26	0.06	11.16	42.27	0.06	8.77	11.75	0.17	8.76	11.72	0.13
	Average	15.94	0.19	19.23	0.13	19.72	23.72	0.13	17.11	7.35	0.36	17.07	7.07	0.28

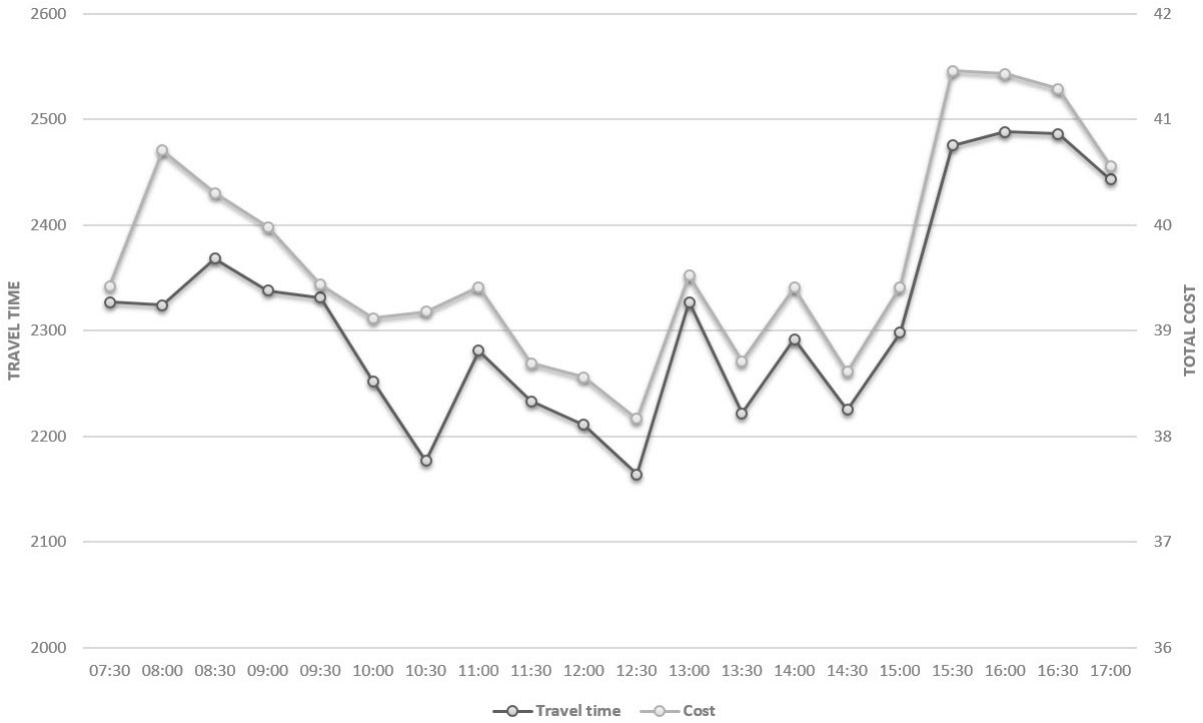

Figure 3.2: Impact of departure time

The final set of experiments presented in Table 3.7 aims at providing some insight on the impact of carried loads over our four performance measures. Results are obtained under the total cost minimization criteria and are averages over all instances. As expected, as the load increases, fuel consumption, and thus the cost, increase for both the TD-Dijkstra-LTM and the TD-Dijkstra-LTM. We can see that for both algorithms the paths are updated (as Distance and Travel Time change) when the load increases from 15 to 20 tons. However, the paths remain the same when the load increases from 20 to 25 tons in the case of the TD-Dijkstra-LTM. For the TD-Dijkstra-FSM, the fuel consumption increases from 7.87 to 8.28 liters (5.21%) from 15 to 17.5 tons and from 8.28 to 8.68 liters (4.83%) from 17.5 to 20 tons. This behavior is coherent with the fact that, proportionally, fuel consumption increases at a slowest rate with respect to the total load.

Table 3.7: Impact of carried load on performance measures

Algorithms	Performance measures	Carried Load				
		Empty Load (15 t)	LTL (17.5 t)	LTL (20 t)	LTL (22.5 t)	TL (25 t)
TD-Dijkstra-LTM	Avg Dist	19657.96	19573.35	19610.46	19610.46	19610.46
	Avg TT	1356.21	1353.25	1358.04	1358.04	1358.04
	Avg Fuel	7.89	8.27	8.71	9.12	9.53
	Avg Cost	20.60	21.02	21.56	22.03	22.50
TD-Dijkstra-FSM	Avg Dist	19642.50	19595.47	19566.88	19550.52	19549.86
	Avg TT	1353.80	1354.66	1356.09	1356.09	1356.09
	Avg Fuel	7.87	8.28	8.68	9.09	9.50
	Avg Cost	20.56	21.04	21.51	21.98	22.45

3.7 Conclusions

The TDQPP-EM extends the TDQPP by considering fuel consumption/GHG emissions minimization. This extension is of high practical relevance since traffic congestion is an important issue for logistics providers. Time-dependent least cost lower and upper bounds were derived based on QPP-EM properties. A fast and effective time-dependent Dijkstra label-setting algorithm and a lower bounding method have been implemented for eighty benchmark instances based on a large road network in Québec City including more than 17000 nodes and 24 million speed observations. The designed algorithms combine pre-existing CMEM and FSM models to compute GHG emissions and costs using time-varying speeds. Our algorithms are highly effective in finding good-quality solutions for benchmark instances of all size.

The extensive computational experiments demonstrated the benefit of choosing alternative paths in congested urban areas that leads to substantial fuel consumption/GHG emissions reduction and cost savings. We clearly demonstrate that using time-dependent algorithms lead to better results with respect to the ones which use constant speeds. Moreover, the required increase in computing time is negligible. An interesting insight derived from this research is that avoiding traffic congestion during peak hours yields substantial GHG emissions reductions and cost savings. Our time-dependent models reproduce expected behavior with respect to optimization criteria, time of the day (level of congestion), carried loads and selected paths. We have also shown that carried loads affect slightly the chosen path, particularly as the vehicle load becomes larger, the potential savings in fuel consumption and GHG emissions increase.

Further research should consider how to embed TDQPP-EM algorithms and our lower bounding method into local search heuristics to efficiently solve real-world time-dependent distribution problems considering emissions minimization based on time-varying speeds. Adding time-dependent quickest path optimization may enhance the resulting route plans that are selected based on dynamic paths to avoid traffic congestion across real road networks.

Acknowledgments

This research was partly supported by grants 2014-05764 and 0172633 from the Natural Sciences and Engineering Research Council of Canada (NSERC) and by the Centre d'Innovation en Logistique et Chaîne d'Approvisionnement Durable (CILCAD). We also thank Mr Jean-Philippe Gagliardi, President of Logix Operations inc, for providing us with real data from an important wholesaler partner in Québec city. This support is highly appreciated.

Appendix A

An integer linear programming formulation for the TDQPP-EM

Let x_{ij} be a binary variable equal to 1 if and only if arc (i, j) is selected, and 0 otherwise, and y_{ijt} be a binary variable equal to 1 if and only if arc (i, j) appears in the solution at entering time t, and 0 otherwise. The formulation is given in a time-dependent network $\mathcal{G}_T = (\mathcal{V}_T, \mathcal{A}_T)$, which is expanded from the original (physical) time-dependent network $\mathcal{G}$ and time-varying travel time and cost. Specifically, $\mathcal{V}_T = \{i_t | i \in \mathcal{V}, t \in T\}$ represents the set of time-dependent nodes, in which each node $i_t \in \mathcal{V}_T$ corresponding to a node-time pair indicates the state of node i and the arrival time t. The set of time-dependent arcs is denoted by $\mathcal{A}_T = \{(i_t, j_{t'}) | (i, j) \in \mathcal{A}, t_0 \leq t \leq t_0 + H\delta\}$, in which time-dependent arc $(i_t, j_{t'})$ exists when the arc originates at a given physical node i at time t and terminates at a physical arc's terminal node j at the time t'. Thus, $t' = \gamma_j^p(t)$, such that $t_0 \leq t \leq t' \leq t_0 + H\delta$. For the same starting time in a time-expanded network, there are multiple time-dependent paths with different arrival times and travel costs. In order to define a standard flow balance constraint, a super-sink node $d'_{t_0+H\delta}$ is introduced to the time-expanded network. It represents the end of the planning horizon, where all incoming arc travel times and costs have null values. For each physical node i, let its successors set be $E^+(i) = \{j : (i, j) \in \mathcal{A}\}$. Similarly, $E^-(i) = \{j : (j, i) \in \mathcal{A}\}$ denote the set of predecessors of node i. Furthermore, for each time-depedent node i_t, its successor node set is denoted by $E_T^+(i_t) = \{j_{t'} : (i_t, j_{t'}) \in \mathcal{A}_T, t \leq t'\}$. Similarly, let $E_T^-(i_t) = \{j_{t'} : (j_{t'}, i_t) \in \mathcal{A}_T, t' \leq t\}$ denote the set of predecessor nodes of the time-dependent node i_t. The following integer programming formulation of the TDQPP-EM is then proposed:

$$\min \sum_{(i,j)\in\mathcal{A}} \sum_{t\in T} c_{ij}(t) y_{ijt} \tag{A.1}$$

subject to

$$\sum_{j \in E^+(i)} x_{ij} - \sum_{j \in E^-(i)} x_{ji} = \begin{cases} 1 & \text{if } i = o \\ -1 & \text{if } i = d \\ 0 & \text{otherwise} \end{cases} \tag{A.2}$$

$$\sum_{j:(i,j) \in \mathcal{A}} x_{ij} \leq 1, i \in \mathcal{V} \tag{A.3}$$

$$\sum_{j:(i_t, j_{t'}) \in E_T^+(i_t)} y_{ijt} - \sum_{j:(j_{t'}, i_t) \in E_T^-(i_t)} y_{jit'} = \begin{cases} 1 & \text{if } i = o, t = t_0 \\ -1 & \text{if } i = d', t = t_0 + H\delta \\ 0 & \text{otherwise} \end{cases} \tag{A.4}$$

$$\sum_{t \in T} y_{ijt} = x_{ij}, (i,j) \in \mathcal{A} \tag{A.5}$$

$$x_{ij}, y_{ijt} \in \{0,1\}, (i,j) \in \mathcal{A}, t \in T. \tag{A.6}$$

The objective function (A.1) minimizes the overall travel cost in time-expanded network as in (3.13). Constraints (A.2) and (A.3) are defined to ensure the feasibility of an elementary path from origin o to destination d. Hence, constraints (A.2) correspond to the physical network flow balance. Constraints (A.3) guarantee that the selected physical arcs constitute a feasible path from the origin to the destination. Constraints (A.4) and (A.5) construct a corresponding time-dependent path in the time-expanded network based on the physical network. Additionally, space-time arc-to-link constraints (A.5) define the mapping between the physical and time-expanded networks. Finally constraints (A.6) define the domain and nature of the variables.

Chapter 4

Time-dependent Vehicle Routing Problem with Emission and Cost Minimization considering Dynamic Paths

Résumé

Le problème de tournées de véhicules dépendant du temps avec minimisation des émissions et des coûts en considérant les chemins dynamiques consiste à acheminer une flotte de véhicules pour desservir un ensemble de clients sur un réseau dépendant du temps modélisé comme étant un multigraphe dans lequel la vitesse de déplacement de chaque arc varie avec le temps. Le problème consiste à déterminer des tournées en fonction du temps tout en minimisant le temps de parcours, les émissions de gaz à effet de serre ou les coûts pour rendre visite à tous les clients en tenant compte de la vitesse instantanée imposée par le trafic sur chaque segment routier du réseau sous-jacent. Pour résoudre le problème, nous proposons une heuristique efficace d'amélioration et de recherche du plus proche voisin qui incorpore une méthode de recherche du chemin le plus rapide dépendante du temps. La méthode proposée fait le calcul de trajets dépendant du temps de façon rapide tout en considérant différentes mesures telles que le temps, la consommation de carburant ou le coût sur un multigraphe représentant de grands réseaux routiers utilisant un algorithme Dijkstra dépendant du temps. Basées sur de nouvelles instances qui représentent de manière réaliste les opérations de distribution de marchandises et capturent les périodes congestionnées en utilisant des réseaux routiers réels et de grands ensembles de données d'observations de vitesse, des expérimentations numériques approfondies ont été menées selon trois critères d'optimisation, notamment minimisation du temps de voyage, des émissions et des coûts totaux. Nous avons effectué également une analyse

de sensibilité pour évaluer les effets du choix du moment de départ, des décisions d'évitement de la congestion et des demandes des clients sur les plans de routage. Notre méthode surpasse significativement les résultats obtenus avec une heuristique classique basée sur les limites de vitesse sans tenir en compte de la congestion du trafic.

Chapter information A research paper based on this chapter, named *Time-dependent Vehicle Routing Problem with Emission and Cost Minimization considering Dynamic Paths*, has been submitted to the journal Transportation Research Part B: Methodological in February 2018 by Heni H., Renaud J., and Coelho L. C. in February 2018.

Abstract

The Time-dependent Vehicle Routing Problem with Emission and Cost Minimization considering Dynamic Paths consists of routing a fleet of vehicles to serve a set of customers across a time-dependent network modeled as a multigraph in which the traveling speed of each arc changes over time. The problem involves determining time-dependent paths minimizing travel time, greenhouse gas emissions, or costs to visit all customers taking into account the instantaneous speed imposed by traffic on each road segment of the underlying network. To solve the problem we propose an efficient nearest neighbor improvement heuristic that incorporates a time-dependent quickest path method. The proposed method involves the fast computation of time-dependent point-to-point paths based on different measures such as time, fuel consumption, or cost on a multigraph representing large road networks using a time-dependent label-setting algorithm. Based on new large-scale benchmark instances that realistically represent typical freight distribution operations and capture congested periods using real-life road networks and large data sets of speed observations, extensive computational experiments are conducted under three optimization criteria, namely minimizing travel time, emissions and total costs. We also carry out sensitivity analysis to assess the effects of departure time choice, congestion avoidance decisions and customer demands on the resulting routing plans. Our method significantly outperforms the results obtained with a classical heuristic based on speed limits without regard to traffic congestion.

Keywords: time-dependent vehicle routing; greenhouse gas emissions; traffic congestion; time-dependent quickest path; multigraph.

4.1 Introduction

In most countries freight transportation in urban areas is among the largest sources of greenhouse gas (GHG) emissions (Demir, Bektaş, and Laporte 2014b). With increasing road transportation activity and the expected growth of freight flows at a fast rate, GHG emissions are expected to continue to increase at a similar pace (Transports Canada 2017). In Canada, the transportation sector (including passenger, freight and off-road emissions) is the second-largest source of GHG, reaching 24% of the country's GHG emissions (Transports Canada 2017).

Large urban areas continue to face congestion due to increased flow of trucks. It is widely recognized that in urban areas, vehicles must often travel at the speed imposed by traffic, which affects travel times at certain periods of the day. The variability of traveling speed has a significant impact on the performance of road freight transportation operations, GHG emissions and fuel consumption (Bektaş and Laporte 2011). Third-party logistics (3PL) providers are nowadays in position to acquire the speed of traffic on the road. Considering time-varying speeds and alternative paths between customers in route planning may lead to effective routes and schedules that avoid congestion, minimize GHG emissions and yield cost savings more than the traditional vehicle routing problem (VRP).

A feature largely overseen in VRPs is that between any pair of customer nodes (see Figure 4.1) there are many links (road segments) connecting them through the underlying physical road network (Figure 4.2), corresponding to multiple time-dependent paths of different travel times, costs and emissions according to time-varying speeds. Hence, routing decisions involve not only sequencing the customers but also path choices depending on departure times, customer demands and the optimization criteria. The main objective is to minimize the sum of operational and environmental costs while respecting capacity constraints. Travel cost is defined with respect to fuel consumption costs and driver wages. Moreover, when a vehicle travels across an arc it emits a certain amount of GHG which is directly proportional to the amount of fuel consumed (Franceschetti et al. 2013). The fuel consumption depends on several factors, such as carried load, speed, road characteristics, among others. The corresponding problem is a Time-dependent Vehicle Routing Problem with Emission and Cost Minimization considering Dynamic Paths (TDVRP-ECMDP) on time-dependent networks where the flow speed of each road link depends on the time. Vehicles must travel at the speed imposed by traffic, which is determined by congestion.

Path selection in time-dependent VRPs (TDVRP) has been considered by few works. Ehmke, Campbell, and Thomas (2016b) and Qian and Eglese (2016) solved the TDVRP considering emissions-minimized paths using a tabu search and their instances was limited to 30 and 60 customers, respectively as the search space increases drastically. Huang et al. (2017) considered path flexibility in the TDVRP with a multigraph through the integration of path selection decision according to departure time and congestion levels. A multigraph model was first

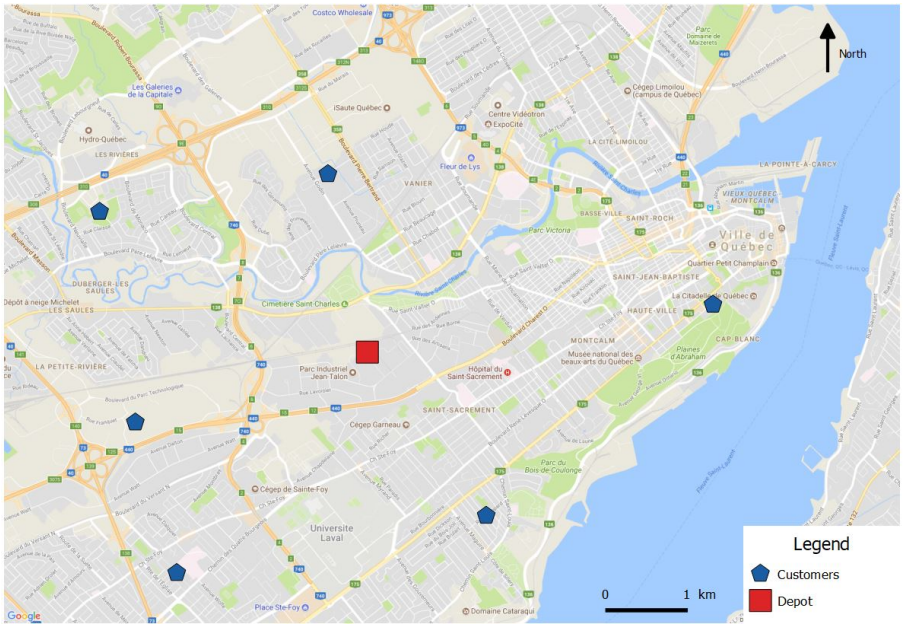

Figure 4.1: Illustration of a classical simplified network

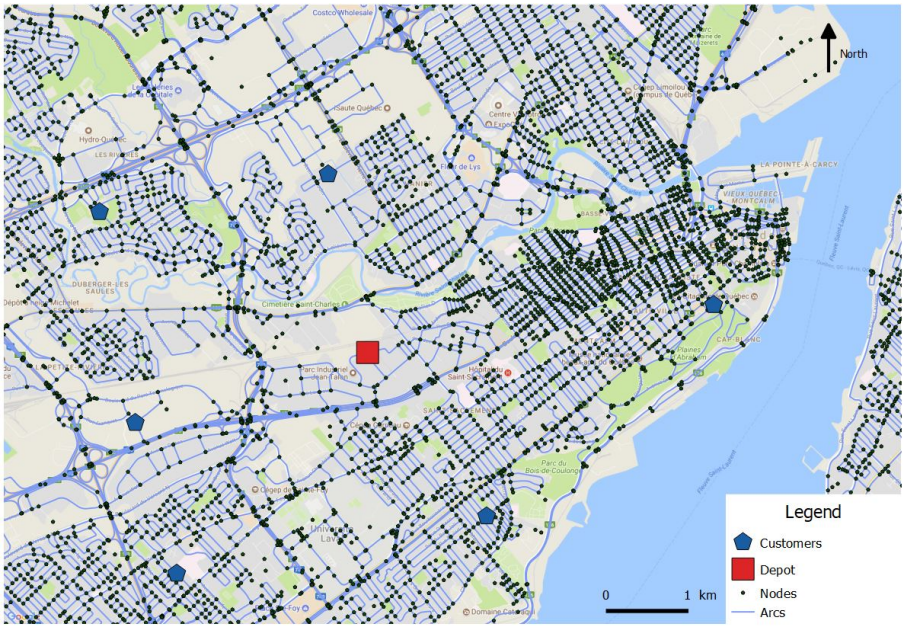

Figure 4.2: Illustration of a subset of customers and segment nodes of the road network of Quebec City

introduced by Garaix et al. (2010) to consider alternative paths between all pairs of key-locations. Letchford, Nasiri, and Oukil (2014), Lai, Demirag, and Leung (2016) and Ticha et al. (2017) used the multigraph representation to solve different VRPs. Their results indicate that the multigraph structure significantly increases computing times. We follow these studies by applying speed-up techniques to efficiently find appropriate time-dependent paths connecting the clients without computing them in advance for very large instances (up to 500 customers), road network (50376 arcs) and number of time slots (buckets of 15 minutes). We compute time-dependent quickest and least emission paths, and use the TD least costly path to investigate the insights related to different optimization objectives. To solve the TDVRP-ECMDP we develop efficient heuristics which are successfully applied to large road networks using a realistic set of large scale benchmark instances from 24 millions speed observations collected by furniture and appliance stores in Quebec City. We conduct sensitivity analysis to shed light on the trade-offs between multiple performance indicators, including driving time, GHG emissions and generalized costs pertaining to fuel consumption, traffic congestion, and drivers costs. Our detailed experimental analysis also quantifies the effects of flexible departure times from the depot and carried load according to customer demands. The scientific contributions of this research are fourfold:

(i) we model the underlying road network using a multigraph, which involves not only the best sequences of nodes across routes but also the fast computation of TD point-to-point quickest paths (TDQP), least emission paths (TDLEP) and least costly paths (TDLCP);

(ii) we create a new large sized benchmark set of instances reflecting real road freight distribution operations and congested areas of the road network from a large data set of speed observations;

(iii) we propose an efficient TD nearest neighbor method adapted to the multigraph representation to solve the TDVRP-ECMDP taking into account the effects of path choice and congestion avoidance decisions on GHG emissions as well as on traveling cost. Significant saving are obtained by integrating TDLCPs into routing decisions, which captures and minimizes fuel consumption along with operational costs;

(iv) we conduct sensitivity analysis to demonstrate that significant saving in terms of emissions and cost is achieved with regard to departure times.

The remainder of this paper is organized as follows. Section 4.2 summarizes the relevant literature. Section 4.3 formally describes the TDVRP-ECMDP. In Section 4.4, a detailed description of the designed TDVRP-ECMDP heuristics is provided. Section 4.5 presents extensive computational experiments and their numerical results. Finally, conclusions are stated in Section 4.6.

4.2 Literature review

In this section, we review the existing contributions on green logistics that consider the impact of GHG emissions in addition to operational issues on vehicle routing models in Section 4.2.1. Then, we look at existing studies on TD routing in Section 4.2.2.

4.2.1 Green logistics problems

Figliozzi (2011) studied a variant of the VRP in which GHG emissions minimization is pursued. He shows the effects of travel time optimization and the location of the depot in reducing emission levels considering scenarios with and without congestion. Likewise, Jabali, Van Woensel, and de Kok (2012) presented a variant of the problem with time-varying traffic. The planning horizon is divided into two periods, the first one is a congested period, whereas the second one considers free-flow.

Moreover, some have considered speed optimization decisions when dealing with emission minimization, as introduced by Bektaş and Laporte (2011). Their model computes the travel cost through a function encompassing fuel consumption, GHG emissions and driver costs. Later, Demir, Bektaş, and Laporte (2014a) introduced the bi-objective PRP in order to analyze trade-offs between fuel consumption and travel time. The authors developed a solution method based on the Adaptive Large Neighborhood Search and the speed optimization algorithm proposed by Demir, Bektaş, and Laporte (2012). They show that there is no need to greatly compromise on driving time in order to achieve a significant reduction in fuel consumption and GHG emissions. In a subsequent work, Kramer et al. (2015b) propose a solution method for the PRP combining a local search with an integer programming approach over a set covering formulation and a recursive speed optimization algorithm. This work was extended by Kramer et al. (2015a) to account for the effects of flexible departure times from the depot.

In their studies, Franceschetti et al. (2013) extend the PRP by capturing traffic congestion in the network. The authors consider three time periods: one congested, a transient one, and a free-flow period. They define conditions under which it is optimal to wait at certain nodes of the network in order to avoid congestion and to reduce GHG emissions. Later, Franceschetti et al. (2017a) developed a metaheuristic to solve the PRP with time-varying traffic congestion, which uses a departure time and speed optimization procedure designed by Franceschetti et al. (2013). In a related study, Xiao and Konak (2016) extend the PRP with time-varying traffic congestion by considering a heterogeneous vehicle fleet. In order to avoid traffic congestion and reduce emissions they designed an algorithm that allows waiting at customers and on the road. Otherwise, Dabia, Demir, and Van Woensel (2017) developed an exact method based on branch-and-price to solve a variant of the PRP in which the speed decision is taken at the route level and is assumed to be the constant along a route. Recently, Behnke and Kirschstein (2017) investigate the effects of path selection on a real world network. They show

that considering emission-minimizing paths between customers can lead to additional emission savings.

4.2.2 Time-dependent routing

Most of the literature in this field relies on the speed model of Ichoua, Gendreau, and Potvin (2003), where they do not assume a constant speed over the entire length of an arc. Thus, the speed on each arc may change when the boundary between two consecutive time intervals is crossed. In this way, this model guarantees the first-in, first-out (FIFO) property (Ghiani and Guerriero 2014b). Another contribution in the context of FIFO dynamics is due to Van Woensel et al. (2008) who proposed a queueing approach to model traffic congestion by tacking into account the change on travel speeds. For a relevant literature review on the TD routing problems, the reader is referred to Gendreau, Ghiani, and Guerriero (2015).

Another research stream has focused on the link travel time model (LTM) (Delling and Nannicini 2012) in which arc travel times are specified upon entrance to an arc and are assumed to be fixed during its traversal. In the LTM, the network does not satisfy the FIFO property, which requires additional algorithmic steps to ensure FIFO dynamics. To model travel times Fleischmann, Gietz, and Gnutzmann (2004) proposed a smoothed travel time function satisfying the FIFO consistency.

Focusing on TD networks Sung et al. (2000) introduced the flow speed model (FSM) for a TD shortest path where the flow speed of each arc depends on the time intervals. The FSM is consistent to the FIFO property. Another recent work by Kok, Hans, and Schutten (2012) investigated the impact of traffic congestion on the performance of vehicle route plans. The authors evaluated multiple strategies for avoiding traffic congestion when solving shortest path and VRPs. They designed a speed model to reflect the key elements of peak hour congestion on urban area networks. To solve the TDVRP they applied a modified Dijkstra algorithm and a dynamic programming heuristic.

Slightly different from the VRP, some have worked on the paths connecting two customers. Ghiani and Guerriero (2014a) and Calogiuri, Ghiani, and Guerriero (2015) studied the TD quickest path problem, which aims to find a least time path. They developed a TD lower bound on the time-to-target that can be computed by ignoring congestion ratios. Many studies have dealt with emission-minimizing paths between customers in vehicle routing (Ehmke, Campbell, and Thomas 2016a, Qian and Eglese 2016, Wen, Çatay, and Eglese 2014). These applied the Methodology for Estimating Emissions from Transport (MEET) (Hickman et al. 1999) to calculate GHG emissions which does not explicitly take the changing weight of the carried load into account. Ehmke, Campbell, and Thomas (2016b) proposed an emissions-minimizing model that explicitly accounts for the path finding problem between stops. The majority of paths between customers are pre-computed in advance using path averaging and approxima-

tion method. However, none of these works considered the effects of flexible departure times or waiting at depot and traffic conditions on both emissions and costs.

Finally, some related works on TD routing have focused on the optimization of routing plans by explicitly considering path flexibility (Androutsopoulos and Zografos 2017, Ehmke, Campbell, and Thomas 2016b, Huang et al. 2017, Qian and Eglese 2016). They also indicate that path flexibility increases the problem size requiring efficient heuristics to solve large scale instances. Although Ehmke, Campbell, and Thomas (2016b) and Qian and Eglese (2016) use finer speed levels to depict the 24 hour traffic conditions, the planning horizon in their instances usually contains only one peak hour or daily period. Even if the benefits of both GHG emissions and cost savings in vehicle routing and scheduling are clear, there is a lack of research on the TDVRP with cost minimization considering TDLCP computation which considers time-varying speeds for each road segment across a road network, and not only for customer links. The only works we are aware of that focused in finding TDLCPs are those of Wen, Çatay, and Eglese (2014), Di Bartolomeo et al. (2017) and Heni, Coelho, and Renaud (2017). Hence, this paper focus on solving large scale instances and deals explicitly with the trade-off between travel time, fuel consumption and cost in TDVRP involving emission and cost optimization considering time-varying speeds, congestion and dynamic paths on the underlying networks.

4.3 Problem description

The TDVRP-ECMDP is defined on a network $\mathcal{G}^T = (\mathcal{V}^T, \mathcal{A}^T, \mathcal{Z}^T)$ representing the road network in which $\mathcal{V}^T = \mathcal{V} \cup \mathcal{V}^g \cup \{0\}$ is the set of all nodes: the depot is represented by node 0, the set of customer nodes is $\mathcal{V}$, and the set $\mathcal{V}^g$ represents the other nodes of the road networks. $\mathcal{A}^T = \{(u,v) : u,v \in \mathcal{V}^T, u \neq v\}$ is the sparse set of all road segments connecting pair of nodes of the network. Let $T = z_0 + H\delta$ be the length of the planning horizon within which all routes must be completed, where $\delta > 0$ represents the smallest increment of time over which a change in the speed happens. This planning horizon is divided into a finite number H of time intervals $Z_h = [z_0 + h\delta, z_0 + (h+1)\delta[$ considering the set $\mathcal{Z}^T = \{z_0, z_0 + \delta \ldots, z_0 + H\delta\}$ of discrete times, with $h = 0, 1, 2, ..., H-1$. With each road segment $(u,v) \in \mathcal{A}^T$ is associated a time-dependent travel speed s_{uv}^h during time interval Z_h. Based on the FSM we assume that the speed of each road segment varies as the time interval changes: when a vehicle travels across a road segment (u,v), its traveling speed is not constant over the full arc, but may change when the boundary between two consecutive time intervals is crossed. Hence, the speed s_{uv}^h on arc (u,v) at time interval Z_h can be defined as:

$$s_{uv}^h = \sigma_{uv}^h \mathcal{U}_{uv}^h, \tag{4.1}$$

where $\sigma_{uv}^h \in [0,1]$ represents the congestion factor of arc (u,v) during the time interval Z_h and $\mathcal{U}_{uv}^h$ is the speed limit imposed by traffic regulations.

For any road segment $(u, v) \in \mathcal{A}^T$ let L_{uv} denote the distance between nodes u and v. Let l^h_{uv} represents the portion of the length L_{uv} covered during time interval Z_h. Let $\gamma_i(t)$ be a function that provides the ready time at node $i \in p$ when service is fulfilled given a starting time t at the depot. Let h_t and h_γ be the indices of time intervals where the start time t at node u and the arrival time $\gamma^p_v(t)$ at node v belong to, respectively, with $h_t \in \{0, ..., H-1\}$ and $h_\gamma \in \{h_t, ..., H-1\}$. Let $\tau_{uv}(t)$, $f_{uv}(t)$ and $c_{uv}(t)$ be the travel time, amount of GHG emissions and travel cost, respectively, related to the time $t \in T$ at which a vehicle leaves node u to node v. The travel time function is piecewise linear and satisfies the FIFO property:

$$\tau_{uv}(t) = \sum_{h=h_t}^{h_\gamma} l^h_{uv}/s^h_{uv}. \tag{4.2}$$

Furthermore, a homogeneous fleet of vehicles with capacity $\mathcal{Q}$ is available at the depot. Each customer $i \in \mathcal{V}$ has a non-negative demand q_i and a service time w_i. We denote the set of customers included in route r as $\mathcal{V}(r) \subseteq \mathcal{V}$. Let Ω_{ij} be the set of all feasible paths on $\mathcal{G}^T$ connecting any pair of depot and/or customers nodes i, j through the underlying road network. Each path $p_{ij} \in \Omega_{ij}$ is composed of an ordered sequence of nodes $[i, \langle u^0_{ij}, ..., u^n_{ij}\rangle, j]$. Considering that the road segments attributes are time-dependent, travel time, fuel consumption and travel cost between a pair of customers is defined by a time-dependent path that varies according to the departure time $\gamma_i(t)$ at node i, which is defined by the schedule of traversing it as $p_{ij}(\gamma_i(t)) = (\gamma_i(t), [i, \langle u^0_{ij}, ..., u^n_{ij}\rangle, j])$, where $u^n_{ij} \in \mathcal{V}^T$. Any scheduled route r must follow an ordered sequence of nodes, and pairs of nodes are connected by time-dependent paths:

$$\Psi_r(t) = (v_0, p_{01}(\gamma_0(t)), \ldots, p_{k-1,k}(\gamma_{k-1}(t)), v_k), \tag{4.3}$$

where $v_k \in \mathcal{V} \cup \{0\}$, $v_0 = v_k = 0$, and k represents the number of stops on the complete route.

The aim of the TDVRP-ECMDP is to construct a set of feasible routes that meet the demand of all customers without split delivery, starting and ending at the depot, driving at the speed of the traffic without exceeding the vehicle capacity nor violating their workday duration, so as to minimize a travel cost function encompassing the cost of drivers' wage, fuel consumption, and GHG emissions.

4.3.1 Modeling GHG emissions

Following relevant works in the literature (e.g., Ehmke, Campbell, and Thomas (2016b), Huang et al. (2017)) we consider the comprehensive modal emissions model (CMEM) (Barth and Boriboonsomsin 2008, 2009) to calculate fuel consumption for heavy duty vehicles. Based on the CMEM with a given speed s, total vehicle weight M^p across a given path p_{ij} and road

gradient θ the resulting instantaneous fuel consumption rate (in liters/second) is computed as follows:

$$e_r = E_0 \left(E_1 + \left(\frac{(\alpha M^p + \beta s^2)s}{E_2} + P_{acc} \right) \right), \tag{4.4}$$

where $E_0 = \frac{\zeta}{\varpi\psi}$, $E_1 = kN_eV$, $E_2 = \frac{1}{\varepsilon 1000\eta_{tf}}$, $M^p = \omega + q_i$, $\alpha = a + g\sin\theta + gC_r\cos\theta$, $\beta = 0.5C_dA\rho$, and P_{acc} are constant parameters related to the vehicle and its engine. All parameter values used are provided in Appendix 4.6.

Moreover, considering only the average speed one may not capture precise GHG emissions. For example, if the travel speed on a road segment often drops far below the average speed during a specific time slot Z_h, then the actual emissions will be much higher than if the trip occurs consistently at the average speed. Thus, to optimize GHG emissions in an urban area, we must explicitly consider the variability of the speed at different times of the day. Hence, for a given path p_{ij} traversed by a vehicle departing from customer i at ready time $\gamma_i^p(t)$, the corresponding fuel consumption (in liters) can be computed as follows:

$$F_{p_{ij}}(t) = \sum_{(u,v)\in p_{ij}} f_{uv}(\gamma_u^p(t)), \tag{4.5}$$

where

$$\gamma_u^p(t) = \begin{cases} t & \text{if } u = 0 \\ \gamma_{u-1}^p(t) + \tau_{u-1,u}(\gamma_{u-1}^p(t)) & \text{if } u \in \mathcal{V}^g \\ \gamma_{u-1}^p(t) + \tau_{u-1,u}(\gamma_{u-1}^p(t)) + w_u & \text{if } u \in \mathcal{V}, \end{cases} \tag{4.6}$$

and $f_{uv}(t) = f_{uv}^1(t) + f_{uv}^2(t) + f_{uv}^3(t)$. The first term f^1 denotes the fuel consumption related to the vehicle weight, f^2 represents the fuel consumption implied by travel time, and component f^3 measures the fuel consumption incurred by the variations in speed:

$$f_{uv}^1(t) = \sum_{h=h_t}^{h_\gamma} \left[\left(\frac{l_{uv}^h}{s_{uv}^h} \right) \frac{\alpha M^p E_0}{E_2} s_{uv}^h \right] = \frac{\alpha M^p E_0}{E_2} \sum_{h=h_t}^{h_\gamma} l_{uv}^h = \frac{\alpha M^p E_0}{E_2} L_{uv}, \tag{4.7}$$

$$f_{uv}^2(t) = \sum_{h=h_t}^{h_\gamma} \left[\left(\frac{l_{uv}^h}{s_{uv}^h} \right) E_0 E_1 \right] = E_0 E_1 \tau_{uv}(t), \tag{4.8}$$

$$f_{uv}^3(t) = \sum_{h=h_t}^{h_\gamma} \left[\left(\frac{l_{uv}^h}{s_{uv}^h} \right) \frac{\beta E_0}{E_2} (s_{uv}^h)^3 \right] = \frac{\beta E_0}{E_2} \sum_{h=h_t}^{h_\gamma} \left[l_{uv}^h . (s_{uv}^h)^2 \right]. \tag{4.9}$$

4.3.2 Modeling travel costs

In this section, we model the TD travel cost of a particular path. Given a departure time t, the driver cost incurred from path p_{ij} can be simply computed by multiplying the sum of the traveling time across road segments connecting customers nodes (i, j) by the driver wage c_d:

$$\mathcal{C}(\Gamma_{p_{ij}}(t)) = c_d \sum_{(u,v)\in p_{ij}} \tau_{uv}(\gamma_u^p(t)). \tag{4.10}$$

The cost of fuel consumption for a given route r can be computed by multiplying the fuel consumption (4.5) by a factor c_e representing the price of a liter of fuel:

$$\mathcal{C}(F_{p_{ij}}(t)) = c_e \sum_{(u,v)\in p_{ij}} f_{uv}(\gamma_u^p(t)). \tag{4.11}$$

The path cost encompasses the path duration and fuel costs:

$$\mathcal{C}_{p_{ij}}(t) = c_d \sum_{(u,v)\in p_{ij}} \tau_{uv}(\gamma_u^p(t)) + c_e \sum_{(u,v)\in p_{ij}} f_{uv}(\gamma_u^p(t)). \tag{4.12}$$

4.4 Heuristic methods for the TDVRP-ECMDP

With respect to exact methods, solving large VRP instances using a multigraph representation of the underlying road network increases significantly the size of the solution space as shown by Garaix et al. (2010) and Letchford, Nasiri, and Oukil (2014) for VRPs, and Huang et al. (2017) for TDVRP with path flexibility. Even with heuristic approaches, Ehmke, Campbell, and Thomas (2016b) solved TDVRP with emissions minimizing paths limited to 30 customers and one-hour time intervals due to computation time. Hence, to efficiently solve large instances of the TDVRP-ECMDP considering time-varying speeds we propose two solution methods. The first one only considers the speed limits on the underlying road network. The second method takes traffic congestion into account by considering time-varying speeds of all transportation links between each pair of customer nodes. The proposed heuristic methods are followed by a TD neighborhood search improvement heuristic (TDNSIH) to enhance the solution by using intra- and inter-route exchanges.

4.4.1 Static nearest neighbor heuristic

The static nearest neighbor heuristic (SNNH) does not take traffic congestion into account and solves the TDVRP-ECMDP considering static scenarios where the paths between customers are fixed. Thus, it works only on the customer network considering speed limits. The static paths used by the SNNH are chosen with respect to the optimization objective by solving the corresponding point-to-point routing problem, namely the Quickest Path Problem (QPP), the

Least Emission Path Problem (LEPP) or the Least Cost Path Problem (LCPP). The SNNH begins each route by determining, from the set of remaining customers, the unrouted customer to be visited next having the least additional increase in the objective function. When the search fails to find unrouted customers who can feasibly be embedded to the end of a route, the heuristic starts a new one.

4.4.2 Time-dependent nearest neighbor heuristic

To solve the TDVRP-ECMDP we also propose a greedy heuristic that accounts for traffic congestion and dynamic paths. The TD nearest neighbor heuristic (TDNNH) solves the problem according to three variants of TD point-to-point routing problems: TDQPP, TDLEPP and TDLCPP. The proposed heuristic considers the multigraph $\mathcal{G}^T$ to construct the set of routes. Table 4.1 shows the notation used to develop the TDNNH.

Table 4.1: Additional notation used by the TDNNH

Notation	Description
E^T	Set of processed nodes
N^T	Set of remaining nodes
N^c	Set of remaining customer nodes
$E^T_+(u)$	Set of successor nodes of node u
Ψ_r	Ordered set of customers visited along a route r
Ψ_R	Set of feasible routes

The TDNNH is briefly introduced in the following algorithmic steps (see Algorithm 4.1). The heuristic starts a time-dependent goal-directed search from the depot. The TDNNH takes into consideration the closeness of the customer node to be examined. The closeness is an estimated goal cost defined based on different measures such as fuel consumption, travel time or cost. At each iteration if the active labeled node having the smallest cost is a customer, then we check if the customer could be added to the current route with respect to the time window associated with the depot and the capacity of the vehicle, otherwise a new route is started. Then, we begin again a new time-dependent goal directed search from the current customer node. The heuristic stops when all customer nodes are processed.

The travel cost of each road link is computed according to the entering time on the arc and to the flow speed at the time of traversing it. The physical network is used to find connecting paths between each pair of nodes in the global network. Algorithm 4.2 is used to compute fuel consumption, travel time and travel cost for a given road segment. Given a starting time $\gamma_u^p(t)$ at node u, the fuel consumption, GHG emissions and travel costs across arc (u, v) are computed using the FSM based on Algorithm 4.2. At each covered time period the time-dependent flow speed is identified and the length of the appropriate portion of the distance L_{uv} is calculated. Hence, at every iteration the time-dependent travel cost and fuel consumption are calculated.

Algorithm 4.1 Determination of a TDVRP-ECMDP solution using the TD quickest path method (TDNNH)

$\Psi_R \leftarrow \emptyset$, $N^c \leftarrow \mathcal{V}$
function TDNNH($\Psi_R, N^c, \mathcal{G}^T, t$)
    $E^T \leftarrow \varnothing$, $N^T \leftarrow \mathcal{V}^T$, $r \leftarrow |\Psi_R|$, $\gamma \leftarrow t$, $c_o \leftarrow 0$, $predecessor(o) \leftarrow 0$, $c_u \leftarrow \infty | \tau_u \leftarrow 0$, $\forall u \in \mathcal{V}^T$
    while $|E^T| < |\mathcal{V}^T|$ or $|N^c| = 0$ **do**
        let $u \in N^T | c_u \leftarrow \min\{c_v : v \in N^T\}$
        $E^T \leftarrow E^T \cup \{u\}$, $N^T \leftarrow N^T \backslash \{u\}$
        if $u \in N^c$ **then**
            $\gamma \leftarrow (\gamma + \tau_u + w_u)$
            if $\Psi = \emptyset$ **then**
                Step 1:
                $\Psi_r \leftarrow \Psi_r \cup \{(u, o)\}$, $\Psi_R \leftarrow \Psi_R \cup \Psi_r$, $N^c \leftarrow N^c \backslash \{u\}$, $r \leftarrow r + 1$
                Start a new route: $TDNNH(\Psi_R, N^c, \mathcal{G}^T, t)$
                if $N^c = \emptyset$ **then**
                    return Ψ_R
                else
                    Go to Step 2
                end if
            else
                $\Gamma_{p_{uo}} \leftarrow TD\_Dijkstra(u, o, \gamma, \mathcal{G}^T)$
                if u can be added to current route r **then**
                    $\Psi_r \leftarrow \Psi_r \cup \{(u, v)\}$, $N^c \leftarrow N^c \backslash \{u\}$
                    Go to Step 2
                else
                    Go to Step 1
                end if
            end if
        end if
        Step 2:
        $\gamma \leftarrow \gamma + \tau_u$
        for each $(u, v) \in E_+^T(u)$ **do**
            if $c_v > \left[TD\_Cost\_FSM(\gamma, (u, v), \mathcal{Z}^T)) \longrightarrow c_{uv}(\gamma)\right]$ **then**
                $c_v \leftarrow c_u + \left[TD\_Cost\_FSM(\gamma, (u, v), \mathcal{Z}^T)) \longrightarrow c_{uv}(\gamma)\right]$
                $\tau_v \leftarrow \tau_u + \left[TD\_Cost\_FSM(\gamma, (u, v), \mathcal{Z}^T)) \longrightarrow \tau_{uv}(\gamma)\right]$
                $predecessor(v) \leftarrow u$
            end if
        end for
    end while
end function

The algorithm stops when node v is reached.

When performing time restriction validation, the TDNNH involves the fast computation of point-to-point TD quickest path, least emission path or least cost path in a time-dependent network using an efficient TD Dijkstra (TD-Dijkstra) label-setting algorithm (see Appendix 4.6) based on Brodal and Jacob (2004) and Dean (2004b). Note that, finding the TDLCP is NP-Hard as stated by Dehne, Omran, and Sack (2012) and demonstrated by Di Bartolomeo et al. (2017). To reduce the computational time our adaptation on the algorithm maintains a single label for each node including travel time, fuel and cost information.

Algorithm 4.2 Computing TD travel time, fuel consumption and cost across a given road segment (u, v) according to the FSM

2

function TD_COST_FSM($\gamma_u^p(t)$, (u,v), $\mathcal{Z}^T$)
  $h|\gamma_u^p(t) \in Z_h = [z_h, z_{h+1}[$
  $k \leftarrow h$, $d \leftarrow L_{uv} - s_{uv}^k(z_{k+1} - \gamma_u^p(t))$
  $l \leftarrow s_{uv}^k(z_{k+1} - \gamma_u^p(t))$
  $g \leftarrow kN_eV\left(\frac{l}{s_{uv}^k}\right) + l\lambda_\varsigma\beta(s_{uv}^k)^2$
  while $d > 0$ **do**
    $k \leftarrow k+1$, $l \leftarrow \delta s_{uv}^k$, $d \leftarrow d - l$
    $g \leftarrow g + E_0E_1\left(\frac{l}{s_{uv}^k}\right) + l\frac{\beta E_0}{E_2}(s_{uv}^k)^2$
  end while
  $\gamma_v^p(t) \leftarrow z_{k+1} + d/s_{uv}^k$
  if $k > h$ **then**
    $l \leftarrow s_{uv}^k(\gamma_v^p(t) - z_k)$
    $g \leftarrow g + E_0E_1\left(\frac{l}{s_{uv}^k}\right) + l\frac{\beta E_0}{E_2}(s_{uv}^k)^2$
  else
    $g \leftarrow E_0E_1\left(\frac{l}{s_{uv}^k}\right) + l\frac{\beta E_0}{E_2}(s_{uv}^k)^2$
  end if
  $\tau_{uv}(\gamma_u^p(t)) \leftarrow \gamma_v^p(t) - t$
  $f_{uv}(\gamma_u^p(t)) \leftarrow \frac{\alpha M E_0}{E_2}L_{uv} + g$
  $c_{uv}(\gamma_u^p(t)) \leftarrow c_d\tau_{uv}(\gamma_u^p(t)) + c_e f_{uv}(\gamma_u^p(t)$
  return $[\tau_{uv}(\gamma_u^p(t)), f_{uv}(\gamma_u^p(t)), c_{uv}(\gamma_u^p(t))]$
end function

4.4.3 Time-dependent nearest neighbor and improvement heuristic

The main components of local search heuristics are the rules applied to generate the neighboring solutions employed to carry out the exploration of the solution space and identify the best neighbor solution. In the TDNSIH, the neighborhoods are constructed by applying efficient implementations of arc-exchange algorithms. Exchanges are performed by replacing some arcs by new ones and moving them within the same route. Note that any modification in a route may need a major recalculation of the paths linking two consecutive customers, starting from the point of modification of the route up to the return to the depot.

The appropriate arc-exchange neighborhoods are defined successively based on six operators commonly applied in the literature (e.g., Zachariadis and Kiranoudis (2010)):

(i) 1-0-Exchange: iteratively removes a node and reinserts it at its best position.

(ii) 1-1-Exchange: the position of customer i is exchanged with that of customer j that yields the largest decrease in cost.

(iii) Or-Opt: sequences of one to three consecutive nodes are moved. This results in replacing up to three arcs in the original route by three new one.

(iv) Intra-2-Opt: tries to improve each route separately by exchanging a pair of arcs. If an improvement is possible, the two arcs that yield the largest decrease in objective value are removed and the resulting paths are reconnected in the reverse order.

(v) Inter-2-Opt*: tries to merge two routes. The first route is simply followed by the second one. The new route, if feasible, has one fewer arc.

(vi) Inter-CROSS-Exchange: is performed by removing two arcs for a first route as well as two arcs from a second route. Then the customers are swapped by introducing new arcs that yields the smallest detour (Taillard et al. 1997). Note that the orientation of both routes is preserved.

The general structure of the designed TDNSIH is summarized in Algorithm 4.3. At each iteration, once a potential neighboring solution is determined at the first neighborhood, it is compared against the current solution Ψ_R. If the new neighboring solution is better, it becomes the current solution, and the exploration of the current neighborhood continues. If no better solution is found through the exploration of the first neighborhood, the TDNSIH starts the search in the second neighborhood. If a better solution is determined, the heuristic goes back to explore the first neighborhood. Otherwise, the TDNSIH selects the next predefined neighborhood $Neighbor_k$ and looks for further improvement of the current solution. The TDNSIH stops if no better solution is found on the set of established neighborhoods.

A new neighbor solution is generated only if the deadline restriction is not exceeded. For inter-route moves new routes are generated with respect to vehicle capacity constraints. The evaluation of each neighbor solution implies the calculation of cost change and the validation of deadline through the fast computation of point-to-point TD paths connecting the new sequence of customers of each updated route on the underlying physical transportation network using a TD-Dijkstra algorithm. In the case in which deadline is not exceeded, we update the cost of each arc using the appropriate TDQP, TDLEP or TDLCP.

Algorithm 4.3 Time-dependent neighborhood search improvement heuristic (TDNSIH)

function TD_NSIH($\Psi_R, \mathcal{G}^T$)
  $nb\_max\_neighbors \leftarrow 6$, $improve \leftarrow 1$, $k \leftarrow 1$
  while $improve = 1$ **do**
    $\Psi_{R'} \leftarrow Neighbor_k(\Psi_R)$, $improve \leftarrow 0$
    if $\mathcal{C}(\Psi_{R'}) < \mathcal{C}(\Psi_R)$ **then**
      $\Psi_R \leftarrow \Psi_{R'}$, $k \leftarrow 1$, $improve \leftarrow 1$
    else
      if $k < nb\_max\_neighbors$ **then**
        $k \leftarrow k + 1$, $improve \leftarrow 1$
      end if
    end if
  end while
  return Ψ_R
end function

4.5 Computational experiments

In this section we provide the results of extensive computational experiments we have conducted to solve the TDVRP-ECMDP and to assess the performance our heuristics. We first explain how the benchmark instances are generated based on real traffic data from the road network of Québec City. We then discuss the results of our experiments. Particularly, a comparison is made between routing strategies with and without time-varying speeds to illustrate several insights concerning the impact of congestion avoidance, path choice decisions, optimization objective, departure time and volume of demand. These are measured and compared in terms of distance, travel time, fuel consumption (GHG emissions) and costs.

4.5.1 Proposed benchmark instances

Benchmark instances are designed using the geospatial road network covering the delivery regions of our industrial partner in Québec City. Each constructed test instance contains up to 50,376 road segments connecting 17,431 geographical nodes, the depot and customers. The speed limit of each road segment depends on the road type, namely highways, urban roads and primary roads. We have defined 60 time periods of 15 minutes from 6h00 to 21h00, which covers a typical workday. Time-varying speed data was extracted and analyzed by geomatic experts (Belhassine et al. 2018). Hence, for each road segment and each time slot the speed is computed based on a large set of real traffic data including more than 24 million of GPS speed observations provided by our logistic partners. We used pgRouting library 2.0 and QGIS 2.18 for the geomatic developments.

As presented in Table 4.2, we propose three classes of instances using three variants of networks, namely small, medium and large to take into account different shipping patterns and number of customers randomly selected from the set of nodes:

- small network sets (S) composed by 10 (S1), 20 (S2), 30 (S3), 40 (S4), and 50 (S5) customers;
- medium network sets (M) composed by 100 (M1), 150 (M2), and 200 (M3) customers;
- and large network sets (L) composed by 300 (L1), 400 (L3), and 500 (L3) customers.

We use the location of the depot of our logistic partner for all instances. Additionally, for each combination of instance classes and number of customers the load scenarios are produced according to three demand patterns: low, medium, and high. Hence, we use three demand distributions to assign small (100 to 500 kg), medium (500 to 2500 kg) and high demand (2500 to 5000 kg) quantities to the customers of each instance.

We also investigate the impact of departure times from the depot to capture the effects of congestion avoidance and waiting at depot decisions considering four departure times associated to each combination of instances class, number of customers, and demand patterns: 07h00, 08h00, 09h00 and 10h00. Therefore, we obtain 132 instances for the TDVRP-ECMDP to build insights on heuristics efficiency according to several loads and departure times settings.

Table 4.2: TDVRP-ECMDP benchmark instances

Instances	Time-dependent networks	Number of customers	Number of nodes	Number of arcs	Departure time	Demand
S1		10				
S2		20				
S3	Small network	30	1612	2810		
S4		40				
S5		50			07h00	Low
M1		100			08h00	Medium
M2	Medium network	175	3859	5388	09h00	High
M3		200			10h00	
L1		300				
L3	Large network	400	17431	50367		
L4		500				

4.5.2 Experimental setting

Computational experiments are carried out by applying the solution methods to assess the benefit of quickest path optimization considering time-varying speeds on the reduction of both operational and environmental costs. Our algorithms were coded in C++ 17 and OpenMP for multithreading programming using Jetbrains CLion release 2.4 and tested on a ThinkCenter workstation with 32-gigabyte RAM and Intel i7 vPro, running Ubuntu Linux 16.05 LTS x86.

Table 4.3 provides an overview of our experimental plan. The experiments are executed considering a heavy-duty vehicle with a gross weight of 25000 kg when it is fully loaded and 15000 kg when it is empty. Each of the 132 instances is solved for three different objective functions minimizing: (i) travel time using quickest paths, (ii) fuel/emission using least emission paths, and (iii) costs using least costly paths. We do this twice, first without considering traffic information using the speed limit of each arc, and then with our real-life traffic information

using time-varying speeds. The solutions will then be compared in terms of their distances (Dist), travel times (TT), fuel consumption, cost, number of routes (#Routes), number of late deliveries (#LD), and number of late returns times to the depot (#LRTD), percentage gap between two solutions calculated as $100 * (Solution - Solution_{best})/Solution_{best}$, and percentage improvement between two solutions.

Table 4.3: Overview of experimental setting

Optimization criteria	Accounting for traffic congestion	Heuristic	Solution evaluation measure
Travel time Fuel (GHG emissions) Costs	No (speed limits)	SNNH	Distance (m) Travel time (s) Fuel consumption (liters) Cost ($) # vehicle routes # late deliveries # late return times to depot Gap (%) Improvement (%)
	Yes (time-varying speeds)	TDNNH	

4.5.3 Experimental results

In this section we analyze the performance of our heuristics. We will first concentrate our analysis for departure times at 08h00 with low demand. Table 4.4 illustrates the effect of fixed speed assumption on the accuracy of travel time, fuel consumption and cost computations, by providing the results over all benchmark instances using the classical SNNH and TDNNH according to three optimization measures. Results are obtained as follows. When an optimization measure is chosen, e.g., travel time, the SNNH algorithm is applied with the corresponding point-to-point algorithm, in this example, the quickest path one. The results, which are obtained without considering congestion, are reported in Table 4 under the columns TT, Fuel and Cost. Then, each solution is evaluated by considering congestion on each of the selected path leading to the results under the columns TD-TT, TD-Fuel and TD-Cost. If we take instance S1 as an example with the travel time as optimization objective, the associated travel time without congestion is 1900. When congestion is applied to this solution, the real travel time increases to 3104. The relative difference between the two solutions, measured as (3104−1900)/3104, is reported under the Gap (%) column. Table 4.4 shows that using the TD algorithm TDNNH for this instance yields a travel time of 2472 leading to an improvement of 20.36% which demonstrates the value of considering congestion during the resolution process.

From Table 4.4 we see that solutions with respect to minimization objectives show similar patterns: SNNH applied on real-world network generates a high gap between 20 and 36.47% for key evaluation metrics, namely, travel time, fuel consumption, and cost under realistic traffic congestion. For example, when applying the cost optimization objective, there is an average gap of 36.47% on travel time (15,309.18 vs 24,096.55 seconds) and 20.66% on fuel (96.43 vs 121.54 liters), leading to a gap of 30.06% on overall cost (241.00 vs 344.59$). Additionally, with the SNNH, on average, in 73.91% (#LRTD is 2.55 out of 3.45 routes) of cases, vehicles return

late to the depot. However, with the TDNNH, all solutions respect the time window associated with the depot (#LRTD is 0 for all instances). One explanation could be the underestimation of congestion effects on delays across selected paths between customers. Hence, fixed speed calculations are not sufficiently accurate compared to TD ones, which affects the efficiency of route plans. Therefore, these results show that time-varying speeds have a strong impact on fuel consumption and cost computations.

As shown in Table 4.4, compared to the SNNH we observe that the TDNNH yields the best solutions over all instances under real-world networks considering time-varying speeds enabling more fuel and cost savings. When looking at the cost optimization objective, we can see that for all S*, M* and L* instances, the TDNNH produces an average travel time of 21,576.82 seconds, which is 10.46% lower than SNNH (24,096.55 seconds). Second, the fuel consumption reported by the TDNNH (under the cost objective) is 116.24 liters for a distance of 246.55 km which corresponds to 47.15 liters/100 km, which is 4.36% lower than the SNNH (121.54 liters). The obtained value is very close to the average consumption of 46.90 reported by the annual statistical report of Transports Canada (2017). Finally, the TDNNH generates global savings on overall cost of 7.98% (317.08 instead of 344.59$). It is remarkable that the same patterns hold for travel time and fuel objectives. This exposes the error margin associated with using speed limits instead of using calculations with time-varying speeds. These results clearly show that the quality of route plans strongly increase if we consider time-varying speeds using TDNNH compared to those generated with SNNH that uses fixed speeds and that are adjusted considering traffic congestion.

Table 4.5 shows that our improvement heuristic TDNSIH is able to improve solutions generated by the TDNNH heuristics using the cost optimization criterion. Regarding the quality of the solution, as measured by fuel consumption reduction and cost improvements when compared to the previous solution, we see that the saving on overall costs with respect to medium demands is of up to 7.51% combined with an overall decrease of travel time by 3.54% and a reduction on fuel consumption by 6.89%. As expected the proposed TD exchange moves produce alternative paths that allow congestion avoidance yielding potential reductions of travel times, fuel consumption and costs. Note that the TDNSIH is time-consuming as it runs multiple exchange operators to improve input solutions, which requires finding and computing alternative paths on the multigraph.

Regarding the performance and scalability of the TDNNH, the results from Table 4.6 reported for instance with medium demand show that in terms of computational time (CPU) our heuristic is very effective even for large instances with 300-500 customers. As an example, for the travel time objective, solving 100 customer instances M1 requires only 8.08–8.80 seconds. The global average runtime over all optimization objectives vary from 17.99 to 26.38 seconds. This is due to the fact that the TDNNH applies a goal directed search based on the fast computation of point-to-point paths between customer nodes.

Table 4.4: Computational results of the SNNH and TDNNH for different optimization criteria considering low demand patterns

Optimization measure	Instances	SNNH												TDNNH									
		Dist	TT	TD-TT	Gap (%)	Fuel	TD-Fuel	Gap (%)	Cost	TD-Cost	Gap (%)	#Routes	#LD	#LRTD	Dist	TD-TT	Imp (%)	TD-Fuel	Imp (%)	TD-Cost	Imp (%)	#Routes	#LD	#LRTD
Travel Time	S1	28787.50	1900	3104	38.79	10.89	14.76	26.22	29.03	43.36	33.05	1	10	0	28992.49	2472	20.36	12.72	13.82	35.64	17.80	1		
	S2	29694.17	2117	3895	45.65	11.98	17.39	31.11	31.77	53.10	40.17	1	20	0	30962.95	2933	24.70	14.65	15.76	41.78	21.32	1		
	S3	39601.42	2794	4903	43.01	16.27	22.55	27.85	42.46	67.61	37.20	1	30	0	42113.26	3766	23.19	19.58	13.17	54.52	19.36	1		
	S4	51468.95	3806	5249	27.49	21.49	25.93	17.12	57.07	74.43	23.32	1	40	0	59307.18	5147	1.94	25.64	-4.94	75.04	-0.82	1		
	S5	61427.71	4413	6363	30.65	25.79	31.72	18.69	67.17	90.56	25.83	1	50	0	59314.43	5305	16.63	28.07	11.51	77.37	14.56	1		
	M1	158886.82	10903	18117	39.82	66.63	87.79	24.10	169.30	254.95	33.59	2	100	2	164008.87	15422	14.88	79.40	9.56	222.40	12.77	3	0	0
	M2	196510.46	14327	23588	39.26	82.70	110.59	25.22	216.88	327.67	33.81	3	150	2	218106.04	20160	14.53	104.61	5.41	291.66	10.99	4		
	M3	241989.70	17167	28292	39.32	101.65	134.18	24.24	262.82	394.79	33.43	4	200	3	274611.38	25329	10.47	131.70	1.85	366.76	7.10	5		
	L1	504617.79	30076	42854	29.82	205.05	242.10	15.30	491.46	642.67	23.53	6	300	5	526368.51	41454	3.27	236.39	2.36	624.21	2.87	7		
	L2	583468.65	35586	55162	35.49	238.12	292.31	18.54	576.32	805.04	28.41	8	400	7	623879.88	51084	7.39	284.31	2.74	761.17	5.45	9		
	L3	691278.03	42872	67142	36.15	283.22	350.32	19.15	690.11	973.58	29.12	10	500	9	714542.23	58942	12.21	331.31	5.43	882.01	9.41	10		
	Average	**235248.29**	15087.36	23515.36	35.84	96.71	120.88	20.00	239.49	338.89	29.33	**3.45**	163.64	2.55	249291.57	**21092.18**	10.30	**115.45**	4.49	**312.05**	7.92	3.91	0	0
Fuel Consumption	S1	27183.97	1948	3082	36.79	10.88	14.26	23.7	29.07	42.6	31.76	1	10	0	27754.5	2526	18.04	12.62	11.50	35.98	15.54	1		
	S2	29603.16	2118	3920	45.97	11.97	17.45	31.40	31.76	53.39	40.51	1	20	0	30960.31	2933	25.18	14.65	16.05	41.78	21.75	1		
	S3	37079.26	2761	5038	45.20	15.42	22.42	31.22	41.19	54.82	24.86	1	30	0	36824.82	3786	24.85	18.45	17.71	53.39	2.61	1		
	S4	47489.11	3595	5067	29.05	20.04	24.53	18.30	53.6	71.28	24.80	1	40	0	49569.13	4857	4.14	24.28	1.04	69.20	2.92	1		
	S5	56903.32	4200	5911	28.95	24.10	29.32	17.80	63.41	83.96	24.48	1	50	0	55676.97	5372	9.12	27.45	6.38	77.23	8.02	1		
	M1	140865.74	10554	17339	39.13	60.61	81.12	25.28	159.42	240.67	33.76	2	100	1	161858.78	16390	5.47	81.60	-0.59	233.16	3.12	3	0	0
	M2	189060.07	14145	23083	38.72	81.20	108.28	25.01	213.63	320.73	33.39	3	150	2	199829.99	20821	9.80	102.84	5.02	295.25	7.94	4		
	M3	239271.14	17681	25376	30.32	102.00	127.39	19.93	267.59	362.19	26.12	4	200	2	240960.33	24894	1.90	123.59	2.98	353.73	2.34	5		
	L1	470094.37	31439	48961	35.79	195.32	246.06	20.62	491.85	699.13	29.65	6	300	5	515976.69	44620	8.87	243.06	1.22	658.79	5.77	7		
	L2	556234.92	38286	60495	36.71	233.00	297.64	21.72	593.38	856.488	30.72	8	400	7	608081.81	54046	10.66	288.48	3.08	791.14	7.63	9		
	L3	606845.94	41756	65138	35.90	254.89	322.66	21.00	648.05	924.73	29.92	10	500	9	679157.74	61334	5.84	324.93	-0.70	895.00	3.21	11		
	Average	**218239.18**	15316.64	23946.36	36.04	91.77	117.38	21.82	235.72	337.27	30.11	**3.45**	163.64	2.36	236968.28	**21961.73**	8.29	**114.72**	2.27	**318.6**	5.54	4	0	0
Cost	S1	27728.22	1908	3076	37.97	10.89	14.38	24.27	28.73	42.69	32.70	1	10	0	28728.49	2472	19.64	12.67	11.89	35.59	16.63	1		
	S2	29603.16	2118	3920	45.97	11.97	17.45	31.40	31.76	53.39	40.51	1	20	0	30960.31	2933	25.18	14.65	16.05	41.78	27.75	1		
	S3	37079.26	2761	5038	45.20	15.42	22.42	31.22	41.19	68.60	39.96	1	30	0	41336.73	3766	25.25	19.41	13.43	54.33	20.80	1		
	S4	51276.43	3844	5281	27.21	21.50	25.91	17.02	57.39	74.69	23.16	1	40	0	50953.14	4920	6.84	24.70	4.67	70.23	5.97	1		
	S5	60293.60	4419	6306	29.92	25.45	31.18	18.38	66.83	89.45	25.29	1	50	0	58066.54	5261	16.57	27.68	11.23	76.56	14.41	1		
	M1	154938.57	11243	18948	40.66	65.68	88.76	26.00	171.09	263.10	34.97	2	100	1	179326.06	16941	10.59	87.07	1.90	244.12	7.21	3	0	0
	M2	190181.47	13625	22529	39.52	79.75	106.39	25.04	207.5	313.85	33.89	3	150	2	188471.62	18441	18.15	94.17	11.49	265.05	15.55	3		
	M3	239333.76	17217	28142	38.82	100.89	133.35	24.34	262.37	392.56	33.16	4	200	3	272926.74	26763	4.90	135.98	-1.97	383.86	2.22	5		
	L1	525223.48	32059	49250	34.91	211.64	258.45	18.11	515.8	715.84	27.94	6	300	6	555539.51	44986	8.66	251.71	2.61	671.84	6.15	7		
	L2	572652.25	35707	56047	36.29	235.81	292.53	19.39	574.69	812.81	29.30	8	400	7	611756.63	51245	8.57	281.88	3.64	759.75	6.53	9		
	L3	678845.67	43500	66525	34.61	281.69	346.08	18.61	693.70	963.46	28.00	10	500	9	693992.86	59617	10.38	328.73	5.01	884.78	8.17	11		
	Average	**233377.81**	15309.18	24096.55	36.47	96.43	121.54	20.66	241.00	344.59	30.06	**3.45**	163.64	2.55	246550.78	**21576.82**	10.46	**116.24**	4.36	**317.08**	7.98	3.91	0	0

Table 4.5: Computational results of the designed TDNSIH according to the cost optimization criterion

Demand	Instances	TDNSIH									
		Dist	%Imp Dist	TT	%Imp TT	Fuel	%Imp Fuel	Cost	%Imp Cost	#Routes	CPU
Low	S1	28728.49	0.00	2472	0.00	12.67	0.00	35.59	0.00	1	39.04
	S2	30638.77	1.04	2915	0.61	14.54	0.75	41.49	0.69	1	767.77
	S3	35850.53	13.27	3403	9.64	17.24	11.18	48.75	10.47	1	3069.89
	S4	48941.98	3.95	4578	6.95	23.34	5.51	65.75	6.38	1	10763.90
	S5	55820.61	3.87	5058	3.86	26.62	3.38	73.61	3.85	1	12397.93
	Average	39996.08	4.43	3685.20	4.21	18.88	4.16	53.04	4.29	1	5407.71
Medium	S1	28778.85	0.00	2470	0.00	13.09	0.00	36.05	0.00	1	74.00
	S2	45679.38	0.06	4324	2.74	21.96	1.92	62.01	2.41	2	767.77
	S3	48001.51	7.47	4544	8.22	23.43	7.72	65.56	8.02	2	3069.89
	S4	57131.20	1.43	5717	2.26	22.66	21.75	63.76	23.20	3	1184.31
	S5	72972.21	1.03	6744	4.49	34.68	3.07	97.21	3.90	3	950.06
	Average	50512.63	2.00	4759.80	3.54	23.16	6.89	64.92	7.51	2.20	1209.21
High	S1	42236.93	0.00	3733	0.00	19.65	0.00	54.32	0.00	2	55.27
	S2	47077.27	1.05	4486	0.04	22.72	0.39	64.26	0.14	3	767.77
	S3	68510.51	2.03	6422	2.07	33.16	2.01	92.73	2.03	4	3069.89
	S4	90856.53	4.73	8467	6.16	43.95	5.00	122.51	5.69	6	527.79
	S5	108855.57	0.70	10347	1.15	53.23	0.95	149.16	1.07	7	715.48
	Average	71507.36	1.70	6691	1.88	34.54	1.67	96.60	1.79	4.40	1027.24

To further assess the impacts of traffic congestion on travel time, fuel consumption and cost, the results from Table 4.6 show solutions according to departure times first at 07h00 with medium demand. Note that the results of the time-independent SNNH are not reported as fixed speed calculations are incoherent with the following analysis. Globally, we note that in most cases the TDNNH produces coherent results with respect to the optimization objective. As expected, when the fuel consumption minimization criterion is applied, the obtained values of fuel consumption (160.66, 165.06, 165.59 and 161.11 liters when starting at 07h00, 08h00, 09h00 and 10h00, respectively) is lower than the values generated by those obtained when optimizing time. The same pattern holds for cost minimization criterion. From these results we can conclude that minimizing the travel time does not minimize the fuel consumption in such environments.

Regarding the cost minimization criterion, we can see from Table 4.6 that the travel cost is effectively lower with respect to its value when compared against the other minimization criteria, as expected. For the case of 07h00 departure, we notice that the cost minimization objective requires less travel time that when minimizing fuel consumption (27989.27 instead of 28806.55 seconds) but an increase in distance (349729.57 instead of 343220.52 meters), yielding a small reduction in the overall cost by 1.64% (422.56 instead of 429.61$). The same observation holds for the other departure times. This pattern is not observed in the other optimization criteria.

From Table 4.6 we also see that delayed departure times can lead to higher fuel consumption. When looking at the cost minimization criteria we observe that fuel consumption increases on average, by 3.56% (160.57 at 07h00 versus 166.29 liters at 08h00), combined with an increase in travel time of up to 6.34% (27989.27 at 07h00 versus 29764.09 seconds at 08h00), leading to a global fluctuation on overall costs of 5.13% (422.56 at 07h00 versus 444.22$ at 08h00). We observe that allowing flexible departures can lead to better route plans using alternative

paths yielding fuel and cost savings.

Additional experiments were performed to study the impact of delayed departure time and rush hours traffic congestion on key performance metrics. Figure 4.3 shows in more details the impact of flexible departure times on fuel consumption and total costs for a 100 customers instance with medium demands. In Figure 4.3, the results of the TDNNH according to 28 departure times between 06h00 and 14h00 replicate the traffic pattern of Québec City with a moderate morning congestion between 06h00 and 07h45. Then, congestion rapidly increases between 07h45 and 09h15. Between 09h30 and 11h00 drivers face a low traffic congestion leading to lower fuel consumption. Hence, all customers can be served with less fuel and costs when starting between 06h00 and 07h45 or 09h30 and 11h00 compared to other periods. In the afternoon congestion impacts traffic between 13h00 and 13h30 leading to much higher fuel consumption. Interestingly, we observe that even with the same number of vehicles (6 routes for all departure times) congestion has a considerable impact on fuel consumption. These results clearly show that allowing delayed or flexible departures may lead to better alternative paths by avoiding traffic congestion yielding better route plans that lead to the reduction of GHG emissions and savings on overall costs.

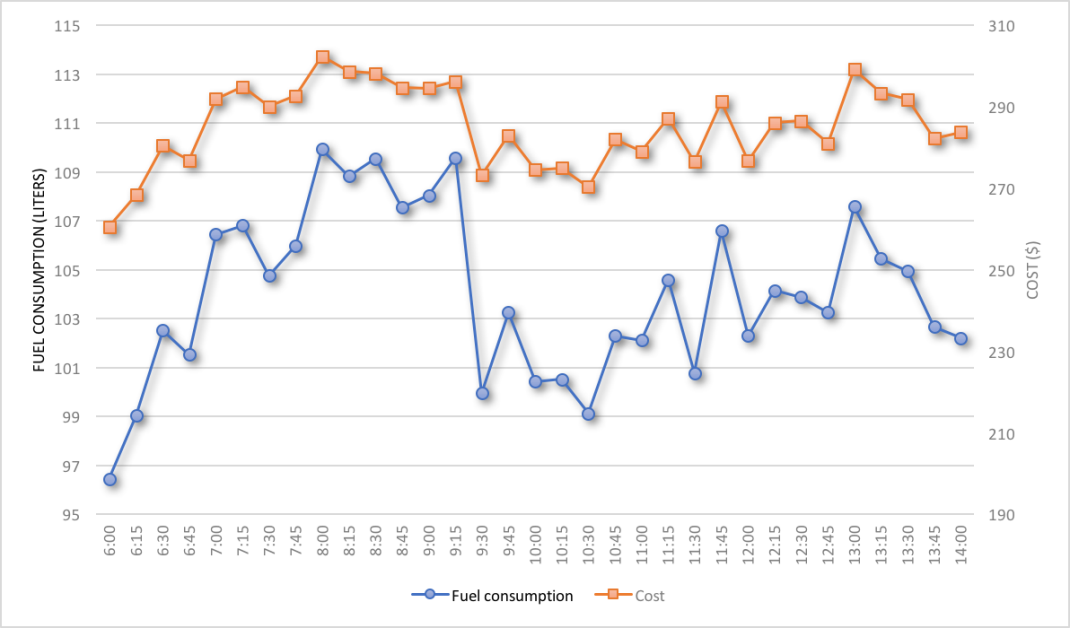

Figure 4.3: Effects of flexible departure times on fuel consumption and costs considering 100 customers with medium demand

Table 4.7 reports the impact of demand size on travel time, fuel consumption and costs. In the light of these results, instances with large demand tend to be more expensive in terms of emission and operational costs compared to low or medium-size ones. Table 4.7 provides some insights on the impact of carried loads over the five performance measures. Results of the TDNNH are obtained under the three minimization criteria. As expected, the number

Table 4.6: Impacts of departure time on the emissions of alternative routes considering medium demand patterns: average using TDNNH for different optimization criteria

Optimization measure	Instances	07h00						08h00						09h00						10h00					
		Dist	TT	Fuel	Cost	#Routes	CPU	Dist	TT	Fuel	Cost	#Routes	CPU	Dist	TT	Fuel	Cost	#Routes	CPU	Dist	TT	Fuel	Cost	#Routes	CPU
Travel Time	S1	30479.42	2470	13.565	36.60	1	0.48	29259.33	2470	13.17	36.14	1	0.48	29515	2636	13.83	38.31	1	0.529	29899.12	2596	13.87	38.01	1	0.48
	S2	45183.64	3964	20.91	57.74	2	0.98	40001.63	3517	18.713	51.42	2	0.86	45966.38	4384	22.25	62.85	2	0.90	40765.36	3661	19.38	53.41	2	0.87
	S3	53283.55	4734	25.03	69.018	2	1.24	50780.25	4719	24.45	68.22	2	1.191	53516.93	5034	26.025	72.72	2	1.223	51015.77	4790	24.753	69.18	2	1.23
	S4	67197.60	5782	30.47	84.19	3	1.83	65390.99	6224	31.49	89.11	3	1.575	69985.27	6292	32.68	91.07	3	1.639	60796.34	5861	29.44	83.68	3	1.55
	S5	77563.11	7049	36.56	101.96	3	2.10	76327.99	7247	36.84	103.96	3	1.96	75196.50	6983	36.00	100.76	3	1.99	77551.74	7038	36.77	102.10	3	2.07
	M1	218023.12	19486	104.75	286.10	6	8.29	214312.95	19193	103.14	281.75	6	8.98	228573.44	19522	107.25	289.28	6	8.24	224089.17	19319	105.57	285.62	6	8.80
	M2	276466.88	23781	130.25	351.92	8	12.66	288301.37	25403	137.85	374.45	8	13.28	270831.92	24063	129.81	353.81	8	13.06	265559.76	22538	124.4	334.63	8	12.26
	M3	365308.21	31395	171.65	464.26	11	16.86	389170.72	34771	187.08	510.70	11	17.49	357800.20	31665	170.96	465.76	11	16.70	365180.53	30021	168.44	448.89	11	16.44
	L1	791357.29	57747	350.72	894.17	16	40.79	782633.89	60278	355.41	921.08	16	39.19	812023.11	59784	364.15	926.93	16	39.46	765692.29	55157	339.18	858.89	16	41.40
	L2	949506.48	70540	427.15	1090.82	21	51.98	991180.12	75926	452.66	1165.92	21	50.70	945550.06	70648	427.16	1091.74	21	56.60	952795.68	69983	425.66	1084.37	21	51.71
	L3	1135763.90	82678	506.25	1284.95	26	63.735	1139216.20	88359	525.10	1354.91	26	62.18	1152256.40	86819	521.53	1337.72	26	61.42	1139656.40	83981	513.45	1304.30	26	61.40
	Average	364557.56	28147.82	165.21	429.25	9	18.27	369688.68	29827.91	171.44	450.70	9	17.99	367383.2	28893.64	168.33	439.18	9	18.34	361182.01	**27722.27**	163.72	423.92	9	18.02
Fuel Consumption	S1	28268.68	2535	13.11	36.63	1	0.65	27728.87	2565	13.14	36.91	1	0.55	28239.25	2689	13.65	38.56	1	0.56	27557.55	2679	13.47	38.26	1	0.58
	S2	43303.85	3971	20.54	57.3724	2	1.07	45663.87	4446	22.38	63.52	2	1.15	45038.12	4392	22.12	62.77	2	1.07	43184.99	4333	21.61	61.68	2	1.07
	S3	50340.76	4711	24.16	67.8214	2	1.38	48312.55	4913	24.39	69.81	2	1.38	49684.01	5039	25.06	71.65	2	1.34	48276.76	4790	23.98	68.29	2	1.40
	S4	56684.72	5416	27.38	77.52	3	1.81	56930.82	5910	28.98	83.56	3	1.81	64412.77	6304	31.48	89.79	3	1.88	57403.19	5934	29.07	83.86	3	1.85
	S5	66279.16	6245	31.91	89.77	3	2.26	72336.26	7102	35.653	101.37	3	2.29	66895.16	6549	32.92	93.53	3	2.23	67149.44	6655	33.26	94.82	3	2.26
	M1	216729.08	20216	105.67	293.36	6	10.13	224435.65	21775	111.61	313.44	6	10.16	219218.81	20736	107.66	300.07	6	10.17	214083.06	19889	104.87	289.66	6	9.97
	M2	263651.68	25379	130.83	366.17	8	15.33	263994.67	26084	132.55	374.14	8	15.27	260370.51	25132	128.97	361.94	8	15.00	242653.86	23219	120.20	335.59	8	15.01
	M3	343197.35	32073	168.03	465.86	11	19.78	326875.12	32713	167.09	470.22	11	19.99	337824.65	31895	166.78	462.90	11	19.76	346888.29	31682	168.05	462.55	11	19.70
	L1	760586.21	59333	344.53	900.55	16	51.71	735637.12	61063	342.73	913.17	16	53.40	779393.06	63408	358.58	951.33	16	50.25	733733.37	59196	337.43	891.21	16	50.59
	L2	884681.06	71607	410.00	1080.16	21	65.82	910252.34	77263	432.43	1154.03	21	63.83	926827.54	75722	430.76	1139.01	21	63.32	890330.51	73301	414.98	1100.29	21	63.22
	L3	1061703.2	85386	491.07	1290.52	26	80.35	1067284.70	90303	504.77	1348.06	26	79.04	1077163.70	88315	503.53	1329.74	26	78.75	1092351.10	87956	505.32	1328.74	26	78.83
	Average	**343220.52**	28806.55	160.66	429.61	9	22.75	**343586.54**	30376.09	**165.06**	448.02	9	22.62	**350460.69**	30016.45	165.59	445.57	9	22.21	**342146.56**	29057.64	**161.11**	432.27	9	22.22
Cost	S1	28590.28	2484	13.072	36.15	1	0.63	28778.85	2470	13.09	36.05	1	0.64	29509.17	2636	13.83	38.31	1	0.63	28596.47	2558	13.31	37.05	1	0.62
	S2	43448.91	3971	20.569	57.41	2	1.14	45707.28	4446	22.39	63.54	2	1.18	45434.61	4384	22.16	62.75	2	1.15	39327.56	3678	18.98	53.09	2	1.14
	S3	53645.44	4654	24.836	68.12	2	1.55	51874.55	4951	25.39	71.28	2	1.55	51059.78	4981	25.17	71.28	2	1.52	49893.00	4802	24.42	68.90	2	1.48
	S4	58800.72	5286	27.476	76.53	3	2.06	57960.88	5849	28.96	83.02	3	2.07	64930.74	6292	31.56	89.77	3	2.09	59000.68	5835	29.07	83.03	3	1.89
	S5	69397.56	6299	32.642	91.08	3	2.50	73734.26	7061	35.78	101.16	3	2.51	73979.65	6882	35.35	99.15	3	2.55	75254.39	6781	35.43	98.38	3	2.57
	M1	218607.40	19497	104.23	285.59	6	11.30	225560.02	20700	109.93	302.37	6	11.74	213804.99	19707	103.62	286.67	6	10.33	210175.53	18713	100.44	274.57	6	10.86
	M2	277086.37	25166	132.95	366.80	8	16.65	282782.19	26091	138.22	380.73	8	18.79	277440.83	24913	132.50	364.13	8	17.26	254759.73	22922	122.07	335.22	8	17.87
	M3	340510.47	30598	164.43	449.18	11	23.43	351031.59	32781	172.82	477.38	11	23.67	346698.40	31189	166.55	456.64	11	23.35	345371.96	30328	163.86	446.23	11	22.97
	L1	779854.70	57737	347.02	889.83	16	59.39	749278.21	59939	345.03	906.26	16	60.10	786083.18	59677	354.11	914.49	16	57.86	793413.91	58210	351.46	898.96	16	57.76
	L2	911031.30	69486	411.07	1063.36	21	75.05	912630.60	74141	424.05	1117.86	21	76.00	889145.04	70469	409.44	1069.85	21	73.45	910834.93	69534	412.11	1064.97	21	74.62
	L3	1066019.10	82704	487.95	1264.13	26	92.62	1099216.10	88976	513.49	1346.81	26	91.94	1115233.90	86046	509.99	1317.88	26	90.50	1105616.90	84137	501.23	1291.58	26	93.03
	Average	349726.57	**27989.27**	**160.57**	**422.56**	9	26.03	352595.87	**29764.09**	166.29	**444.22**	9	26.38	353938.21	**28834.18**	**164.02**	**433.72**	9	25.52	352022.28	27954.36	161.13	**422.91**	9	25.89

routes increases when the volume of orders increases, which has a considerable impact on the level of fuel consumption and overall costs. For the cost minimization objective, both fuel consumption and cost doubled from 116.24 liters and 318.01$ (case of low demands) to 280 liters and 736.29$ (case of high demands). This behavior is coherent with the fact that, proportionally, fuel consumption increases as both load and the number of routes increase, on average, from 3.91 to 20.27. Additionally, we have noticed that fuel consumption increases by 43.06% (116.24 vs 166.29 liters) in the case of medium demand against 140.88% (116.24 vs 280 liters) for high demand one. A key finding is that combining heterogeneous loads (case of medium demand) could be beneficial in optimizing both fuel consumption and costs.

4.6 Conclusions

In this paper we have studied the Time-dependent Vehicle Routing Problem with Emission and Cost Minimization considering time-varying speeds and dynamic paths. In order to solve it, we have developed an efficient method combining a goal directed search heuristic, called Time-dependent Nearest Neighborhood heuristic (TDNNH) with a Time-dependent Neighborhood Search Improvement heuristic (TDNSIH). An efficient adaptation of the Dijkstra label-setting algorithm to a time-dependent setting is embedded into the solution methods to perform the fast computation of time-dependent point-to-point paths connecting pairs of customers nodes based on different measures, namely fuel consumption (TDLEP), time (TDQP) or cost (TDLCP) leading to a larger search space and further opportunities of optimization in large time-dependent road networks. The results of extensive computational experiments on real-life benchmark instances demonstrate that taking dynamic paths into account according to time-varying speeds yields good quality solutions in a very consistent manner using the TDNSIH, outperforming the classical SNNH with fixed speed limits. In fact, some routes that were evaluated as profitable can now appear as not viable candidates in the case of time-dependent network modeled as a multigraph which reflect more realistic scenarios.

Moreover, our analyses have shown that potential reduction in GHG emissions and costs are achievable through flexible departure times, which allows congestion avoidance considering alternative paths between customers. Additionally, we have observed that the size of orders affects paths choice decision yielding different route plans with higher level of fuel consumption. Further research can now focus on generalizing these methods to broader distribution problems, namely the time-dependent inventory-routing and dynamic vehicle routing problems.

Acknowledgments

This research was partly supported by grants 2014-05764 and 0172633 from the Natural Sciences and Engineering Research Council of Canada (NSERC) and by the Centre d'Innovation

Table 4.7: Impact of the variation in demand on the emissions of routes: average across TDVRP-ECMDP benchmark instances using the TDNNH

Optimization measure	Instances	Low demand					Medium demand					High demand				
		Dist	TT	Fuel	Cost	#Routes	Dist	TT	Fuel	Cost	#Routes	Dist	TT	Fuel	Cost	#Routes
Travel Time	S1	28992.49	2472	12.72	35.64	1	29259.33	2470	13.17	36.14	1	42626.35	3733	19.72	54.41	2
	S2	30962.95	2933	14.65	41.78	1	40001.63	3517	18.71	51.42	2	48052.05	4480	22.90	64.41	3
	S3	42113.26	3766	19.58	54.52	1	50780.25	4719	24.45	68.22	2	74419.39	6604	34.99	96.37	4
	S4	59307.18	5147	27.21	75.04	1	65390.99	6224	31.49	89.11	3	103226.39	9436	49.17	136.75	6
	S5	59314.43	5305	28.07	77.37	1	76327.99	7247	36.837	103.962	3	111835.09	10446	54.10	151.01	7
	M1	164008.87	15422	79.40	222.40	3	214312.95	19193	103.14	281.75	6	315950.70	28722	153.02	420.11	13
	M2	218106.04	20160	104.61	291.66	4	288301.37	25403	137.85	374.45	8	435925.17	38231	208.21	564.41	18
	M3	274611.38	25329	131.70	366.76	5	389170.72	34771	187.08	510.70	11	582756.17	51558	279.64	759.832	25
	L1	526368.51	41454	236.39	624.21	7	782633.89	60278	355.41	921.079	16	1323580.20	99727	599.26	1536.83	36
	L2	623879.88	51084	284.31	761.17	9	991180.12	75926	452.66	1165.92	21	1630572.70	124152	742.55	1909.22	48
	L3	714542.23	58942	331.31	882.01	10	1139216.20	88359	525.10	1354.91	26	2081732.70	158484	948.21	2437.56	61
	Average	249291.57	21092.18	115.45	312.05	3.91	369688.68	29827.91	171.45	450.70	9	613697.90	48688.45	282.89	739.17	20.27
Fuel Consumption	S1	27754.50	2526	12.62	35.98	1	27728.87	2565	13.14	36.91	1	40886.59	3784	19.46	54.5429	2
	S2	30960.31	2933	14.65	41.78	1	45663.87	4446	22.38	63.52	2	47578.51	4484	22.81	64.35	3
	S3	36824.82	3786	18.45	53.39	1	48312.55	4913	24.39	69.81	2	73882.84	6982	36.05	100.80	4
	S4	49569.13	4857	24.28	69.20	1	56930.82	5910	28.98	83.56	3	92940.35	9079	45.88	129.93	6
	S5	55676.97	5372	27.45	77.23	1	72336.26	7102	35.65	101.37	3	105710.78	10443	53.28	150.04	7
	M1	161858.78	16390	81.60	233.16	3	224435.65	21775	111.61	313.44	6	281374.75	27751	142.54	399.80	12
	M2	199829.99	20821	102.84	295.25	4	263994.67	26084	132.55	374.14	8	401711.55	39298	202.62	567.04	18
	M3	240960.33	24894	123.59	353.73	5	326875.12	32713	167.09	470.22	11	555849.38	52904	276.51	767.67	25
	L1	515976.69	44620	243.06	658.79	7	735637.12	61063	342.73	913.17	16	1277676.6	102856	592.24	1555.35	36
	L2	608081.81	54046	288.48	791.139	9	910252.34	77263	432.43	1154.03	21	1613860.5	133783	756.42	2007.04	48
	L3	679157.74	61334	324.93	895.004	11	1067284.70	90303	504.77	1348.06	26	1970353.5	162889	927.37	2451.03	61
	Average	236968.28	21961.73	114.72	318.60	4	343586.54	30376.09	165.06	448.02	9	587438.67	50386.64	279.56	749.78	20.18
Cost	S1	28728.49	2472	12.67	35.59	1	28778.85	2470	13.09	36.05	1	42236.93	3733	19.6	54.32	2
	S2	30960.31	2933	14.65	41.78	1	45707.28	4446	22.39	63.54	2	47578.51	4484	22.81	64.35	3
	S3	41336.73	3766	19.41	54.33	1	51874.55	4951	25.39	71.28	2	69933.53	6558	33.84	94.65	4
	S4	50953.14	4920	24.70	70.23	1	57960.88	5849	28.96	83.02	3	95368.84	9023	46.26	129.90	6
	S5	58066.54	5261	27.68	76.56	1	73734.26	7061	35.78	101.16	3	109621.49	10467	53.74	150.77	7
	M1	179326.06	16941	87.07	244.12	3	225560.02	20700	109.93	302.37	6	298359.01	27595	146.00	402.45	12
	M2	188471.62	18441	94.17	265.05	3	282782.19	26091	138.22	380.73	8	434687.07	37380	205.40	553.94	18
	M3	272926.74	26763	135.98	383.86	5	351031.59	32781	172.82	477.38	11	549997.86	48975	264.77	720.78	25
	L1	555539.51	44986	251.71	671.84	7	749278.21	59939	345.03	906.26	16	1324648.10	98306	598.40	1523.76	36
	L2	611756.63	51245	281.88	759.75	9	912630.60	74141	424.05	1117.86	21	1673384.10	126721	761.85	1953.26	49
	L3	693992.86	59617	328.73	884.78	11	1099216.10	88976	513.49	1346.81	26	2046900.60	152708	929.63	2367.09	61
	Average	246550.78	21576.82	116.24	317.08	3.91	352595.87	29764.09	166.29	444.22	9	601469.90	48739.18	280.00	736.29	20.27

en Logistique et Chaîne d'Apporovisionnement Durable (CILCAD). We also thank Mr Jean-Philippe Gagliardi, President of Logix Operations inc, for providing us with real data from an important wholesaler partner in Québec city. This support is highly appreciated.

Appendix B

CMEM parameters

We set the values of the CMEM input parameters based on the specification of Barth and Boriboonsomsin (2009) as follows: the curb-weight $\omega = 15000\ kg$, carried load q between 0-10000 kg, fuel-to-air mass ratio $\zeta = 1$, engine friction factor $k = 0.25\ kJ/rev/L$, engine speed $N_e = 60$, engine displacement $V = 7\ L$, gravitational constant $g = 9.81\ m/s^2$, air density $\rho = 1.2041\ k/m^3$, coefficient of aerodynamic drag $C_d = 0.7$, frontal surface area $A = 3.912\ m^2$, coefficient of rolling resistance $C_r = 0.01$, vehicle drive train efficiency $\eta_{tf} = 0.4$, efficiency parameter for diesel engines $\eta = 0.9$, fuel and GHG emissions cost per liters $c_f = 1.2$ \$CAD/liters, driver wage $c_d = 0.0085$ \$CAD/s, heating value of a typical diesel fuel $\varpi = 44\ kJ/g$, conversion factor from g/s to L/s $\psi = 737$, lower speed limit $s^l = 1.388\ m/s$, upper speed limit $s^u = 30.555\ m/s$, acceleration $a = 0\ m/s^3$, and roadway gradient $\theta = 0$ degree.

Appendix C

Time-dependent Dijkstra label-setting algorithm

The TD-Dijkstra algorithm is applied to determine time-dependent paths by using a node-examination process considering time-varying speeds from an origin o to a destination d. A pseudocode is presented in Algorithm 3.1.

Algorithm 3.1 Time-dependent Dijkstra label-setting algorithm (TD-Dijkstra)

function TD_DIJKSTRA($o, d, t, \mathcal{G}^T$)
  $E \leftarrow \varnothing$, $N \leftarrow \mathcal{V}^T$, $predecessor(o) \leftarrow o$, $c_o \leftarrow 0$, $c_u \leftarrow \infty | \tau_u \leftarrow 0$, $\forall u \in \mathcal{V}^T$
  while $|E| < n$ **do**
    let $u \in N$ be a node for which $c_u \leftarrow \min\{c_v : v \in N\}$
    $E \leftarrow E \cup \{u\}$, $N \leftarrow N \backslash \{u\}$
    if $u = d$ **then**
      Stop
    end if
    $t \leftarrow t + \tau_u$
    for each $(u, v) \in E_+^T(u)$ **do**
      if $c_v > \left[TD\_Cost\_FSM(t, (u, v), \mathcal{Z}^T) \longrightarrow c_{uv}(t)\right]$ **then**
        $c_v \leftarrow c_u + \left[TD\_Cost\_FSM(t, (u, v), \mathcal{Z}^T) \longrightarrow c_{uv}(t)\right]$
        $\tau_v \leftarrow c_u + \left[TD\_Cost\_FSM(t, (u, v), \mathcal{Z}^T) \longrightarrow \tau_{uv}(t)\right]$
        $predecessor(v) \leftarrow u$
      end if
    end for
  end while
end function

Chapter 5

Measuring emissions in vehicle routing: new emission estimation models using supervised learning

Résumé

Dans cet article, nous proposons et évaluons la précision de nouveaux modèles d'estimation des émissions pour le routage des véhicules. En se basant sur des données réelles de consommation instantanée de carburant, de vitesses variables dans le temps et des données de trafic liées à un grand nombre de livraisons, nous proposons des méthodes efficaces d'estimation des émissions de gaz à effet de serre (GES). En effectuant une analyse de régression non linéaire à l'aide de méthodes d'apprentissage supervisé, à savoir les réseaux neuronaux, les machines à vecteurs de support, les arbres d'inférence conditionnelle et la descente de gradient, nous développons de nouveaux modèles d'émission plus précis que les modèles classiques. Nous estimons correctement les émissions pour un déplacement de bout en bout en fonction du temps dans des conditions réalistes en tenant compte des opérations de transport de marchandises pendant l'heure de pointe, des schémas de conduite arrêt-départ, des états de ralenti et de la variation des charges. Des expérimentations numériques approfondies sur un jeu de données réelles montrent l'efficacité des modèles d'émissions basés sur l'apprentissage automatique, dépassant nettement le modèle CMEM (Comprehensive Modal Emissions Model) et celui du MEET (Predictive Pollution Emissions Transport) en termes de la prévision des émissions en se référant aux mesures de l'erreur quadratique moyenne. Sur la base des indicateurs de performance, nous montrons que le MEET sous-estime les émissions de GES réelles de 24,94% et que le CMEM conduit à une surestimation des émissions de 13,18% en fonction de la consommation de carburant observée, alors que l'écart de précision de notre meilleur modèle d'apprentissage (Gradient Boosting Machines) est de seulement 1,70% par rapport aux conditions de conduite réelles. Des tests statistiques confirment l'efficacité de nos nouveaux

modèles.

Chapter information A research paper based on this chapter, named *Measuring emissions in vehicle routing: new emission estimation models using supervised learning*, has been submitted to the journal Production Operations Management (POMS) by Heni H., Diop S. A., Coelho L. C., and Renaud J. in March 2018.

Abstract

In this paper we propose and assess the accuracy of new emission models for vehicle routing. Based on real-world data of instantaneous fuel consumption, time-varying speeds observations, and traffic data related to a large set of shipping operations we propose effective methods to estimate greenhouse gas (GHG) emissions. By carrying out nonlinear regression analysis using supervised learning methods, namely Neural Networks, Support Vector Machines, Conditional Inference Trees, and Gradient Boosting Machines, we develop new emission models that provide more prediction accuracy than classical models. We correctly estimate emissions for time-dependent point-to-point routing under realistic conditions taking into account freight transportation operations during peak hour traffic congestion, stop and go driving patterns, idle vehicle states, and the variation of vehicle loads. Extensive computational experiments under real data sets show the effectiveness of the proposed machine learning emissions models, clearly outperforming the Comprehensive Modal Emissions Model (CMEM) and the Methodology for Estimating air pollutant Emissions from Transport (MEET) in the prediction of hot running traffic emissions according to root mean square error metrics. Based on performance indicators we show that MEET underestimates real-world GHG emissions by 24.94% and CMEM leads to an overestimation of emissions by 13.18% according to observed fuel consumption, while our best machine learning model (Gradient Boosting Machines) exhibited superior estimation accuracy and is off by only 1.70% considering real-world driving conditions. Statistical tests confirm the efficiency of our new models.

Keywords: emissions models; time-dependent routing; traffic congestion; machine learning.

5.1 Introduction

Freight transportation is known to be an important source of greenhouse gas (GHG) emissions (Transports Canada 2017). GHG emissions are proportional to the fuel consumption which in turn, depends on several factors including speed, acceleration, distance, weight of the vehicle, backhauls and roadway slope (Demir, Bektaş, and Laporte 2014b).

Accurate emissions estimation is a valuable information for transportation experts in making effective decisions that improve routing operations. The current literature on GHG emissions for road freight transportation offers different models for estimating emission and fuel consumption, the more well-known being the Comprehensive Modal Emissions Model (CMEM) (Barth and Boriboonsomsin 2009) and the Methodology for Estimating air pollutant Emissions from Transport (MEET) (Hickman et al. 1999). Over the last few years, CMEM and MEET have been integrated into various routing models, with a focus on environmental impacts in addition to economic implications.

The CMEM is designed for heavy duty vehicles. It computes GHG emissions of route plans considering the traveled distance, vehicle speed, carried load and roadway gradient. Relevant studies on green vehicle routing calculating the amount of GHG emissions following CMEM are those of Bektaş and Laporte (2011), Demir, Bektaş, and Laporte (2012), and Franceschetti et al. (2017b) in which the objective is to minimize a function comprising emissions and driver costs. Pathak et al. (2016) used CMEM to estimate emissions under real-world driving patterns. Androutsopoulos and Zografos (2017) and Huang et al. (2017) integrated path selection decision on the vehicle routing problems considering a multigraph representation (Garaix et al. 2010, Ticha et al. 2017) for the road network that incorporates the set of candidates paths between all pairs of key-destinations.

Figliozzi (2011), Jabali, Van Woensel, and de Kok (2012), Qian and Eglese (2016), and Ehmke, Campbell, and Thomas (2016a) derived emissions from the MEET model, which allows the conversion of speeds into emissions based on fuel consumption rates that have been derived from engine test-bed measurements. MEET considers the impact of load and roadway gradient through error-corrective parameters.

Real-time traffic congestion, the behavior of freight vehicles across road networks, timely fuel consumption data collected by various sensors, and Global Positioning System (GPS) devices are becoming more present in commercial operations (Hess et al. 2015). With such rich amount of traffic-related data much attention is now accorded to the computation of emission-minimizing paths on very large road networks based on time-dependent speed observations provided by logistics companies using Intelligent Transportation System (ITS) technology (Belhassine et al. 2018). However, different emission estimation models exist and they are based on very distinct assumptions and yield contrasting results. Making an accurate prediction of fuel consumption and emissions is an important aspect of a firm's decision-making

process as realized emissions and fuel price affects the profitability (Drake, Kleindorfer, and Van Wassenhove 2016).

Demir, Bektaş, and Laporte (2011) elaborated a comparative analysis of several vehicle emission models that have been developed to compute GHG emissions associated with road freight transportation. Emission models vary in their performance according to numerous factors such as speed, acceleration, and vehicle types. Turkensteen (2017) evaluated the accuracy of CMEM, indicating that we cannot take for granted that fuel consumption computations assuming fixed speed are accurate in time-dependent routing. The author observed that fixed average speed computations are likely to underestimate emissions. Through sensitivity analysis he showed that much emissions is produced when speed fluctuates and vehicle load increases.

Jaikumar, Nagendra, and Sivanandan (2017) performed a modal analysis of vehicular emissions under real-world driving conditions. They found out that short term events such as acceleration and braking significantly affect emissions. Despite their findings that CMEM underestimates emissions they have only used average speed and acceleration for distances ranging from 1 to 10 km based on field data obtained from an on-board diagnostic tool.

It follows from previous studies that approaches based on aggregated speeds can underestimate GHG emissions. Greater estimation accuracy relies on data that reflects real-world operations in road networks. The last decade has seen substantial advances in building prediction models using machine learning methods, which capture complex nonlinear relationships in the systems under study and produce accurate estimations by learning from the available data (Choi, Wallace, and Wang 2018, Lee 2018). There have been a few studies on the application of machine learning methods for establishing practical emission models that can be used in routing problems with both environmental and operational considerations. Inspired by the need of emissions prediction Zeng, Miwa, and Morikawa (2016) proposed a new emission model derived from the theory of vehicle dynamics. The parameters of their model were computed with the maximum likelihood estimation (MLE), and its accuracy was validated using GPS data collected for a light duty passenger car through a comparative analysis with the Virginia Tech Microscopic Energy and Emission Model (VT-Micro) (Rakha, Ahn, and Trani 2004), Support Vector Machines (SVM) model and Neural Networks (NNET) model. Liu et al. (2016) proposed an effective emissions prediction model of a diesel engine using SVM that can be used by diesel engine manufacturers to accurately measure emissions. Due the growing interest of accurate emissions estimations in road freight transportation field, the current study follows previous streams of literature by applying Gradient Boosting Machines (GBM) method in addition to NNET, SVM and Conditional Inference Trees (CIT) machine learning methods to predict emissions considering relevant variables derived from in-field emissions data considering real-world driving conditions.

From a machine learning point of view a number of opportunities may exist with the availabil-

ity of time-varying speeds observations, instantaneous fuel consumption, roadway gradient, vehicle load, and stop-and-go traffic data related to vehicle trips of logistics and freight companies across large cities. GPS and on-board real-time emission measurement devices provide real-world observations of emissions of micro scale events under real-world traffic congestion. In this work, we used field data collected across the entire road network of Québec City, which contains up to 50,000 road links. The obtained GPS data set contains 58,215 instantaneous fuel consumption and speed observations for 1406 deliveries monitored over 97 days between November 2016 and March 2017. In terms of prediction accuracy, families of supervised learning algorithms are shown to be effective in fitting artificial outputs to the real one. Therefore, using supervised learning methods we build nonlinear emission models considering time-varying speeds, vehicle load fluctuations, stop-and-go driving patterns, acceleration, and breaking events. The contributions of this paper are fourfold:

(i) we propose an effective approach for the computation of GHG emissions in routing considering time-varying speeds;

(ii) we provide several insights concerning fuel consumption through the analysis of real-world emission data considering shipping operations under a large road network with fluctuating traffic congestion and stop-and-go driving patterns;

(iii) we develop efficient nonlinear emission models using NNET, SVM, CIT, and GBM supervised learning methods, which are trained by applying the k-fold cross validation method on real-life GHG emission data acquired by a private-sector retailer from thousands of trips over the course of several months;

(iv) we demonstrate the effectiveness of the proposed supervised learning models at micro scale events compared to MEET and CMEM that incorrectly predicted emissions under realistic driving conditions.

The remainder of this paper is organized as follows. In the following section we review the literature on emissions models for road freight transportation. Section 3 describes the data collection procedure and provides some initial analysis of the available data. In Section 4 we describe the proposed approach for modeling GHG emissions using supervised learning methods. In Section 5, we present results of our extensive computational experimentation and sensitivity analysis of several existing and newly introduced emissions models. Conclusions and directions for future research are stated in Section 6.

5.2 Existing emission estimation models

Motivated by the need to account for traffic congestion effects considering variable speeds, this section describes the existing methods to compute emissions in time-dependent networks

(multigraphs) using CMEM and MEET. To do so, let $\mathcal{G}^T = (\mathcal{V}, \mathcal{A}, \mathcal{Z})$ be a multigraph, where $\mathcal{V}$ is the set of nodes of the road network and $\mathcal{A}$ is the set of arcs or road segments connecting some pairs of nodes in the network (see Figure 5.1). Let $T = z_0 + H\delta$ be the length of the planning horizon, where $\delta > 0$ represents the smallest increment of time over which a change in the speed happens. T is divided into a finite number H time intervals $Z_h = [z_0 + \delta(h-1), z_0 + \delta h[$ considering the set $\mathcal{Z} = \{z_0, z_0 + \delta \, ..., z_0 + H\delta\}$ of discrete times, with $h = 1, 2, ..., H$.

Furthermore, let $\gamma_u(t)$ be a function that provides the arrival time at node u given a starting time t at the source. Any path p from an origin o to a destination d follows an ordered sequence of nodes on the road network and is defined by the schedule of traversing it as:

$$p_{od} = (\gamma_o(t), [o = v_0, v_1, ..., v_{k-1}, v_k = d]) \tag{5.1}$$

where $v_k \in \mathcal{V}$ are road nodes, and k represents the number of nodes of the complete path.

For any road segment $(u, v) \in \mathcal{A}$ let l_{uv} denote the distance between nodes u and v. Let $\tau_{uv}(t)$ and $F_{uv}(t)$ be the time-dependent travel time and the amount of GHG emissions, respectively, related to traveling across the road segment (u, v) when the vehicle leaves node u at time $t \in T$. The travel time function is piecewise linear and satisfies the first-in, first-out (FIFO) rule. With each road segment (u, v) across a given path is associated a time-dependent travel speed $s_{uv}(t)$ when the vehicle leaves node u at time t.

5.2.1 Time-dependent emission function using CMEM

The CMEM is one of the most used emission models in green vehicle routing. It was designed by Barth and Boriboonsomsin (2009) to estimate the amount of emissions generated by a wide variety of vehicles. According to this model, vehicle emissions depend on many environmental and traffic-related parameters, namely load, speed, roadway gradient, among others. Considering vehicle speed s (m/s), total vehicle weight M and roadway gradient θ, CMEM calculates the instantaneous fuel consumption rate (in liters/second) using the following polynomial function:

$$e_r = E_0 \left(E_1 + \left(\frac{(\alpha M + \beta s^2)s}{E_2} + P_{acc} \right) \right), \tag{5.2}$$

where $E_0 = \frac{\zeta}{\varpi\psi}$, $E_1 = kN_eV$, $E_2 = \frac{1}{\varepsilon 1000\eta_{tf}}$, $M = \omega + q$, $\alpha = a + g\sin\theta + gC_r\cos\theta$, and $\beta = 0.5C_dA\rho$ are constant parameters related to the vehicle and its engine such as inertia force, rolling resistance, and other vehicle characteristics. P_{acc} is the engine power demand associated with running losses of the engine and additional vehicle accessories such as air conditioning, typically assumed to be zero. All parameter values used are shown in Table 5.1. Those related to the vehicle specifications are provided and calibrated by the manufacturer.

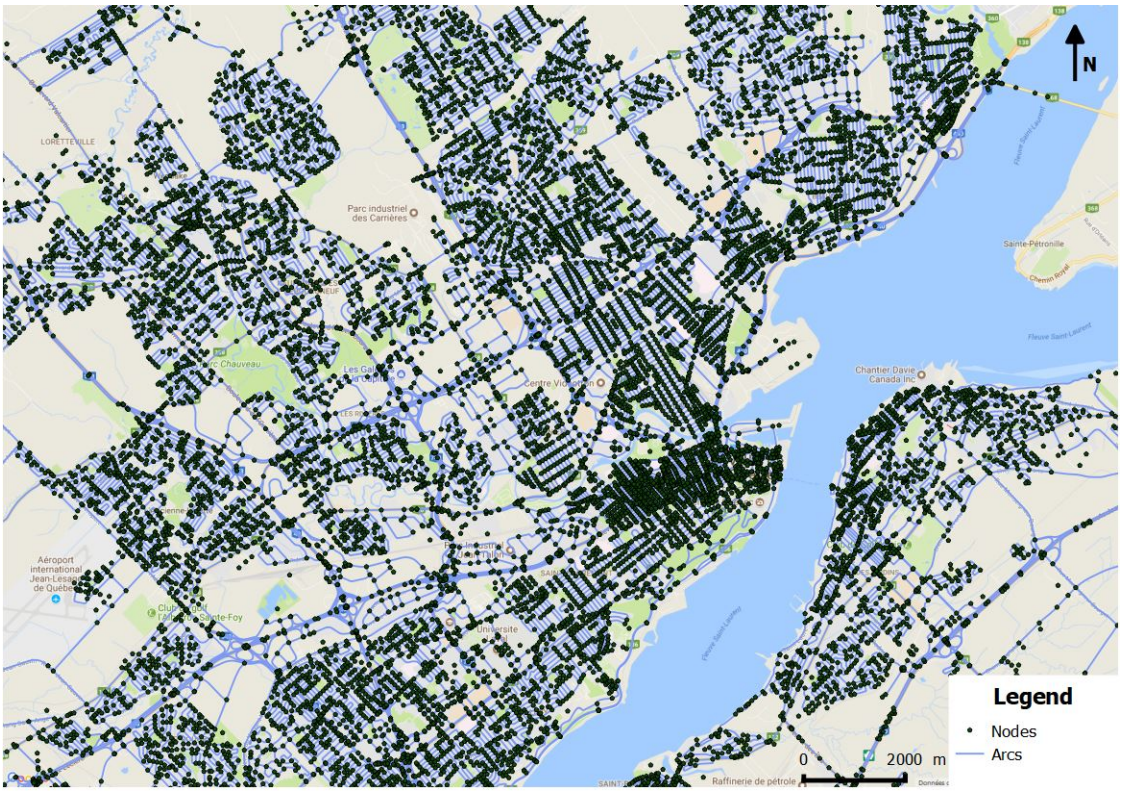

Figure 5.1: Illustration of a portion of the road network in Québec City

Table 5.1: Parameters used by CMEM for the computation of fuel consumption

Notation	Description	Typical values
w	Curb-weight (kg)	4500
q	Carried load (kg)	0-4350
ζ	Fuel-to-air mass ratio	1
k	Engine friction factor $(kJ/rev/liter)$	0.25
N_e	Engine speed (rev/s)	40
V	Engine displacement $(liter)$	5.12
g	Gravitational constant (m/s^2)	9.81
ρ	Air density (k/m^3)	1.2041
C_d	Coefficient of aerodynamic drag	0.7
A	Frontal surface area (m^2)	4.6
C_r	Coefficient of rolling resistance	0.01
η_{tf}	Vehicle drive train efficiency	0.4
η	Efficiency parameter for diesel engines	0.9
c_f	Fuel and GHG emissions cost per liter ($CAD/$liter$)	1.05
c_d	Driver wage ($CAD/$s$	0.0085
ϖ	Heating value of a typical diesel fuel (kJ/g)	44
ψ	Conversion factor $(g/s$ to $liter/s)$	737
s^l	Lower speed limit (m/s)	5.555
s^u	Upper speed limit (m/s)	22.222
s	Average speed at a portion of segment (m/s)	
a	Acceleration (m/s^3)	$[-3, 1]$
θ	Roadway gradient (degree)	0

For a given path p traversed by a vehicle departing from node o at time t, the corresponding fuel consumption (in liters) can be computed based on equation (5.3):

$$F_p(t) = \sum_{(u,v)\in p} \mathcal{F}^1_{uv}(t) + \mathcal{F}^2_{uv}(t). \tag{5.3}$$

The term $\mathcal{F}^1$ describes the emissions related to the vehicle weight and $\mathcal{F}^2$ represents the fuel consumption unrelated to the vehicle load:

$$\mathcal{F}^1_{uv}(t) = \tau_{uv}(\gamma_u(t))\frac{\alpha M E_0}{E_2} s_{uv}(\gamma_u(t)) = \frac{\alpha M E_0}{E_2} l_{uv}, \tag{5.4}$$

and

$$\mathcal{F}^2_{uv}(t) = \tau_{uv}(\gamma_u(t))E_0\left(E_1 + \frac{\beta}{E_2}(s_{uv}(\gamma_u(t)))^3\right) = E_0 E_1 \tau_{uv}(\gamma_u(t)) + \frac{\beta E_0}{E_2} l_{uv}.(s_{uv}(\gamma_u(t)))^2 \tag{5.5}$$

5.2.2 Time-dependent emission function using MEET

The MEET emission model was developed by Hickman et al. (1999) for estimating vehicle emissions using a variety of polynomial functions of speed and acceleration levels. It computes GHG emissions produced by a vehicle of weights ranging from 3.5 to 32 tons according to travel speed and a wide range of input parameters related to the type of vehicle. Given an unloaded vehicle traveling at speed s (km/h) on a flat surface the MEET calculates the rate of emissions (g/km) using the following function:

$$\eta_r = K + as + bs^2 + cs^3 + d\frac{1}{s} + e\frac{1}{s^2} + f\frac{1}{s^3}. \tag{5.6}$$

The coefficients (K, a, b, c, d, e, f) are defined based on the vehicle type and weights. For example, if we consider the case of a vehicle weighing 3.5-7.5 tons the coefficients for the GHG emissions function for this specific vehicle category are $(K, a, b, c, d, e, f) = (110, 0, 0, 0.000375, 8702, 0, 0)$.

To consider the effect of road gradient for each vehicle category, pollutant and gradient class, MEET proposes the following road gradient correction factor:

$$\eta_g = A_0 + A_1 s + A_2 s^2 + A_4 s^4 + A_3 s^3 + A_5 s^4 + A_6 s^6. \tag{5.7}$$

where $(A_0..A_6)$ are coefficients for CO_2 pollutant that vary according to the vehicle category and gradient class. Moreover, to take the effect of the load into account, MEET applies the following load correction factor:

$$\eta_l = \kappa + n\theta + \rho\theta^2 + q\theta^3 + rs + ys^2 + zs^3 + \frac{\varrho}{s}, \tag{5.8}$$

where θ is the roadway gradient in percent and $(\kappa, n, \rho, q, r, y, z, \varrho)$ are coefficients of the load correction function.

Based on MEET the amount of GHG emissions $E_{p_{ij}}(t)$ in grams produced by traversing path p at time t (with time-varying speeds taken into account) is given by:

$$E_{p_{ij}}(t) = \sum_{(u,v)\in p} \eta_r(t)\eta_g(t)\eta_l(t)l_{uv}. \tag{5.9}$$

As GHG emissions are directly proportional to fuel consumption, the amount of fuel consumed can be derived from the amount of emissions according to the study of Coe (2005) that set the CO_2 emission from a liter of fuel to 2.66 $kg/liters$ (10.1 $kg/gallon$).

5.3 Data collection and analysis of emissions

In collaboration with an important furniture, appliances and electronics retailer from Québec City, on-road fuel consumption data collection was conducted with HINO SERIES 195 heavy-duty vehicles across different time periods of each workday during shipping operations, which covers rush hours times. The vehicles were monitored with a GPS on-board diagnostics and data logging device, which can measure the instantaneous fuel consumption between GPS points. The device incorporates a fuel analyzer sensor, an engine scanning tool, and a communication port for obtaining accurate measurements.

During 97 days between November 2016 and March 2017 up to 58,215 instantaneous speed and fuel consumption observations were collected. Real-time information includes fuel consumption, travel speed, acceleration, deceleration, GPS coordinates and vehicle load. The average travel time between two consecutive measurements is 14.54 seconds.

We now present the characteristics and analysis of real-world, on-road vehicle emissions. The main goal is to quantify and characterize the emissions in a real-world road freight distribution environment regarding relevant input variables. For data validation the daily observed fuel consumption was fitted to fuel invoices showing that the consumption device yields perfect accuracy. Yet, outliers analysis of emission data was done to ensure that there is no time lag between instantaneous emission observations. Hence, this section describes how data analysis were offset to cleanup any lags in the emission sample that will be used by our machine learning algorithms.

For each observed workday the vehicle travels on average through 14 paths corresponding to shipping trips. Translating journeys into trips involves three main steps:

- geomatics and geospacial manipulations by geomatic specialists allow us to match GPS coordinates of each trip to the road links of Québec City. It is therefore essential to

combine road segments that form part of a single trip but which have been divided into individual paths according to service time at customers, refueling stops, and/or driver breaks.

- identification of whether a break is a refueling stop or driver break, or service time at a customer where goods are picked up or dropped off, by grouping the observations according to when the vehicle ignition is turned on or off. For the purpose of this study, a trip is defined as a combination of paths traveled across a given workday where the ends are the real location of a pickup or delivery, thus grouping subsequent journeys that include breaks at fuel stations or truck-stops.
- matching the information of GPS points, starting time and idle time with orders details from another database to identify the vehicle load at each GPS point, which is constant throughout the path connecting two customers.

A cleanup process is applied on the prepared data to remove observations corresponding to idle state during breaks or delivery operations. Then, based on the obtained emission sample composed of 46,476 observations we define five explanatory variables: travel speed, acceleration, vehicle load, stop-and-go driving pattern, traveled distance, while the output variable is the amount of fuel consumption produced between two GPS points.

The frequency of link-based fuel consumption observations is displayed in Figure 5.2. We see that the number of observations is high for low fuel volumes. As shown in Figure 5.2 the mean of fuel consumption considering all observations is 0.033 liters, respectively.

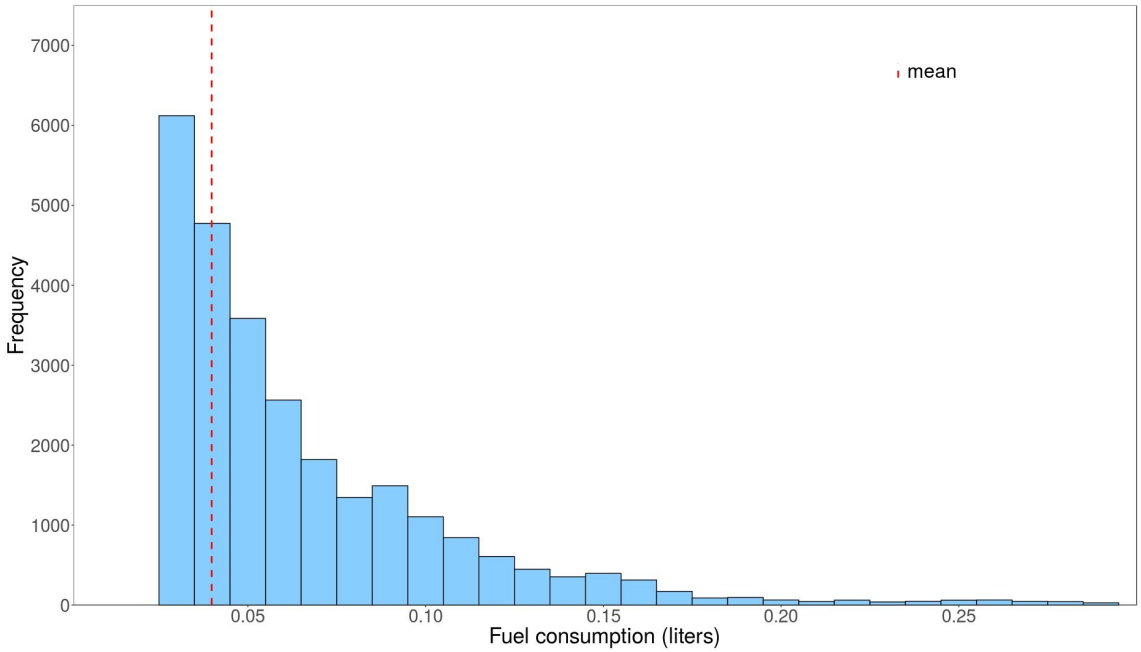

Figure 5.2: Fuel consumption histogram of real-world shipping trips in Québec City

Figure 5.3 presents the daily variation of fuel consumption. The different consumption levels between journeys are due to several factors including number of orders, traffic congestion and traveled distance, among others.

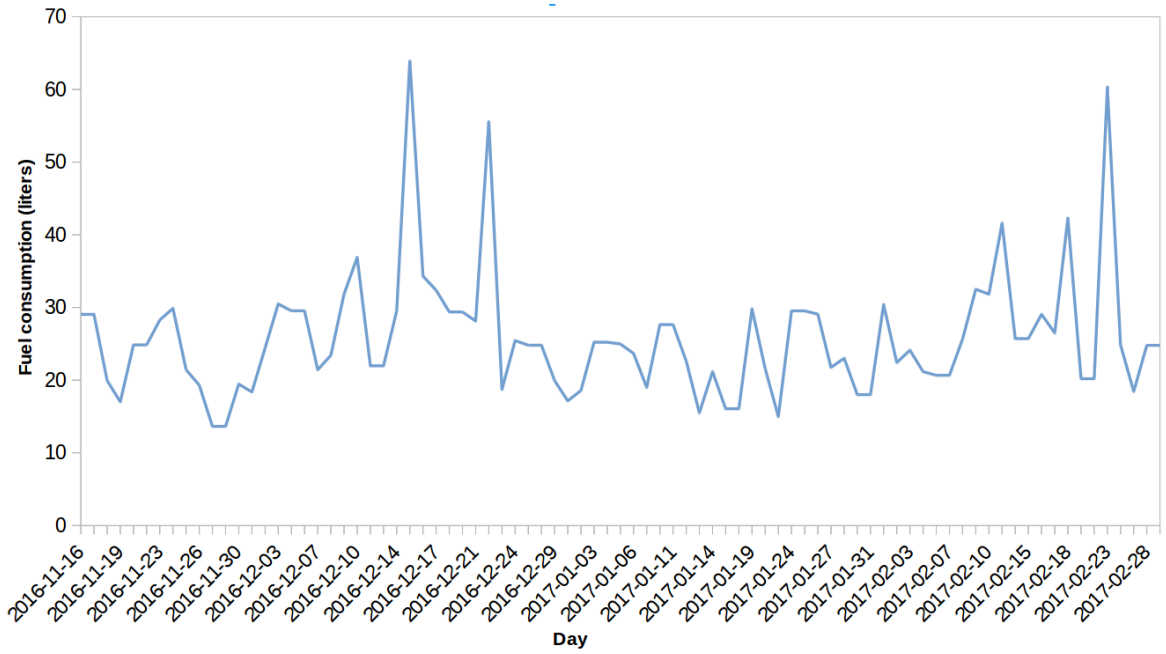

Figure 5.3: Variation of daily fuel consumption of real-world shipping trips in Québec City

A subset of data composed by observations corresponding to steps of 11 seconds is presented in Figure 5.4. We see a high level of fuel consumption variability based on speed and acceleration levels. It also illustrates the nonlinear behavior of fuel consumption as a function of travel speed and acceleration. When acceleration and speed levels increase, consumption tends to increase. In deceleration, consumption values are generally low.

Figure 5.5 shows the trade-off between fuel consumption and travel speed over different times of a typical shipping workday. It is remarkable that the fluctuation of fuel consumption is impacted by the speed in the underlying road network. The shape of curves has two distinct phases. In a first stage, we observe that fuel consumption increases with speed. This phase is characterized by a regular form of speed (ascending or descending). The second phase, marked by erratic fluctuations of speed, gives a very accidental relationship between speed and fuel consumption. This situation corresponds to the different phases of acceleration and deceleration. We can see that vehicular consumption during idling and cruising are generally low compared to consumption during acceleration. We also observe that fuel consumption depends on short term events such as rapid acceleration and braking (stop-and-go). The majority of microscopic emission models assume a constant consumption rate when a vehicle is decelerating.

To summarize, there is a clear need to perform an effective predictive modeling that takes

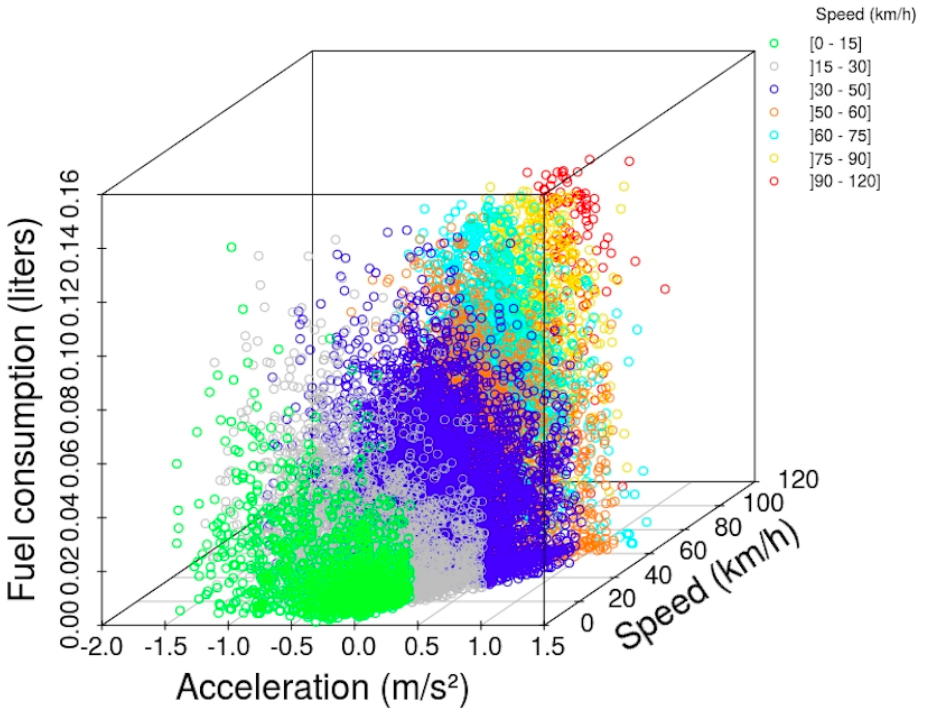

Figure 5.4: Fuel consumption as a function of instantaneous speed and acceleration for all observations with a travel time of 11 seconds

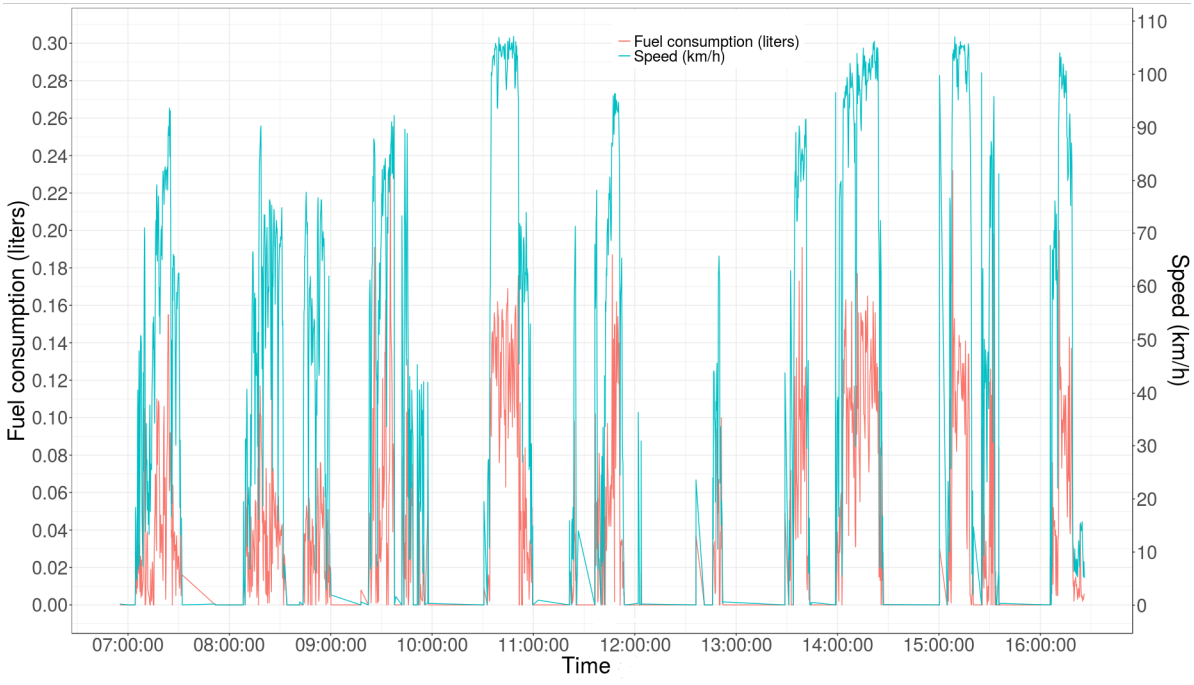

Figure 5.5: Instantaneous variation in fuel consumption and speed during a typical shipping day

into account the specificity of fuel consumption/emissions data structures. Therefore, in this study we used model-based machine learning for predicting vehicle emissions.

5.4 Emission modeling with supervised learning methods

This section shows the development of multiple nonlinear emission models using four supervised learning methods: Neural Networks (NNET), Support Vector Machines (SVM), Conditional Inference Trees (CIT) and Gradient Boosting Machines (GBM). Each model-based machine learning uses a set of tuning parameters. These determine the performance profile of each model. To choose the appropriate combination of parameters values while avoiding over-fitting we used grid search method for SVM and CIT and trial-and-error approach for NNET and GBM. For each model we define a set of candidate values for the appropriate tuning parameters according to the relevant literature, sample size and computational resources. We then fit each model with each candidate set using the training data set on which we apply the k-fold cross validation method (Kuhn and Johnson 2013) for estimating prediction error. The k-fold cross validation works by splitting the training data set into k roughly equal-sized subsamples or folds. Each supervised learning method performs k iterations and at each time it excludes one held-out fold in turn to evaluate their prediction accuracy once the model is estimated using the remaining $k-1$ folds. There is no formal rule of defining the value of k, and we used k=10. The prediction accuracy of each model is given by the average of k obtained prediction error measures. For each candidate machine learning model, the optimal setting of tuning parameters is determined according to the obtained performance metrics. Then, we evaluate the performance of their accuracy prediction using a testing data set (see Section 5.5).

5.4.1 Neural Networks

NNET learning methods allow the extraction of linear combinations of the inputs to produce a nonlinear emission model. NNET is composed of a set of neurons connected together (Dreyfus 2005). It uses massive interconnections to fit nonlinear models to multidimensional data (Haykin 1994). Figure 5.6 shows a schematic diagram of the proposed NNET used to model GHG emissions. In the network diagram the nodes are the neurons and the arcs are the connections. NNET is a multi-layer network composed of three layers: input layer, hidden layer and output layer. The input layer incorporates five input variables $x_1, ..., x_5$ defined based on the chosen parameters affecting emissions, namely speed, acceleration, vehicle load, stop-and-go driving patterns, and distance. The hidden layer incorporates a set of hidden units or unobserved variables used to model the outcome Kuhn and Johnson (2013). These hidden units perform intermediate computations using linear combinations of the input variables. The output layer is the combination of obtained hidden units to perform the prediction of emissions.

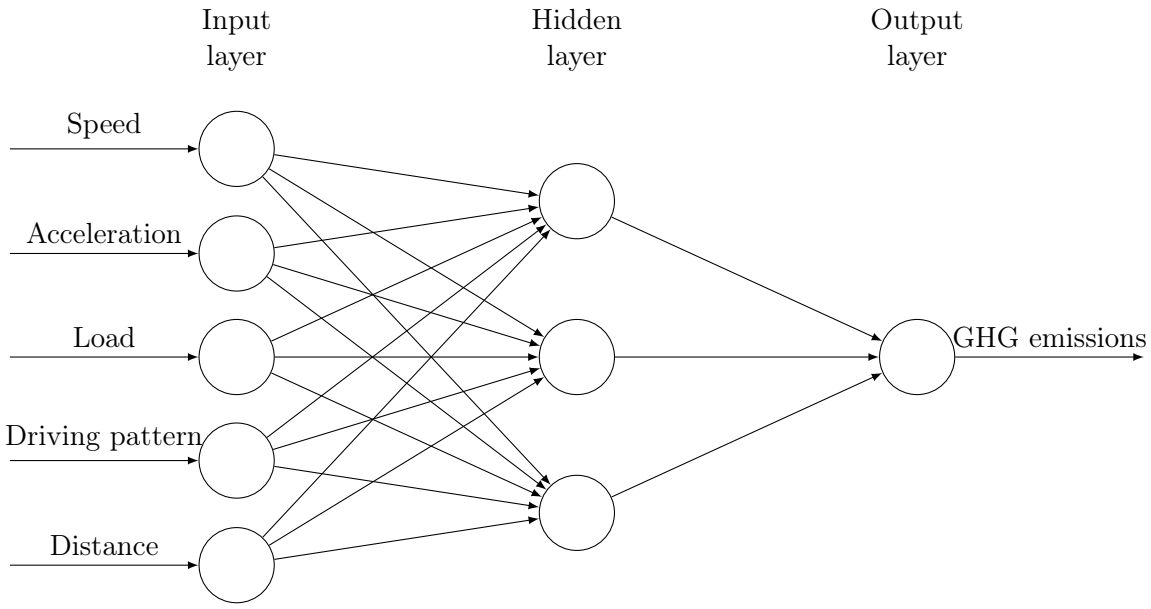

Figure 5.6: Schematic diagram of the NNET emission model

In this study, several NNET tasks were performed to accurately predict traffic emissions by studying field data. We applied the quasi-Newton back propagation learning algorithm (Battiti 1990). The linear combinations of the predictors are transformed by a nonlinear activation function (sigmoidal). To reduce over-fitting our NNET algorithm minimizes the following function Kuhn and Johnson (2013):

$$G = \sum_{i=1}^{N}(y_i - f_i(x))^2 + \eta \left(\sum_{k=1}^{H}\sum_{j=0}^{P} \beta_{jk}^2 + \sum_{k=0}^{H} \gamma_k^2 \right), \tag{5.10}$$

where N is the total number of observations, P is the number of predictors, H represents the number of hidden units, η is the weight decay, and y_i is the outcome. The coefficient β_{jk} represents the effect of the jth predictor on the kth hidden unit. The function f defines a linear combination that connects the hidden units to the outcome:

$$f(x) = \gamma_0 + \sum_{k=1}^{H} \gamma_k h_k, \tag{5.11}$$

where γ_k are the regression coefficients of hidden layers.

Several combinations of NNET parameter values were investigated by trial-and-error to identify the best learning performance. Four different weight decay $\eta \in \{15^{-4}, 15^{-3}, 15^{-2}, 15^{-1}\}$ were evaluated along with one hidden layer including between one and 10 hidden units. The

convergence to the best NNET model is achieved with a maximum number of iterations equal to 2000. The optimal NNET model used $\eta = 15^{-3}$ and $H = 9$ hidden units.

5.4.2 Support Vector Machines

SVMs is a supervised learning method applied for classification and nonlinear regression (Vapnik 2013). SVM algorithms use a kernel function allowing this model to transform input data to the required form of relationships. There are multiple kinds of kernel functions, such as linear kernel, polynomial, radial basis function, and sigmoid. After several trials, we used a linear kernel function defined as a simple sum of cross products, which have been shown to be effective for the current study.

The SVM regression tries to minimize the following regularized function:

$$W = C \sum_{i=1}^{N} L(y_i, F(x_i)) + \sum_{j=1}^{P} \beta_j^2, \tag{5.12}$$

where x_i is the input space-vector, $L(.)$ is the loss function, β are coefficients used by the regularization term considering P predictors, and constant C is the error penalty factor for adjusting the complexity of the model (Kuhn and Johnson 2013). F is a prediction equation defined as follows:

$$F(x) = \sum_{i=1}^{N} \alpha_i \varphi(x) + \beta_0, \tag{5.13}$$

where $\varphi(x)$ is the linear kernel function.

The tuning of regularization parameter C through grid search method produced a constant with a value of 1.

5.4.3 Conditional Inference Trees

CIT is a machine learning method that uses unbiased tree-based models for regression and classification (Hothorn, Hornik, and Zeileis 2006). CIT algorithm's estimates regression relationship using a binary recursive partitioning method, which efficiently performs the exhaustive search across the predictors according to split points. A simplified description of this method is provided by the following steps:

1. perform the null hypothesis test of independence between each input variable and the outcome one. The algorithm continues until the hypothesis cannot be rejected;

2. apply a binary split to the selected input variable;

3. recursively repeat steps 1 and 2.

The p-value statistical test is applied for candidate splits by evaluating the difference between the means of two groups. On our preliminary tests with the training data set we found that the optimal CIT model is obtained with a value of $1 - p$ equal to 0.821.

5.4.4 Gradient Boosting Machines

GBM is gaining a considerable interest in a wide range of data driven applications such as travel time prediction (Zhang and Haghani 2015) and the modeling of the energy consumption (Touzani, Granderson, and Fernandes 2018). It is a highly adaptable supervised learning method encompassing both classification and regression in order to find an additive model that minimizes the loss function (Friedman 2001). GBM iteratively investigates decision trees (basic learner) to reduce the loss function and improve prediction accuracy. The GBM model is defined as follows (Friedman 2001).

Let $\hat{R}(x)$ be the regression function that minimizes the expectation of loss function $S(y, R)$ over the joint distribution:

$$\hat{R}(x) = \arg\min_{R(x)} E_{x,y}[S(y, R(x))], \tag{5.14}$$

where $R(x)$ can be formulated as a function with a finite number of parameters β estimated by selecting those values that minimize the loss function S using the training sample as shown in equation 5.15:

$$\hat{R}(x) = \arg\min_{\beta} \sum_{i=1}^{N} S(y_i, \beta)). \tag{5.15}$$

To optimize the GBM model we have performed the tuning of several regularization parameters:

- d: the depth of decision trees that controls the maximum interaction order of the model;
- I: the number of boosting iterations, which also corresponds to the numbers of decision trees;
- α: the learning rate that controls the contribution of each base model or decision trees by shrinking its contribution by a factor between 0 and 1;
- δ: the subsampling rate or fraction of the training set observations, which is randomly selected to propose the next tree in the expansion.

After the training of the model, the depth of the decision trees d was selected in the set $\{2, 5, 7, 9\}$, the learning rate α was chosen from 0.01 to 0.5 with a granularity of 0.02. The number of iterations I was selected within a set spanning from 50 to 250 iterations with a granularity of 50 iterations. The minimum number of observations in trees terminal nodes φ was defined between 5 and 10. The subsampling rate δ was fixed to 0.5. The final combination of values used for the GBM model was $d = 9$, $I = 250$, and $\alpha = 0.07$.

5.5 Numerical experiments

It is not recommended to use the same set of observations for both training and testing. Hence, in this work the assessment of predictive performance has been carried out on an independent sample of field data in order to avoid over-fitting, which is the tendency of the models to fit the training sample too well, at the expense of the predictive accuracy. The preprocessed field data set composed of 46,476 fuel consumption observations (1406 paths) was split randomly on two subsets using days as the splitting criterion:

- training sample: composed by 80% of days corresponding to 38,004 observations (1263 paths);
- testing sample: composed by 20% of days including 8,472 observations (143 paths).

Each model was trained with the same training data set with R version 3.4.3 through R-Studio 1.0.153 using a ThinkCenter professional workstation with Intel i7 vPro (8 cores) and 32-gigabyte RAM, running Ubuntu Linux 16.04 LTS x86 operating system. The following R machine learning packages were used to generate nonlinear emission models: nnet, e1071, party, gbm, and caret. The evaluation process was initiated by comparing the models prediction outcomes on in-field observations. More specifically, we assessed the accuracy of studied emissions models considering realistic driving conditions that take into account several factors, such as carried loads, speed, and stop-and-go events. The obtained models were then evaluated on the testing data set. Their effectiveness was validated by computing and analyzing the following accuracy measures:

- Root Mean Squared Error (RMSE): interpreted as the average distance between the observed values and the model predictions. The RMSE is then computed by taking the square root of the Mean Squared Error (MSE). The smaller the values of RMSE, the closer the predicted values are to the observed ones. The RMSE is computed by squaring the residuals, summing them up and dividing by the number of observations as $\frac{1}{n}\sum_i^n (y_i - \hat{y}_i)^2$, where y_i is the observed value, $\hat{y}$ is the predicted output, and n is the total number of observations;

- Mean Absolute Error (MAE): is the average magnitude of the errors in a set of predictions. It is computed as $\frac{1}{n}\sum_i^n \mid y_i - \hat{y}_i \mid$.
- Std Error: is the standard error of the mean. It is computed as $\frac{\sigma}{\sqrt{n}}$, where $\sigma = \sqrt{\frac{\sum_i^n (y_i-\mu)^2}{n-1}}$ is the standard deviation of the mean μ.
- Mean: is the average of the corresponding predicted outcomes. It is calculated as $\mu = \frac{1}{n}\sum_i^n \hat{y}_i$.
- Gap (%): reports how close the corresponding predicted outcome is to the observed value. The percentage gap values are calculated as $100(y_i - \hat{y}_i)/y_i$.

5.5.1 Experimental results and analysis

In this section we provide the experimental results and analysis. Table 5.2 shows the accuracy metrics of CMEM, MEET, NNET, SVM, CIT and GBM predictions. In this table, successive columns give for each emission model the RMSE, the MAE, the Standard Error (Std Error), the mean value, the Gap (%) aggregated across all paths (trips) in the testing data set, and the computational time (CPU) of training (seconds). Doing so, we estimate the fuel consumption for each road segment, then we aggregate the obtained values for each path. The results obtained for the RMSE metric show that the proposed nonlinear emission models, namely GBM, NNET, CIT and SVM outperform CMEM and MEET and appear to be more accurate in estimating instantaneous vehicle fuel consumption. In fact, we see that the average RMSE ranges from 0.258 to 0.315 for the machine learning models, which are lower than those of the CMEM and MEET models (0.501 and 0.850). More specifically, it can be clearly seen that GBM model exhibited the best estimation accuracy as the fuel consumption predictions are very consistent in trends with in-field observations, with the lowest RMSE of 0.258.

Figure 5.7 also illustrates that GBM outperforms MEET and CMEM that were found to respectively under- and over-predict fuel consumption. Note however, that GBM algorithm is computationally demanding as it takes over 32354.44 seconds of execution time compared to the case of NNET (5188.85 seconds), SVM (1743.11 seconds) and CIT (404.10 seconds) models.

Regarding the obtained percentage gap values, we observe from Table 5.2 that the machine learning models give the best prediction results with a gap ranging from -1.930% to 6.173% when compared against MEET underestimating fuel consumption on average by 24.942% and CMEM overestimating fuel consumption by 13.184%. We also see that GBM and CIT yield the lowest underestimation with a gap of -1.709% and -1.453%, respectively.

Additional experiments were performed to study the performance of the developed machine learning models. Figure 5.8 shows scatter plots that illustrate graphically the prediction accuracy of the studied models superimposed on the field data. On the vertical scale, the

Table 5.2: Comparative performance of the proposed machine learning models against MEET and CMEM regarding emission prediction aggregated by paths

Emission models	RMSE	MAE	Std Error	Mean	Gap (%)	CPU of training (seconds)
Real-world	0	0	0	1.539	0	-
CMEM	0.501	0.305	0.459	1.742	−13.184	-
MEET	0.850	0.404	0.760	1.155	24.942	-
SVM	0.315	0.170	0.301	1.444	6.173	1743.110
CIT	0.264	0.151	0.263	1.561	−1.453	404.100
NNET	0.271	0.155	0.270	1.569	−1.930	5188.850
GBM	0.258	0.150	0.257	1.565	−1.709	32354.440

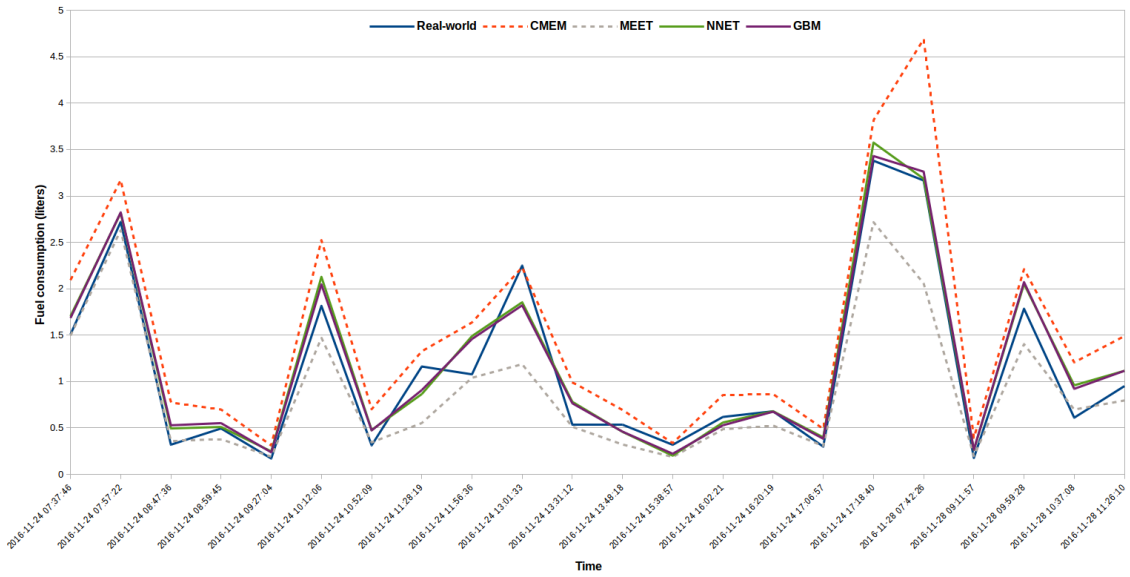

Figure 5.7: Sample of the estimations produced by CMEM, MEET, NNET and GBM models against real-world fuel consumption.

observed value of fuel consumption is displayed, whereas the predicted values are presented on the horizontal scale. We observe that NNET, GBM, SVM and CIT models fit similarly as their prediction outcomes are more concentrated and closer to the identity lines represented by red color indicating that the observed and predicted emission values are very close. This implies that the machine learning models yield more effective prediction of fuel consumption than those produced by the classical CMEM and MEET. As expected, machine learning models provide good fitting regarding observed fuel consumption as they are able to reflect differences in vehicle emissions that result from traveling on congested areas with frequent stop-and-go events impacting the traffic speed.

Figure 5.8 also illustrates the difference observed between the identity red line and the black regression line, which shows the variation in prediction between each model results compared

to observed data. Notably, this graphical trend was validated by the goodness of fit test. The null hypothesis of this test is performed with a slope=1 and intercept=0. This test leads to the rejection of the null hypothesis with very low p-value (<2.2e-16), lower than the threshold 0.05. Hence, these two models are not preferred candidates for predicting fuel consumption considering estimation at points level. More specifically, the best prediction accuracy belongs to the GBM model yielding the lowest p-value of 0.314, which is larger than the threshold 0.05. Therefore, the null hypothesis is not rejected which indicates that the prediction outcome of the GBM model is similar to the observed values.

In order to make further analysis on the prediction accuracy of the proposed models the boxplots presented on Figure 5.9 illustrate numerical outcomes of the studied emission models through their quartiles. Clearly, the median thicknesses of GBM, CIT and NNET models (represented by the lines in the middle of the boxes) seem to be very close to the observed fuel consumption one, exhibiting superior accuracy regarding fuel consumption. When looking at the boxplots of CMEM and MEET, we can see a difference between the medians, indicating that these models tend to incorrectly predict fuel consumption.

To further evaluate the performance of the proposed emission models, a sensitivity analysis is performed to compare their prediction accuracy under multiple criteria: congested (low speeds) and free flow (high speeds) situations, empty and loaded vehicle, stop-and-go driving patterns, and peak and non-peak periods. In Table 5.3 the performance of emissions estimation of CMEM and MEET is compared against the proposed models with in-field measurements considering each criterion, which includes corresponding mean and gap for the best machine learning model, CMEM, and MEET. Clearly, the degree of estimation varies for all criteria according to real-world driving conditions. We have noticed that the estimation of CMEM and MEET are deteriorated in the case of low speeds with an overestimation of 107.032% and 11.800%, respectively. The result obtained for CMEM is conform with previous literature indicating that potential under prediction is due to it deterministic nature (Jaikumar, Nagendra, and Sivanandan 2017). However, GBM provides a low overestimation of only 3.776%.

For driving pattern criterion, we see that the prediction of CMEM and MEET are affected in the cases of acceleration and deceleration events. As an example, for acceleration observations our experiments indicate that CMEM and MEET emission estimations are inaccurate under fluctuating speeds as they produce a gap of -28.222% and 30.701%, respectively. As expected the GBM model adequately handles acceleration variability when congestion occurs as it has the smallest gap (-1.564%). Regarding loads, GBM gives the lowest gaps (-1.666% for empty vehicles and -1.716% for loaded ones). Interestingly, NNET model shows its performance in peak period cases during the morning between 08h00 and 09h00 providing a gap ranging from 1.107% to 2.783% compared to CMEM and MEET which have a much higher absolute gap between 4.265% and 30.692%.

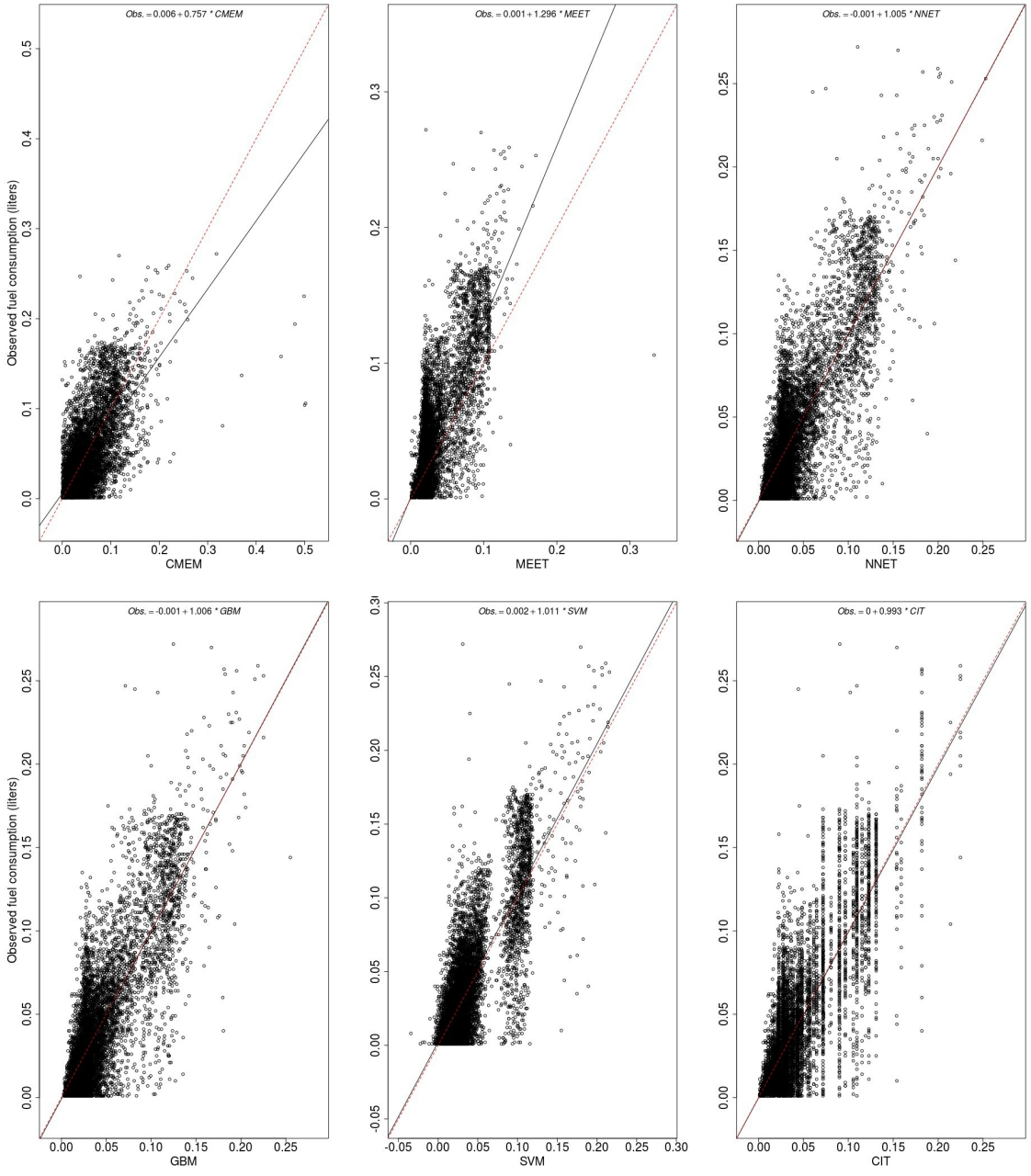

Figure 5.8: Scatter plots of predicted outcomes by CMEM, MEET and machine learning models against observed fuel consumption

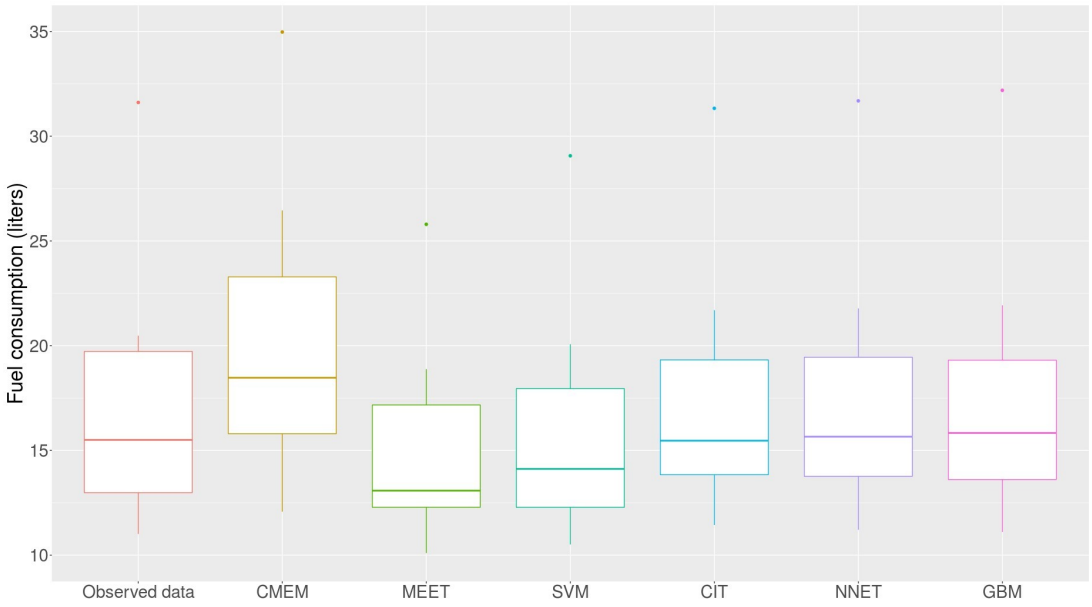

Figure 5.9: Boxplots of emissions models prediction performance against observed fuel consumption aggregated by days

Based on the results presented in Table 5.3 it can be argued that GBM and NNET models give the best results and are the most accurate for all aspects, exhibiting a gap just over 3.776%. Further, we can see that the overall performance of both models is very good not only in normal or moderate traffic conditions, but also during traffic congestion. Compared to CMEM and MEET, machine learning models are less sensitive to input variables and maintain superior prediction accuracy.

To summarize, even if emissions estimation is complex and challenging, it is clearly shown that machine learning models enhance emission prediction accuracy by taking into account the interactions among different combinations of input variables. In all experiments presented in this section, we conclude that the proposed machine learning models significantly outperform CMEM and MEET. In fact, machine learning-based emission models, and in particular GBM and NNET models are able to fit complex nonlinear relationship of vehicle emissions leading to superior emissions prediction accuracy.

5.6 Conclusions and future research

In this paper we have proposed nonlinear emission models using supervised learning methods. The prediction accuracy was compared to the classical MEET and CMEM methods under real-world driving conditions with stop-and-go events, fluctuating speeds and varying road geometry. In our numerical experiments, we have observed that MEET and CMEM incorrectly predicted emissions by 24.942% and −13.18%, respectively. Results revealed that the pro-

Table 5.3: Comparative performance statistics of the GBM, NNET, CMEM and MEET models regarding multiple performance indicators

Criterion	Aspects	NB Obs.	Mean real-world	Best model (RMSE)	Mean BM	Gap BM (%)	CMEM	Gap CMEM (%)	MEET	Gap MEET (%)
All observations	Testing data set	8472	0.041	GBM	0.041	−1.709	0.046	−13.184	0.031	24.942
Speed	Low speeds (0-15 km/h)	1832	0.017	GBM	0.017	−3.776	0.034	−107.032	0.018	−11.800
	Moderate speed (∼50 km/h)	175	0.034	GBM	0.035	−2.533	0.043	−28.210	0.022	34.444
	High speed (>75 km/h)	1573	0.101	NNET	0.101	0.529	0.090	11.252	0.074	27.160
Load	Empty vehicle	1377	0.037	GBM	0.038	−1.666	0.041	−11.414	0.028	23.101
	Loaded vehicle	7095	0.041	GBM	0.042	−1.716	0.047	−13.490	0.031	25.26
Driving pattern	Acceleration	4703	0.044	GBM	0.044	−1.564	0.056	−28.222	0.030	30.701
	Deceleration	3691	0.036	GBM	0.037	−2.081	0.033	9.002	0.031	16.255
Period	07h30 - 08h00	744	0.060	NNET	0.060	0.867	0.062	−2.671	0.044	26.650
	08h00 - 08h30	776	0.050	NNET	0.049	1.107	0.051	−4.265	0.036	26.630
	08h30 - 09h00	359	0.038	NNET	0.037	2.783	0.043	−13.490	0.026	30.692

posed NNET, SVM, CIT and GBM models outperform CMEM and MEET as they improve prediction accuracy in the case of traffic congestion and stop-and-go driving patterns with recurrent acceleration and breaking events. It was also shown that GBM produces the best predictability which is off by only 1.70% according to real-world data. This indicates that we cannot take for granted that existing emission models are sufficiently accurate to be used in green vehicle routing, which requires machine learning models that update them by applying supervised learning methods on collected real-time traffic data and on-road vehicular exhaust emissions.

The results of this work show that using machine learning models and more specifically the GBM and NNET models enhance the prediction accuracy of emissions prediction. A direction of future research is to evolve machine learning emission models by investigating the effects of weather, driver profiles and road-wide factors such as temperature, rain, snow, road maintenance events, etc. Another area of future work will be the integration of machine learning emission models in routing problems and practical road freight transportation applications.

Acknowledgments

This research was partly supported by grants 2014-05764 and 0172633 from the Natural Sciences and Engineering Research Council of Canada (NSERC) and by the Centre d'Innovation en Logistique et Chaîne d'Approvisionnement Durable (CILCAD). The CILCAD receives financial support from the Green Fund under Priority 15.2 of the 2013-2020 Action Plan on Climate Change, a priority implemented by Transition Énergétique Québec (TEQ). We also thank Mr Jean-Philippe Gagliardi, President of Logix Operations inc, for providing us with real data from an important wholesaler partner in Québec City. This support is highly appreciated.

Conclusion

In this thesis we have introduced, modeled and solved several types of time-dependent distribution problems considering dynamic paths and GHG emissions. Particularly, we have explicitly considered the time-varying flow speed model and time-dependent FIFO network within these problems, and have developed heuristics, time-to-target travel time and cost bounds, and optimization methods for their resolution. The main scientific contributions of this thesis are the incorporation of time-dependent optimization and path flexibility on the definition, models and solution algorithms for the Quickest Path Problem (QPP) and the Green Vehicle Routing Problem (GVRP). These allow for more realistic and efficient solutions from a cost perspective and from an environmental standpoint.

Research synthesis

We have proposed a comprehensive literature review in Chapter 2. On the one hand, the history of the time-dependent shortest path problem (TDSPP), which was introduced more than 50 years ago, was presented along with a number of variants of the problem, their properties, models and solution methods. A systematic review of recent research on the TDSPP and green routing problems is provided.

In Chapter 3 we have introduced the time-dependent quickest path problem with emission minimization (TDQPP-EM), which extends the TDQPP by considering GHG emissions and costs minimization. This extension is of high practical relevance since traffic congestion is an important issue for logistics providers. A fast and effective time-dependent Dijkstra label-setting algorithm and a lower bounding method have been implemented and tested using the road network of Québec City with a large data set of speed observations. Our algorithms are highly effective in finding good-quality solutions for benchmark instances of all sizes. Our extensive computational experiments have demonstrated the benefits of choosing alternative paths in congested urban areas that lead to substantial GHG emission reduction and cost savings. We have clearly demonstrated that using time-dependent algorithms leads to solutions with high degree of accuracy. An interesting insight derived from this research is that avoiding traffic congestion during peak hours yields substantial GHG emissions reductions and cost savings. Our time-dependent models reproduce the expected behavior with respect to different

optimization criteria, time of the day (level of congestion), carried loads and selected paths. We have also shown that carried loads affect the chosen path, particularly as the vehicle load becomes larger, the potential savings in fuel consumption and GHG emissions increase.

We have studied in Chapter 4 the Time-dependent Vehicle Routing Problem with Emission and Cost Minimization considering time-varying speeds and dynamic paths. In order to solve it, we have developed an efficient method combining a goal directed search heuristic, called Time-Dependent Nearest Neighborhood Heuristic (TDNNH) with a Time-Dependent Neighborhood Search Improvement Heuristic (TDNSIH). Solving this problem requires an efficient adaptation of the Dijkstra label-setting algorithm to a time-dependent setting to perform the fast computation of time-dependent point-to-point paths connecting pairs of customers nodes based on different measures, namely fuel consumption, time or cost leading to a larger solution space and further opportunities of optimization in large scale time-dependent road networks. The results of extensive computational experiments on real-life benchmark instances have demonstrated that taking dynamic paths into account according to time-varying speeds yields good quality solutions in a very consistent manner using the TDNSIH. In fact, some paths that were evaluated as profitable in a static setting can now appear as not viable candidates in the case of time-dependent network modeled as a multigraphs which reflects more realistic scenarios. Moreover, we have shown that potential reductions in GHG emissions and costs are achievable through flexible departure times, which allows congestion avoidance considering alternative paths between customers. As expected, we have observed that the size of orders affects paths choice decision yielding different route plans with higher levels of fuel consumption.

Finally, in Chapter 5 we have proposed nonlinear emission estimation models using supervised learning methods. The prediction accuracy was compared to the classical Comprehensive Modal Emissions Model (CMEM) and Methodology for Estimating air pollutant Emissions from Transport (MEET) methods under real-world driving conditions with stop-and-go events, fluctuating speeds, loads, and varying road geometry. Results have revealed that the proposed Neural Networks (NNET), Support Vector Machines (SVM), Conditional Inference Trees (CIT) and Gradient Boosting Machines (GBM) models outperform the CMEM and the MEET as they improve prediction accuracy in the case of traffic congestion and recurrent acceleration and breaking events. It was also shown that GBM produces the best predictability according to real-world data. Our computational analysis have demonstrated that one cannot take for granted that existing emission models are sufficiently accurate to be used in green vehicle routing, which requires machine learning models that update them by applying supervised learning methods on collected real-time traffic data and instantaneous fuel consumption.

Main contributions

This thesis makes a number of contributions to literature. The first one is the introduction, modeling and resolution of two meaningful Time-dependent Distribution Problems, namely the *Time-dependent Quickest Path problem with Emission Minimization* (TDQPP-EM) and the *Time-dependent Vehicle Routing Problem with Emission and Cost Minimization considering Dynamic Paths* (TDVRP-ECMDP). These are variants of the minimum-cost path across time-dependent network, where arc costs are time-dependent and are evaluated by explicitly considering GHG emissions and fuel consumption as parts of the cost components.

The second contribution is the design of an effective approach for computing travel cost and GHG emissions in time-dependent networks under the FIFO dynamic, ensuring that our solution methods account for the impact of speed variations on the optimization of a chosen path.

The third key contribution is the design of an efficient method to obtain tight time-dependent bounds, reducing the computational burden, and investigate when it is important to incorporate the load carried by the vehicle and traffic congestion factors into the lower and upper bounding algorithms. These bounds seem a worthwhile feature for validating the quality and the accuracy of solutions.

This thesis also investigates the benefits of incorporating road-network and traffic information within a time-dependent setting. The decisions to make are involving not only routing decisions but also the effects of path choice and congestion avoidance decisions on GHG emissions as well as on traveling cost. Thereby, incorporating path flexibility enlarges the problem size leading to more realistic route plans. Doing so, we have proposed an efficient time-dependent nearest neighbor method adapted to the multigraph representation to solve large-scale instances of the TDVRP-ECMDP. Significant saving is obtained by embedding TDLCPs into routing decisions, which captures and minimizes fuel consumption along with operational costs.

Finally, the fifth key contribution is the development of efficient nonlinear emission models using NNET, SVM, CIT, and GBM supervised learning methods, which are trained by applying the k-fold cross validation method on real-life GHG emission data acquired by a private-sector retailer from thousands of trips over the course of several months. We believe our work increases the awareness of both temporal and environmental dimensions leading to new perspectives in the evolution of road freight transportation field.

Perspectives for further research

In spite of the strong evidence of the validity and need for road network and traffic information in green logistics, and the solid theoretical foundations for integrating both temporal

and environmental dimensions into the field, we do not pretend to cover all the aspects related to this subject. Throughout this thesis, we highlight the importance of time-dependent feature and paths selection within the resolution methods and we show how to use them to strengthen formulations and enhance routing algorithms. Further research should consider how to embed TDQPP-EM algorithms and lower bounding methods into local search heuristics to efficiently solve real-world time-dependent distribution problems considering emissions minimization based on time-varying speeds. Adding time-dependent quickest path optimization may enhance the resulting route plans that are selected based on dynamic paths to avoid traffic congestion across real road networks. Another promising avenue is to enhance the proposed bounds and algorithms.

Many research avenues stem from the introduction of new nonlinear emissions models. In this thesis, we have primarily focused on solving two time-dependent distribution problems: the TDQPP-EM and the TDVRP-ECMDP. Our analyses have shown that potential reduction in GHG emissions and costs are achievable through flexible departure times, which allows congestion avoidance considering alternative paths between customers. Developing a scientific approach to build and study new logistic problems at even larger scales is another research opportunity to capture more of the potential impacts of routing on economic, environmental, and sustainability. Further research can now focus on generalizing these methods to broader distribution problems, namely the time-dependent inventory-routing, dynamic vehicle routing, and autonomous vehicle routing problems. Modeling these problems would require a large increase in the number of variables, parameters and constraints, probably making it significantly harder to solve. A more extensive investigation is necessary to identify whether to adapt the same framework, to build new ones, or to construction different combinations.

Finally, from a research perspective, it is clear that there is room for meaningful work to be done around exploiting high-frequency traffic data. An interesting extension is addressing distribution problems from a big data and artificial intelligence standpoints which have the potential for generating enormous contributions in operation research and more specifically to the road transportation field. The range of options available in this context is clearly very wide. The results of this work show that using machine learning models and more specifically the GBM and NNET models enhance the prediction accuracy of emissions. A direction of future research is to evolve machine learning emission models by investigating the effects of weather, driver profiles and road-wide factors such as temperature, rain, snow, road maintenance events, etc. Another area of future work will be the integration of machine learning emission models in routing problems and practical road freight transportation applications. New algorithms for constructing effective routing plans could be developed and tested. It is reasonable to think that other forms of high-dimensional problems can be conceptualized and studied which may result in further changes to the current visions and the ways of doing things, as well as leading to new perspectives and potential in this exciting and challenging field.

Bibliography

Ahuja RK, Orlin JB, Pallottino S, Scutella MG, 2003 *Dynamic shortest paths minimizing travel times and costs. Networks* 41(4):197–205.

Androutsopoulos KN, Zografos KG, 2017 *An integrated modelling approach for the bicriterion vehicle routing and scheduling problem with environmental considerations. Transportation Research Part C: Emerging Technologies* 82:180–209.

Bander JL, White CC, 2002 *A heuristic search approach for a nonstationary stochastic shortest path problem with terminal cost. Transportation Science* 36(2):218–230.

Barth M, Boriboonsomsin K, 2008 *Real-world carbon dioxide impacts of traffic congestion. Transportation Research Record: Journal of the Transportation Research Board* 2058:163–171.

Barth M, Boriboonsomsin K, 2009 *Energy and emissions impacts of a freeway-based dynamic eco-driving system. Transportation Research Part D: Transport and Environment* 14(6):400–410.

Barth M, Younglove T, Scora G, 2005 *Development of a heavy-duty diesel modal emissions and fuel consumption model. UC Berkeley: California Partners for Advanced Transit and Highways, San Francisco* .

Battiti R, 1990 *Optimization methods for back-propagation: Automatic parameter tuning and faster convergence. International Joint Conference on Neural Networks*, volume 1, 593–596.

Bauer R, Delling D, Sanders P, Schieferdecker D, Schultes D, Wagner D, 2010 *Combining hierarchical and goal-directed speed-up techniques for Dijkstra's algorithm. Journal of Experimental Algorithmics* 15:2–3.

Behnke M, Kirschstein T, 2017 *The impact of path selection on GHG emissions in city logistics. Transportation Research Part E: Logistics and Transportation Review* 106:320–336.

Bektaş T, Demir E, Laporte G, 2016 *Green vehicle routing.* Psaraftis HN, ed., *Green Transportation Logistics. The Quest for Win-Win Solutions*, 243–265 (Kgs. Lyngby, Denmark: Springer).

Bektaş T, Laporte G, 2011 *The pollution-routing problem. Transportation Research Part B: Methodological* 45(8):1232–1250.

Belhassine K, Coelho LC, Renaud J, Gagliardi JP, 2018 *Improved home deliveries in congested areas using geospatial technology.* Technical Report CIRRELT-2018-02, Montreal, Canada.

Bellman R, 1958 *On a routing problem. Quarterly of Applied Mathematics* 16(1):87–90.

Ben Ticha H, Absi N, Feillet D, Quilliot A, 2018 *Vehicle routing problems with road-network information: State of the art. Networks* 00:1–14.

Brodal GS, Jacob R, 2004 *Time-dependent networks as models to achieve fast exact time-table queries. Electronic Notes in Theoretical Computer Science* 92:3–15.

Calogiuri T, Ghiani G, Guerriero E, 2015 *The time-dependent quickest path problem: Properties and bounds. Networks* 66(2):112–117.

Carey M, 1986 *A constraint qualification for a dynamic traffic assignment model. Transportation Science* 20(1):55–58.

Chabini I, 1998 *Discrete dynamic shortest path problems in transportation applications: Complexity and algorithms with optimal run time. Transportation Research Record: Journal of the Transportation Research Board* (1645):170–175.

Chabini I, Lan S, 2002 *Adaptations of the A* algorithm for the computation of fastest paths in deterministic discrete-time dynamic networks. IEEE Transactions on Intelligent Transportation Systems* 3(1):60–74.

Cheung RK, 1998 *Iterative methods for dynamic stochastic shortest path problems. Naval Research Logistics* 45(8):769–789.

Choi TM, Wallace SW, Wang Y, 2018 *Big data analytics in operations management. Production and Operations Management* forthcoming.

Coe E, 2005 *Average carbon dioxide emissions resulting from gasoline and diesel fuel.* Technical report, United States Environmental Protection Agency.

Cooke KL, Halsey E, 1966 *The shortest route through a network with time-dependent internodal transit times. Journal of Mathematical Analysis and Applications* 14(3):493–498.

Cordeau JF, Ghiani G, Guerriero E, 2014 *Analysis and branch-and-cut algorithm for the time-dependent travelling salesman problem. Transportation Science* 48(1):46–58.

Crainic TG, 2000 *Service network design in freight transportation. European Journal of Operational Research* 122(2):272–288.

Crainic TG, 2003 *Long-haul freight transportation. Handbook of Transportation Science*, 451–516 (Springer).

Crainic TG, Gendreau M, Potvin JY, 2009 *Intelligent freight-transportation systems: Assessment and the contribution of operations research. Transportation Research Part C: Emerging Technologies* 17(6):541–557.

Crainic TG, Roy J, 1988 *OR tools for tactical freight transportation planning. European Journal of Operational Research* 33(3):290–297.

Dabia S, Demir E, Van Woensel T, 2017 *An exact approach for a variant of the pollution-routing problem. Transportation Science* 51(2):607–628.

Dabia S, Ropke S, Van Woensel T, De Kok T, 2013 *Branch and price for the time-dependent vehicle routing problem with time windows. Transportation science* 47(3):380–396.

Dean BC, 2004a *Algorithms for minimum-cost paths in time-dependent networks with waiting policies. Networks* 44(1):41–46.

Dean BC, 2004b *Shortest paths in FIFO time-dependent networks: Theory and algorithms.* Technical report, Massachusetts Institute of Technology.

Dehne F, Omran MT, Sack JR, 2012 *Shortest paths in time-dependent FIFO networks. Algorithmica* 62(1-2):416–435.

Dekker R, Bloemhof J, Mallidis I, 2012 *Operations research for green logistics–an overview of aspects, issues, contributions and challenges. European Journal of Operational Research* 219(3):671–679.

Delling D, Nannicini G, 2012 *Core routing on dynamic time-dependent road networks. INFORMS Journal on Computing* 24(2):187–201.

Delling D, Wagner D, 2007 *Landmark-based routing in dynamic graphs. International Workshop on Experimental and Efficient Algorithms*, 52–65 (Springer).

Demir E, Bektaş T, Laporte G, 2011 *A comparative analysis of several vehicle emission models for road freight transportation. Transportation Research Part D: Transport and Environment* 16(5):347–357.

Demir E, Bektaş T, Laporte G, 2012 *An adaptive large neighborhood search heuristic for the pollution-routing problem. European Journal of Operational Research* 223(2):346–359.

Demir E, Bektaş T, Laporte G, 2014a *The bi-objective pollution-routing problem. European Journal of Operational Research* 232(3):464–478.

Demir E, Bektaş T, Laporte G, 2014b *A review of recent research on green road freight transportation. European Journal of Operational Research* 237(3):775–793.

Desaulniers G, Villeneuve D, 2000 *The shortest path problem with time windows and linear waiting costs. Transportation Science* 34(3):312–319.

Di Bartolomeo M, Grande E, Nicosia G, Pacifici A, 2017 *Cheapest paths in dynamic networks. Networks* 55(2):23–32.

Dijkstra EW, 1959 *A note on two problems in connexion with graphs. Numerische mathematik* 1(1):269–271.

Drake DF, Kleindorfer PR, Van Wassenhove LN, 2016 *Technology choice and capacity portfolios under emissions regulation. Production and Operations Management* 25(6):1006–1025.

Dreyfus G, 2005 *Neural Networks: Methodology and Applications* (Berlin Heidelberg, Germany: Springer Science & Business Media).

Dreyfus SE, 1969 *An appraisal of some shortest-path algorithms. Operations Research* 17(3):395–412.

Eglese R, Bektas T, 2014 *Green vehicle routing.* Psaraftis HN, ed., *Vehicle Routing: Problems, Methods, and Applications*, volume 18, 437–458 (University of Bologna, Bologna, Italy: MOS-SIAM Series on Optimization).

Ehmke JF, Campbell AM, Thomas BW, 2016a *Data-driven approaches for emissions-minimized paths in urban areas. Computers & Operations Research* 67:34–47.

Ehmke JF, Campbell AM, Thomas BW, 2016b *Vehicle routing to minimize time-dependent emissions in urban areas. European Journal of Operational Research* 251(2):478–494.

Ehmke JF, Meisel S, Mattfeld DC, 2012 *Floating car based travel times for city logistics. Transportation research part C: emerging technologies* 21(1):338–352.

Environment Canada, 2014 *Canada's emissions trends*, URL https://ec.gc.ca/ges-ghg/E0533893-A985-4640-B3A2-008D8083D17D/ETR_E%202014.pdf, available online (accessed on April 16, 2018).

Europeia C, 2012 *EU transport in figures-statistical pocketbook 2012.*

Figliozzi MA, 2007 *Analysis of the efficiency of urban commercial vehicle tours: Data collection, methodology, and policy implications. Transportation Research Part B: Methodological* 41(9):1014–1032.

Figliozzi MA, 2010 *The impacts of congestion on commercial vehicle tour characteristics and costs. Transportation Research Part E: Logistics and Transportation Review* 46(4):496–506.

Figliozzi MA, 2011 *The impacts of congestion on time-definitive urban freight distribution networks CO_2 emission levels: Results from a case study in Portland, Oregon. Transportation Research Part C: Emerging Technologies* 19(5):766–778.

Fleischmann B, Gietz M, Gnutzmann S, 2004 *Time-varying travel times in vehicle routing. Transportation Science* 38(2):160–173.

Ford Jr LR, 1956 *Network flow theory.* Technical report, DTIC Document.

Franceschetti A, Demir E, Honhon D, Van Woensel T, Laporte G, Stobbe M, 2017a *A metaheuristic for the time-dependent pollution-routing problem. European Journal of Operational Research* 259(3):972–991.

Franceschetti A, Demir E, Honhon D, Van Woensel T, Laporte G, Stobbe M, 2017b *A metaheuristic for the time-dependent pollution-routing problem. European Journal of Operational Research* 259(3):972–991.

Franceschetti A, Honhon D, Van Woensel T, Bektaş T, Laporte G, 2013 *The time-dependent pollution-routing problem. Transportation Research Part B: Methodological* 56:265–293.

Frank H, 1969 *Shortest paths in probabilistic graphs. Operations Research* 17(4):583–599.

Friedman JH, 2001 *Greedy function approximation: a gradient boosting machine. Annals of Statistics* 29:1189–1232.

Fu L, Rilett LR, 1998 *Expected shortest paths in dynamic and stochastic traffic networks. Transportation Research Part B: Methodological* 32(7):499–516.

Gajanand M, Narendran T, 2013 *Green route planning to reduce the environmental impact of distribution. International Journal of Logistics Research and Applications* 16(5):410–432.

Garaix T, Artigues C, Feillet D, Josselin D, 2010 *Vehicle routing problems with alternative paths: An application to on-demand transportation. European Journal of Operational Research* 204(1):62–75.

Gendreau M, Ghiani G, Guerriero E, 2015 *Time-dependent routing problems: A review. Computers & Operations Research* 64:189–197.

Ghiani G, Guerriero E, 2014a *A lower bound for the quickest path problem. Computers & Operations Research* 50:154–160.

Ghiani G, Guerriero E, 2014b *A note on the Ichoua, Gendreau, and Potvin (2003) travel time model. Transportation Science* 48(3):458–462.

Hart PE, Nilsson NJ, Raphael B, 1968 *A formal basis for the heuristic determination of minimum cost paths. IEEE Transactions on Systems Science and Cybernetics* 4(2):100–107.

Haykin S, 1994 *Neural Networks: A Comprehensive Foundation* (New York: Macmillan, Prentice Hall PTR).

Heni H, Coelho LC, Renaud J, 2017 *Time-dependent quickest path problem with emission minimization.* Technical Report CIRRELT-2017-62, Montreal, Canada.

Hess S, Quddus M, Rieser-Schüssler N, Daly A, 2015 *Developing advanced route choice models for heavy goods vehicles using GPS data. Transportation Research Part E: Logistics and Transportation Review* 77:29–44.

Hickman J, Hassel D, Joumard R, Samaras Z, Sorenson S, 1999 *Methodology for calculating transport emissions and energy consumption. European Commission, DG VII. Technical Report*, URL `http://www.transport-research.info/sites/default/files/project/documents/meet.pdf`, available online (accessed on April 16, 2018).

Hothorn T, Hornik K, Zeileis A, 2006 *Unbiased recursive partitioning: A conditional inference framework. Journal of Computational and Graphical Statistics* 15(3):651–674.

Huang B, Wu Q, Zhan F, 2007 *A shortest path algorithm with novel heuristics for dynamic transportation networks. International Journal of Geographical Information Science* 21(6):625–644.

Huang H, Gao S, 2012 *Optimal paths in dynamic networks with dependent random link travel times. Transportation Research Part B: Methodological* 46(5):579–598.

Huang Y, Zhao L, Van Woensel T, Gross JP, 2017 *Time-dependent vehicle routing problem with path flexibility. Transportation Research Part B: Methodological* 95:169–195.

Ichoua S, Gendreau M, Potvin JY, 2003 *Vehicle dispatching with time-dependent travel times. European Journal of Operational Research* 144(2):379–396.

Jabali O, Van Woensel T, de Kok AG, 2012 *Analysis of travel times and CO_2 emissions in time-dependent vehicle routing. Production and Operations Management* 21(6):1060–1074.

Jaikumar R, Nagendra S, Sivanandan R, 2017 *Modal analysis of real-time, real world vehicular exhaust emissions under heterogeneous traffic conditions. Transportation Research Part D: Transport and Environment* 54:397–409.

Jula H, Dessouky M, Ioannou PA, 2008 *Real-time estimation of travel times along the arcs and arrival times at the nodes of dynamic stochastic networks. IEEE Transactions on Intelligent Transportation Systems* 9(1):97–110.

Kaufman DE, Smith RL, 1993 *Fastest paths in time-dependent networks for intelligent vehicle-highway systems application. Journal of Intelligent Transportation Systems* 1(1):1–11.

Kim J, Han WS, Oh J, Kim S, Yu H, 2014 *Processing time-dependent shortest path queries without pre-computed speed information on road networks. Information sciences* 255:135–154.

Kim S, Lewis ME, White CC, 2005 *Optimal vehicle routing with real-time traffic information. IEEE Transactions on Intelligent Transportation Systems* 6(2):178–188.

Koç Ç, Bektaş T, Jabali O, Laporte G, 2014 *The fleet size and mix pollution-routing problem. Transportation Research Part B: Methodological* 70:239–254.

Koenig S, Likhachev M, Furcy D, 2004 *Lifelong planning A*. Artificial Intelligence* 155(1):93–146.

Kok AL, Hans E, Schutten J, 2012 *Vehicle routing under time-dependent travel times: the impact of congestion avoidance. Computers & Operations Research* 39(5):910–918.

Kopfer HW, Schönberger J, Kopfer H, 2014 *Reducing greenhouse gas emissions of a heterogeneous vehicle fleet. Flexible Services and Manufacturing Journal* 26(1-2):221–248.

Kramer R, Maculan N, Subramanian A, Vidal T, 2015a *A speed and departure time optimization algorithm for the pollution-routing problem. European Journal of Operational Research* 247(3):782–787.

Kramer R, Subramanian A, Vidal T, Lucídio dos Anjos FC, 2015b *A matheuristic approach for the pollution-routing problem. European Journal of Operational Research* 243(2):523–539.

Kuhn M, Johnson K, 2013 *Applied Predictive Modeling*, volume 810 (New York, USA: Springer).

Lahyani R, Khemakhem M, Semet F, 2015 *Rich vehicle routing problems: From a taxonomy to a definition. European Journal of Operational Research* 241(1):1–14.

Lai DS, Demirag OC, Leung JM, 2016 *A tabu search heuristic for the heterogeneous vehicle routing problem on a multigraph. Transportation Research Part E: Logistics and Transportation Review* 86:32–52.

Laporte G, 2016 *Scheduling issues in vehicle routing. Annals of Operations Research* 236(2):463–474.

Lee HL, 2018 *Big data and the innovation cycle. Production and Operations Management* forthcoming.

Letchford AN, Nasiri SD, Oukil A, 2014 *Pricing routines for vehicle routing with time windows on road networks. Computers & Operations Research* 51:331–337.

Lin C, Choy KL, Ho GT, Chung S, Lam H, 2014 *Survey of green vehicle routing problem: past and future trends. Expert Systems with Applications* 41(4):1118–1138.

Liu B, Hu J, Yan F, Turkson RF, Lin F, 2016 *A novel optimal support vector machine ensemble model for NOx emissions prediction of a diesel engine. Measurement* 92:183–192.

MDDELCC, 2016 *Inventaire québécois des émissions de gaz à effet de serre en 2014 et leur évolution depuis 1990. Ministère du Développement Durable, de l'Environnement et de la Lutte contre les Changements Climatiques, 32 pages*, URL http://www.mddelcc.gouv.qc.ca/changements/ges/2014/Inventaire1990-2014.pdf, available online (accessed on April 16, 2018).

Miller-Hooks E, Yang B, 2005 *Updating paths in time-varying networks given arc weight changes. Transportation Science* 39(4):451–464.

Miller-Hooks ED, Mahmassani HS, 2000 *Least expected time paths in stochastic, time-varying transportation networks. Transportation Science* 34(2):198–215.

Ministère de l'Énergie et des Ressources Naturelles, 2014 *Facteurs d'émission et de conversion. Bureau de l'Efficacité et de l'Innovation Énergétique, Gouvernement du Québec*, URL http://www.transitionenergetique.gouv.qc.ca/fileadmin/medias/pdf/Facteurs_emissions.pdf, available online (accessed on April 16, 2018).

Moore EF, 1959 *The shortest path through a maze* (Bell Telephone System.).

Nannicini G, Delling D, Liberti L, Schultes D, 2008 *Bidirectional A* search for time-dependent fast paths. International Workshop on Experimental and Efficient Algorithms*, 334–346 (Springer).

Nannicini G, Delling D, Schultes D, Liberti L, 2012 *Bidirectional A* search on time-dependent road networks. Networks* 59(2):240–251.

Nie YM, Wu X, 2009 *Shortest path problem considering on-time arrival probability. Transportation Research Part B: Methodological* 43(6):597–613.

Orda A, Rom R, 1990 *Shortest-path and minimum-delay algorithms in networks with time-dependent edge-length. Journal of the ACM* 37(3):607–625.

Orda A, Rom R, 1991 *Minimum weight paths in time-dependent networks. Networks* 21(3):295–319.

Pallottino S, Scutella MG, 1998 *Shortest path algorithms in transportation models: classical and innovative aspects. Equilibrium and Advanced Transportation Modelling*, 245–281 (Montréal: Springer).

Pallottino S, Scutella MG, 2003 *A new algorithm for reoptimizing shortest paths when the arc costs change. Operations Research Letters* 31(2):149–160.

Pathak SK, Sood V, Singh Y, Channiwala S, 2016 *Real world vehicle emissions: Their correlation with driving parameters. Transportation Research Part D: Transport and Environment* 44:157–176.

Patier D, et al., 2002 *La logistique dans la ville.* Technical Report HALSHS-00069760, Laboratoire d'Économie des Transports, France.

Piecyk MI, McKinnon AC, 2010 *Forecasting the carbon footprint of road freight transport in 2020. International Journal of Production Economics* 128(1):31–42.

Psaraftis HN, et al., 2016 *Green Transportation Logistics* (Springer).

Qian J, Eglese R, 2014 *Finding least fuel emission paths in a network with time-varying speeds. Networks* 63(1):96–106.

Qian J, Eglese R, 2016 *Fuel emissions optimization in vehicle routing problems with time-varying speeds. European Journal of Operational Research* 248(3):840–848.

Rakha H, Ahn K, Trani A, 2004 *Development of VT-micro model for estimating hot stabilized light duty vehicle and truck emissions. Transportation Research Part D: Transport and Environment* 9(1):49–74.

Ross M, 1994 *Automobile fuel consumption and emissions: Effects of vehicle and driving characteristics. Annual Review of Energy and the Environment* 19(1):75–112.

Savelsbergh M, Van Woensel T, 2016 *City logistics: Challenges and opportunities. Transportation Science* 50(2):579–590.

Sbihi A, Eglese RW, 2010 *Combinatorial optimization and green logistics. Annals of Operations Research* 175(1):159–175.

Scora G, Barth M, 2006 *Comprehensive modal emissions model (CMEM), version 3.01* .

Sherali HD, Hobeika AG, Kangwalklai S, 2003 *Time-dependent, label-constrained shortest path problems with applications. Transportation Science* 37(3):278–293.

Short J, 2008 *Transport and energy: the challenge of climate change: for transport, a major contributor to greenhouse gases, the challenge to reduce emissions is immense, particularly as most forecasts see transport activity doubling or tripling in the next 30 years. OECD Observer* (266):20–22.

Southworth F, Peterson BE, 2000 *Intermodal and international freight network modeling. Transportation Research Part C: Emerging Technologies* 8(1):147–166.

Speranza MG, 2018 *Trends in transportation and logistics. European Journal of Operational Research* 264(3):830–836.

Stern NH, 2007 *The economics of climate change: the Stern review* (Cambridge University Press).

Sun Y, Yu X, Bie R, Song H, 2017 *Discovering time-dependent shortest path on traffic graph for drivers towards green driving. Journal of Network and Computer Applications* 83:204–212.

Sung K, Bell MG, Seong M, Park S, 2000 *Shortest paths in a network with time-dependent flow speeds. European Journal of Operational Research* 121(1):32–39.

Suzuki Y, 2016 *A dual-objective metaheuristic approach to solve practical pollution routing problem. International Journal of Production Economics* 176:143–153.

Taillard É, Badeau P, Gendreau M, Guertin F, Potvin JY, 1997 *A tabu search heuristic for the vehicle routing problem with soft time windows. Transportation Science* 31(2):170–186.

Tajik N, Tavakkoli-Moghaddam R, Vahdani B, Mousavi SM, 2014 *A robust optimization approach for pollution routing problem with pickup and delivery under uncertainty. Journal of Manufacturing Systems* 33(2):277–286.

Ticha HB, Absi N, Feillet D, Quilliot A, 2017 *Empirical analysis for the VRPTW with a multigraph representation for the road network. Computers & Operations Research* 88:103–116.

Touzani S, Granderson J, Fernandes S, 2018 *Gradient boosting machine for modeling the energy consumption of commercial buildings. Energy and Buildings* 158:1533–1543.

Transports Canada, 2011 *Transportation in Canada 2011*, URL https://www.tc.gc.ca/media/documents/policy/Transportation_in_Canada_2011.pdf, available online (accessed on April 16, 2018).

Transports Canada, 2017 *Transportation in Canada 2016*, URL https://www.tc.gc.ca/media/documents/policy/comprehensive_report_2016.pdf, available online (accessed on April 16, 2018).

Turkensteen M, 2017 *The accuracy of carbon emission and fuel consumption computations in green vehicle routing. European Journal of Operational Research* 262(2):647–659.

United States Department of Transportation, 2017 *Freight facts and figures 2017*, URL https://www.bts.gov/sites/bts.dot.gov/files/docs/FFF_2017.pdf, available online (accessed on April 16, 2018).

Van Woensel T, Kerbache L, Peremans H, Vandaele N, 2008 *Vehicle routing with dynamic travel times: A queueing approach. European Journal of Operational Research* 186(3):990–1007.

Vanek FM, Morlok EK, 2000 *Improving the energy efficiency of freight in the united states through commodity-based analysis: justification and implementation. Transportation Research Part D: Transport and Environment* 5(1):11–29.

Vapnik V, 2013 *The Nature of Statistical Learning Theory* (USA: Springer Science & Business Media).

Verbeeck C, 2016 *Optimizing practical orienteering problems with stochastic time-dependent travel times: towards congestion free routes*. Ph.D. thesis, Ghent University.

Wen L, Çatay B, Eglese R, 2014 *Finding a minimum cost path between a pair of nodes in a time-varying road network with a congestion charge. European Journal of Operational Research* 236(3):915–923.

Wen L, Eglese R, 2015 *Minimum cost VRP with time-dependent speed data and congestion charge. Computers & Operations Research* 56:41–50.

Winebrake JJ, Corbett JJ, Falzarano A, Hawker JS, Korfmacher K, Ketha S, Zilora S, 2008 *Assessing energy, environmental, and economic tradeoffs in intermodal freight transportation. Journal of the Air & Waste Management Association* 58(8):1004–1013.

Xiao Y, Konak A, 2016 *The heterogeneous green vehicle routing and scheduling problem with time-varying traffic congestion. Transportation Research Part E: Logistics and Transportation Review* 88:146–166.

Yang L, Zhou X, 2014 *Constraint reformulation and a lagrangian relaxation-based solution algorithm for a least expected time path problem. Transportation Research Part B: Methodological* 59:22–44.

Zachariadis EE, Kiranoudis CT, 2010 *A strategy for reducing the computational complexity of local search-based methods for the vehicle routing problem. Computers & Operations Research* 37(12):2089–2105.

Zeng W, Miwa T, Morikawa T, 2016 *Prediction of vehicle CO_2 emission and its application to eco-routing navigation. Transportation Research Part C: Emerging Technologies* 68:194–214.

Zenghelis D, 2006 *Stern review: The economics of climate change. HM Treasury* .

Zhang Y, Haghani A, 2015 *A gradient boosting method to improve travel time prediction. Transportation Research Part C: Emerging Technologies* 58:308–324.

Ziliaskopoulos AK, Mahmassani HS, 1993 *Time-dependent, shortest-path algorithm for real-time intelligent vehicle highway system applications. Transportation Research Record* 94–94.

Ziliaskopoulos AK, Mandanas FD, Mahmassani HS, 2009 *An extension of labeling techniques for finding shortest path trees. European Journal of Operational Research* 198(1):63–72.